

DOPING OF VACUUM DEPOSITED ZINC OXIDE THIN FILMS

Thesis

Submitted in partial fulfillment of the requirements for the degree of

DOCTOR OF PHILOSOPHY

by

SOWMYA PALIMAR



DEPARTMENT OF PHYSICS
NATIONAL INSTITUTE OF TECHNOLOGY KARNATAKA, SURATHKAL
MANGALORE - 575 025

JANUARY, 2013

DECLARATION

by the Ph.D. Research Scholar

I hereby *declare* that the Research Thesis entitled **DOPING OF VACUUM DEPOSITED ZINC OXIDE THIN FILMS**, which is being submitted to the *National Institute of Technology Karnataka, Surathkal* in partial fulfillment of the requirements for the award of the Degree of *Doctor of Philosophy* in **Physics** is a *bonafide report of the research work carried out by me*. The material contained in this Research Thesis has not been submitted to any University or Institution for the award of any degree.

PH08F04 **Sowmya Palimar**

(Register Number Name Signature of the Research Scholar)

Department of Physics

Place: NITK - Surathkal

Date:

CERTIFICATE

This is to *certify* that the Research Thesis entitled **DOPING OF VACUUM DEPOSITED ZINC OXIDE THIN FILMS** submitted by **Ms. Sowmya Palimar (Register Number: PH08F04)** as the record of the research work carried out by her, is *accepted as the Research Thesis submission* in partial fulfillment of the requirements for the award of degree of **Doctor of Philosophy**.

Prof. G. K. Shivakumar
Research Guide

Prof. (Mrs.) Kasturi. V. Bangera
Additional Research Guide

Prof. N. K. Udayshankar
Chairman - DRPC

Acknowledgement

I owe my most sincere gratitude to my research guides Prof. G. K. Shivakumar and Prof. Kasturi V. Bangera for considering me as their research student. I heartily acknowledge the help, support and encouragement I received from them during the course of my research. The research work presented here would have been impossible without the able guidance, valuable suggestions and generous help of my research guides. I sincerely thank my research panel members Prof. G. Umesh and Prof. M. C. Narasimhan for their valuable suggestions and excellent advice in accomplishing this work. I must thank my research seniors, Dr Raviprakash, Dr Prakash Shenoy, Dr. Gowrish Rao and my present colleagues, Mr Sadananda Kumar, and Mr. Shashidar, for their help, encouragement and wishes. The help received by Dr. Anandan C, Scientist-F, National Aerospace Laboratories (CSIR), Bangalore in my research work is greatly acknowledged. I thank all faculty members, staff and research students of the Department of Physics, for their kind and sincere support throughout my work. I am grateful to the present Head of the Department Prof. N. K. Udayashankar for supporting me to attend various conferences and workshops, which in turn helped me to understand the current research trends.

I also acknowledge, with gratitude, *National Institute of Technology Karnataka, Surathkal* for providing financial support throughout my research work.

Abstract

The main objective of present work is to study the doping of vacuum evaporated zinc oxide (ZnO) thin films. Initially, optimum conditions required to obtain good quality of undoped ZnO thin films is determined by depositing films using two evaporation sources (boats) namely molybdenum and tungsten and annealing them under different conditions. Compositional analysis of films showed incorporation of boat atoms in to ZnO thin films prepared using molybdenum as well as tungsten boat. A considerable reduction in atomic percentage incorporated boat atoms on annealing was observed in both cases. ZnO thin films obtained under optimum conditions were found to be amorphous in nature with good combination of visible region transmittance of up to 90% and room temperature conductivity of $92 \Omega^{-1}\text{cm}^{-1}$. XPS analysis has shown that the film is approximately stoichiometric with slight oxygen deficiency. From the measurements of activation energy it is observed that ZnO thin film is having two donor levels below the conduction band. Further, ZnO films are doped with third group dopants to improve their n-type conductivity. Investigation has been carried out to know the optimum percentage of dopant to be added to retain the transmittance of the film. Role of third group elements as n-type dopants in the form of pure metals and metal oxides is studied by doping the film with indium and indium oxide separately. It is observed that contribution of indium oxide dopants is more than indium dopants in improving the conductivity of films. ZnO films were then doped with other two third group oxides, namely gallium oxide and aluminum oxide. From structural, optical and electrical properties of these oxide doped ZnO films it is found that all films have smooth surface with visible region transparency of above 90% and significantly high room temperature conductivity of the order of $10^3 \Omega^{-1}\text{cm}^{-1}$, which are well suited for the application of transparent electrodes.

Keywords : Zinc Oxide, Thin Film, Vacuum Deposition, Doping, Conductivity, Transmittance.

Contents

1	Introduction	1
1.1	Thin films	1
1.1.1	Physical deposition	3
1.1.2	Chemical deposition	5
1.2	Zinc oxide	7
1.2.1	Importance of zinc oxide	7
1.2.2	Deposition techniques	9
1.3	Literature survey	12
1.4	Scope and objectives of the present work	18
2	Growth and characterization	20
2.1	Growth technique	20
2.2	Thickness measurement methods	29
2.3	Characterization	33
2.3.1	Structural characterization	33
2.3.2	Compositional characterization	40
2.3.3	Optical characterization	46
2.3.4	Electrical characterization	52
3	Effect of evaporation source materials	59
3.1	X-ray diffraction study	60
3.2	Scanning electron microscopy analysis	62
3.3	EDAX analysis	65
3.4	Optical characterization	70

4	Study of undoped ZnO thin films	76
4.1	Optimization of annealing duration	78
4.2	Structural characterization	82
4.3	Compositional characterization	82
4.4	Electrical characterization	87
4.4.1	Measurement of electrical conductivity	87
4.4.2	Measurement of activation energy	90
5	Doping of thermally evaporated ZnO thin films	94
5.1	Introduction	94
5.2	Doping of ZnO thin films	97
5.2.1	n-Type doping	98
5.2.2	p-Type doping	100
5.3	Indium doped ZnO thin films	104
5.4	Indium oxide doped ZnO thin films	114
5.5	Gallium oxide doped ZnO thin films	122
5.6	Aluminum oxide doped ZnO thin films	129
6	Summary and conclusions	137
6.1	Summary of the present work	137
6.2	Conclusions of the present work	142
6.3	Scope for further work	144
	References	146

List of Tables

3.1	Percentage variation of incorporated evaporation source atoms in thermally evaporated ZnO thin film with annealing	66
4.1	Conductivity and % transmittance ZnO thin films obtained from different methods reported in the literature compared with our results . . .	88
5.1	Opto electronic properties of undoped and doped ZnO thin films studied in the present work.	136

List of Figures

2.1	Schematic diagram of vacuum coating unit	26
2.2	Vacuum coating unit (HIND HIVAC 12A4D) used in the present work	27
2.3	Appearance of ZnO thin film in the (A) as deposited condition and (B) after annealing	28
2.4	Schematic representation of X-Ray diffractometers: (A) $\theta - \theta$ - type (b) $\theta - 2\theta$ type	38
2.5	Schematic diagram of scanning electron microscope <i>Ref:Schroder (2005)</i>	39
2.6	Schematic diagram of a XPS mechanism	45
2.7	The optical absorption phenomenon: (a) Conservation of energy and momentum, (b) Transition in direct bandgap material (c) Transition in indirect bandgap material	50
2.8	Schematic diagram of a typical spectrophotometer	51
2.9	Three different structures used for making contacts to thin films. (a) Bridge structure, (b) Planar structure and (c) sandwich Structure . .	56
2.10	Schematic diagram of the experimental setup for hot probe technique	57
2.11	Keithley Multimeter (2000) and Keithley Sourcemeters (2400) used in the present study	58
3.1	Typical XRD pattern of thermally evaporated ZnO thin films	61
3.2	SEM image of ZnO thin films deposited by W source in the (A) as deposited condition and (B) after annealing at 400°C for 4 hours . . .	63
3.3	SEM image of ZnO thin films deposited using Mo source in the (A) as deposited condition and (B) after annealing at 400°C for 4 hours . . .	64

3.4	EDAX Spectra of ZnO thin film deposited using Mo source in the (A) as deposited condition and (B) after annealing at 400°C for 4 hours	67
3.5	EDAX Spectrum of ZnO thin film deposited using Mo source after annealing at 500°C for 4 hours	68
3.6	EDAX Spectra of ZnO thin film deposited using W source in the (A) as deposited condition and (B) after annealing at 400°C for 4 hours	69
3.7	Transmittance spectrum of ZnO thin film deposited using W source after annealing at 400°C for 4 hours	72
3.8	Transmittance spectra of ZnO thin films deposited using Mo source after annealing at (A) 400°C for 4 hours and (B) 500°C for 4 hours	73
3.9	Optical Band gap calculation of ZnO thin films deposited using (A) W source and (B) Mo source, after annealing at 400°C for 4 hours	74
3.10	Optical band gap calculation of ZnO thin films deposited using Mo source after annealing at (A) 400°C for 4 hours and (B) 500°C for 4 hours	75
4.1	Transmittance spectra of ZnO thin films annealed at 300°C for (A) 60 mins, (B) 90 mins and (C) 120 mins	80
4.2	Optical band gap variation of ZnO thin films annealed at 300°C for (A) 60 mins, (B) 90 mins and (C) 120 mins	81
4.3	XPS Survey scan for ZnO thin film	84
4.4	Zn2p core level spectrum for ZnO thin film	85
4.5	O1s core level spectrum for ZnO thin film	86
4.6	I-V Characteristics of undoped ZnO thin film	92
4.7	Logarithmic resistance profile of ZnO thin film with respect to reciprocal of the temperature	93
5.1	Transmittance spectra of ZnO thin films doped with (A) 3% of indium, (B) 5 % of indium and (C) 7% of indium	107
5.2	I-V characteristics of ZnO thin films doped with (A) 3% of indium, (B) 5 % of indium and (C) 7% of indium	108
5.3	SEM image of ZnO thin film doped with 5 % of indium	109
5.4	Transmittance spectra of (A)undoped and (B) 5 % of indium doped ZnO thin films	110

5.5	Optical band gap measurements of (A)undoped and (B) 5 % of indium doped ZnO thin films	111
5.6	I-V Characteristics of (A)undoped and (B) 5 % of indium doped ZnO thin films	112
5.7	Logarithmic resistance profile of 5 % of indium doped ZnO thin film with respect to the reciprocal of temperature	113
5.8	SEM image of the surface of ZnO:In ₂ O ₃ thin film	117
5.9	Transmittance spectra of (A) undoped and (B) ZnO:In ₂ O ₃ thin films	118
5.10	Optical band gap measurements of (A) undoped and (B) ZnO:In ₂ O ₃ thin films	119
5.11	I-V characteristics of (A) undoped and (B) ZnO:In ₂ O ₃ thin films . . .	120
5.12	Logarithmic resistance profile of ZnO:In ₂ O ₃ thin film with respect to the reciprocal of temperature	121
5.13	SEM image of ZnO:Ga ₂ O ₃ thin film	124
5.14	Transmittance spectra of (A) undoped and (B) ZnO:Ga ₂ O ₃ thin films	125
5.15	Optical band gap measurements of (A) undoped and (B) ZnO:Ga ₂ O ₃ thin films	126
5.16	I-V characteristic ZnO:Ga ₂ O ₃ thin film	127
5.17	Logarithmic resistance profile of of ZnO:Ga ₂ O ₃ thin film with respect to the reciprocal of temperature	128
5.18	SEM image of ZnO:Al ₂ O ₃ thin film	131
5.19	Transmittance spectra of (A) undoped and (B) ZnO:Al ₂ O ₃ thin films	132
5.20	Optical band gap measurements of (A) undoped and (B) ZnO:Al ₂ O ₃ thin films	133
5.21	I-V characteristic ZnO:Al ₂ O ₃ thin film	134
5.22	Logarithmic resistance profile of of ZnO:Al ₂ O ₃ thin film with respect to the reciprocal of temperature	135

*No, it's not as deep as a well, or as wide as a church door,
but it's enough. It'll do the job.*

William Shakespeare

Chapter 1

Introduction

1.1 Thin films

A thin film is a two dimensional material normally nano to micro-metric thickness but not necessarily thin, created ab-intio on to a substrate by depositing atoms/molecules/ions/radicals one by one through a nucleation and growth process dictated by minimization of associated surface interfacial and strain energies. Thin film technology is a large branch of generic technology that has to do with surface modifications and coatings. In the surface modification process the properties of surface to substrate material is changed as exemplified by the hardening of steel, by introducing carbon or nitrogen to the surface or as in doping of semiconductor to change its electrical properties. Thin films can be fabricated to the thickness of one monolayer when the surface effects are predominant.

The microstructures of thin films can be quite different than the bulk material with respect to grain size and texture. Kinetic effects are considerably different in thin films than in bulk. Thin film process are essential to make nanometer materials such as quantum dots, quantum wires and super lattices. The consequence of all these makes thin film studies not only more interesting, highly material and process dependent, but also provides considerable challenges in gaining the physical understanding of the phenomena.

One of the simplest reasons which makes thin films important is that we desire to produce properties in a material that are often conflicting in nature if we use one single homogeneous material. Semiconductor materials are fabricated on a thin layer deposited on a semiconducting substrate. The integrated electronic circuits depend on the confinement of electric charges which relies on the interface between materials with different electronic properties. There are also many occasions when the properties demand for engineering applications involve features that are different than that for the bulk.

Optical interference films, the deposition of transparent films is vital in altering the functionality of a product. Depositing metal and patterning them on the surface are relatively easy to secure electrical connections between semiconductor devices. Titanium nitride coating on tool bits offer hardness and reduce friction and provide a chemical barrier of the tool to alloying with work piece. Epitaxial films are required to fabricate many devices where the deposited atoms are aligned with atoms in the underlying single crystal surface. The deposition of films such as chromium for corrosion protection and titanium nitride for improving the wear resistance are important in improving the product life. Even when the bulk material can perform a desired function it may be necessary to use the material in thin film form on some suitable, less expensive and widely available material. This option in design eliminates the need to use costly material in bulk form there by saving precious resources and conserve materials. There are many applications where the uniqueness of thin films is essential to the observed behavior. Examples include super lattice films, magneto resistance films, thin film super conductors, heterostructure lasers etc. Thin films offer a unique design opportunity and flexibility to create products in a cost effective way.

The technology of thin films receives its impetus for growth from the increased performance, reduced cost and control of properties different from that of the substrate. These features have permitted the addition of and development of an entirely new products, provided additional features in design and manufacturing, permit the achievement of improved functionality in the products, conserve resources and reduce the wastage encountered in traditional manufacturing. The electronic, magnetic

and optical properties of thin films are the key to the convergence of computing, communication and consumer electronics. It is therefore clear that thin films have important role to play in shaping society in future (Shree Harsha 2006).

We observe that thin films can be deposited with very well-defined and controlled dimensions, down to unit cell dimensions that enable us to create superlattices. The devices can be fabricated by lithographic, and dry etching techniques to make the manufacture of devices within acceptable costs. Frequently, the deposition conditions are carried out so far from equilibrium conditions that metastable phases can form and provide the means to search for some unusual structures and phases in creative ways. At present many deposition techniques have been emerged to deposit thin films on various substrates. Most of the deposition techniques allow layer thickness to be controlled with in a few tens of nanometers and some allow single layer of atoms to be deposited at one time. Deposition techniques fall in to two broad categories depending on whether the process is primarily chemical or physical.

1.1.1 Physical deposition

Physical deposition uses mechanical or thermal means to produce a thin film. The material to be deposited is placed in an energetic environment so that the particle of the material escapes from its surface. The substrate draws energy from these particles to travel as freely as possible. Since particles tend to follow a straight path, films deposited by physical means are usually directional rather than conformal. Some widely used physical deposition techniques are as follows.

A. Thermal evaporation technique

Evaporation of a material and its subsequent condensation on the substrate is one of the simplest process for thin film deposition. In this method the material to be deposited will be in the form of solid or liquid phase and requires thermal energy to transfer in to vapor phase. Vapor condenses on the substrate which is maintained at lower temperature than the evaporation source. The process is usually carried out under vacuum (typically 10^{-5} torr to 10^{-6} torr) so that the evaporated atoms undergo

an essentially collision less transport prior to the condensation on the substrate.

B. Electron beam evaporation

An electron beam evaporation system consists of a cathode and anode, between which a potential difference is maintained. In a simple system, cathode emits electron which are then accelerated to the anode that is the work piece to be heated across the potential drop. It is necessary to maintain this arrangement in the vacuum chamber in order to produce and control the flow of electrons since they are easily scattered by gas molecules.

C. Sputtering

The physical sputtering is a process which involves the physical (not thermal) vaporization of atoms by momentum transfer by bombarding energetic atomic sized particles. The energetic particles are usually ions of a gaseous material accelerated in an electric field and particles to be deposited will sputter from a surface called target. Sputter deposition can be used to deposit films of compound material either by sputtering from a compound target or by sputtering from an elemental target in a partial pressure of a reactive gas (usually known as “reactive sputtering”).

D. Pulsed laser deposition (PLD)

In the pulsed laser deposition high power laser pulses are used to evaporate a material from the target surface such that stoichiometry of the material is preserved in the interaction. The main advantages of PLD are its ability to create high energy source particles and permitting high quality film growth at low substrate temperature. Most commonly used lasers in PLD technique are UV excimer lasers and Nd:YAG pulsed lasers.

E. Molecular beam epitaxy (MBE)

Molecular beam epitaxy is a particular sophisticated form of thermal evaporation technique. In MBE, slow streams of an element can be directed at the substrate so that material deposits one atomic layer at a time. The beam of material can be

generated by either physical means or by chemical reaction (chemical beam epitaxy). MBE takes place in high or ultra high vacuum. The main advantage of molecular beam epitaxy is its precise control over the deposition parameter and insitu diagnostic capabilities. In this method growth mode can be monitored with the feed back from reflection high energy electron diffraction (RHEED).

1.1.2 Chemical deposition

In chemical deposition a fluid precursor undergoes chemical change on the solid surface, leaving a solid layer. Since the fluid surrounds the solid object, deposition happens on every surface, with little regard to direction. Hence the films prepared by chemical deposition techniques tend to be conformal, rather than directional. Chemical deposition is further categorized as follows.

A. Chemical vapor deposition (CVD)

Chemical Vapor Deposition technique is particularly interesting, because it gives raise to high quality films and it is applicable to large scale production. In CVD method deposition occurs as a result of chemical reaction of vapor precursors on the substrate which are delivered in to the growth zone by carrier gas. There are several techniques depending on precursors used. If metal organic precursor is used then the technique is called as Metal Organic Chemical Vapor Deposition (MOCVD).

B. Spray pyrolysis

Spray Pyrolysis is a process in which a thin film is deposited by spraying the solution on a heated surface, where the constituents react to form a chemical compound. The chemical reactions are selected such that, products other than the desired compound are volatile at the temperature of deposition. This process is particularly useful for the deposition of oxides.

C. Electroplating

Electroplating relies on liquid precursors, often a solution of water with a salt of the metal to be deposited. Though electroplating was not commonly used in semiconductor processing for many years it is one of the commercially important process with more wide spread use of chemical-mechanical polishing techniques.

D. Plasma enhanced CVD (PECVD)

Plasma enhanced CVD uses an ionized vapor or plasma as a precursor. Commercial PECVD relies on electromagnetic means (electric current, microwave excitation), rather than a chemical reaction to produce plasma.

The higher end techniques such as molecular beam epitaxy produce high quality films but at the same time they prove to be very expensive. The methods such as vacuum deposition, on the other hand are cost effective, and hence they are preferred for mass production in the industries.

1.2 Zinc oxide

1.2.1 Importance of zinc oxide

Zinc oxide (ZnO) is a very promising material for semiconductor device applications. Over the past two decades we have witnessed a significant improvement in the ZnO single crystal and epitaxial films. The prospects of ZnO as a complement in optoelectronics has driven many research groups world wide to focus on its semiconductor properties. This in turn has lead to the revival of the idea of using ZnO as optoelectronic or dielectric applications in its own right. The wide range of useful properties displayed by ZnO has been recognized for a long time. What has captured most of the attention in recent years is that ZnO is a semiconductor of band gap 3.37 eV which in principle enables the optoelectronic applications in blue and UV region of the spectrum. The prospectus of such application is fueled by impressive progress in bulk crystals as well as in thin films over past few years. A partial list of the properties of ZnO that distinguish it from other semiconductors or oxides or render it useful for applications include;

A. Direct and wide band gap

The band gap of ZnO is 3.44 eV at low temperatures and 3.37 eV at room temperature (Janotti *et al* 2009). For comparison, the respective values for wurtzite GaN are 3.50 eV and 3.44 eV (Özgür *et al* 2005). As mentioned above, this enables applications in optoelectronics in the blue/UV region, including light-emitting diodes, laser diodes and photodetectors (Look *et al* 2001). Optically pumped lasing has been reported in ZnO platelets (Reynolds *et al* 1996), thin films (Bagnall *et al* 1997), clusters consisting of ZnO nanocrystals (Cao *et al* 1999) and ZnO nanowires (Haung *et al* 2001) .

B. Large exciton binding energy

The free-exciton binding energy in ZnO is 60 meV, which could lead to lasing action based on exciton recombination even above room temperature. Since the oscillator strength of excitons is typically much larger than that of direct electron hole

transition in direct band gap semiconductors (Özgür *et al* 2005), the large exciton binding energy makes ZnO a promising material for optical devices that are based on excitonic effects.

C. Large piezoelectric constants

The low symmetry of the wurtzite crystal structure combined with a large electromechanical coupling in ZnO gives rise to strong piezoelectric and pyroelectric properties. Piezoelectric ZnO film with uniform thickness and orientation have been grown on a variety of substrates using different deposition techniques including sol-gel process, chemical vapor deposition, spray pyrolysis and sputtering (Janotti *et al* 2009).

D. Strong sensitivity of surface conductivity to the presence of adsorbed species

The conductivity of ZnO thin film is very sensitive to the exposure of the surface to various gases. It can be used as a cheap smell sensor capable of detecting the freshness of foods and drinks, due to the high sensitivity to tri-methylamine present in the odor. The gas sensitivity of ZnO thin film is studied by many research groups to understand the mechanism of sensor action (Janotti *et al* 2009).

E. High thermal conductivity

This property makes ZnO useful as an additive. It also increases the appeal of ZnO as a substrate for homo-epitaxy and hetero-epitaxy. High thermal conductivity translates into high efficiency of heat removal during device operation (Florescu *et al* 2002).

F. Amenability to wet chemical etching

Semiconductor device fabrication process generally benefit from the amenability to low temperature chemical etching. It has been reported that ZnO thin films can be etched with acidic, alkaline, as well as mixture of solutions (Özgür *et al* 2005, Janotti *et al* 2009). This possibility of low temperature chemical etching adds great

flexibility in the processing, designing and integration of electronic and optoelectronic devices.

G. Radiation hardness

Radiation hardness is important for applications at high altitude or in space. It has been observed that ZnO is very resistive to high energy radiation, making it a very suitable candidate for space applications. (Özgür *et al* 2005, Janotti *et al* 2009).

In addition to the above mentioned properties and applications ZnO has recently found other niche applications as well, such as fabrication of transparent thin film transistors, where the protective covering preventing light exposure is eliminated since ZnO based transistors are insensitive to visible light. Also up to $2 \times 10^{21} \text{ cm}^{-3}$ charge carriers can be introduced by heavy substitutional doping into ZnO. By controlling the doping level in ZnO its electrical properties can be changed from insulator through n-type semiconductor to metal while maintaining optical transparency that makes it useful for transparent electrodes in flat panel displays and solar cells. ZnO is also a promising candidate for spintronics applications.

1.2.2 Deposition techniques

Most of the current technological applications of ZnO, such as varistors, transparent conductive electrodes for solar cells, piezoelectric devices and gas sensors, have made use of thin films that are grown by a variety of deposition techniques, mostly on glass substrates. Some of the commonly used deposition techniques of ZnO thin films include,

A. Sputtering

One of the most popular growth techniques for early ZnO investigations was sputtering (DC sputtering, RF magnetron sputtering and reactive sputtering). The magnetron sputtering was a preferred method because of its low cost, simplicity, and low operating temperature. In this method ZnO films can be grown at a certain substrate temperature by sputtering from a high-purity ZnO target using a RF

magnetron sputter system. The growth is usually carried out in the growth ambient with $O_2 / Ar + O_2$ ratios ranging from 0 to 1 at a pressure of 10^3 - 10^2 torr. O_2 serves as the reactive gas and Ar acts as the sputtering enhancing gas. ZnO can also be grown by DC sputtering from a Zn target in an Ar+ O_2 gas mixture. The RF power applied to the plasma is tuned to regulate the sputtering yield rate from the ZnO target (Bachari *et al* 1999, Özgür *et al* 2005, Gong *et al* 2002).

B. Pulsed laser deposition (PLD)

For the growth of ZnO by PLD technique, usually UV excimer lasers KrF: $\lambda = 248$ nm and ArF: $\lambda = 193$ nm and Nd: yttrium aluminum garnet YAG pulsed lasers $\lambda = 355$ nm are used for ablation of the ZnO target in an oxygen environment. In some cases, Cu-vapor laser emitting at $\lambda = 510 - 578$ nm was also used for the same purpose. Cylindrical ZnO tablets made from pressed ZnO powder are usually used as targets. Single-crystal ZnO has been used to grow high-quality ZnO thin films very recently. A pure Zn metal is used only in rare cases. The properties of the grown ZnO films depend mainly on the substrate temperature, ambient oxygen pressure, and laser intensity (Özgür *et al* 2005, Craciun *et al* 1994).

C. Molecular beam epitaxy (MBE))

For ZnO thin-film deposition by MBE, Zn metal and O_2 are usually used as the source materials. High-purity Zn metal is evaporated from an effusion cell, where the cell temperature can be varied to examine the effect of the Zn flux on the growth rate and material properties. The oxygen radical beam, which can be generated by an ECR or a RF plasma source is directed on the film surface to obtain high-oxidation efficiency. When the O plasma is used, the chamber pressure during growth is in the 10^{-5} torr range (Özgür *et al* 2005).

D. Spray pyrolysis technique

Spray pyrolysis technique was used as early as 1910 to obtain transparent oxide films. In the preparation of ZnO thin films aqueous or alcoholic solution of zinc acetate, zinc chloride or zinc nitrate is sprayed on the hot substrate using air as

the carrier gas. The sprayed droplet reaching the hot substrate undergoes pyrolytic action and forms a single crystalline or cluster of crystallites of ZnO thin films. The other volatile by-product and excess solvent escapes in the vapor phase. The substrate provides thermal energy for thermal decomposition and subsequent recombination of the consequent species followed by sintering and recrystallization of clusters of crystallites giving rise to coherent films (Prasada and Santhosh 2010, Hichou *et al* 2005).

E. Chemical vapor deposition (CVD)

In the CVD method, ZnO deposition occurs as a result of chemical reactions of vapor-phase precursors on the substrate, which are delivered into the growth zone by the carrier gas. The reactions take place in a reactor where a necessary temperature profile is created in the gas flow direction. For hydride vapor phase epitaxy (VPE) growth of ZnO, hydrogen will be employed as a carrier gas and targets made using pure ZnO powder will be placed in the evaporation zone maintained at high temperature (Funakubo *et al* 1999, Özgür *et al* 2005).

Most of the growth techniques mentioned here produce ZnO thin film that is highly n-type. This high level n-type conductivity is very useful for some applications, such as transparent conductors, but in general it would be desirable to have a better control over the conductivity. In particular, the ability to reduce the n-type background and to achieve p-type doping would open up tremendous possibilities for semiconductor device applications in general and for light emitting diodes and laser diodes .

1.3 Literature survey

ZnO thin film has gained substantial interest in the research community due to its coexistence of transparency and conductivity. There has been a great deal of interest in zinc oxide thin films as seen from the surge of a relevant number of publications in the past two decades. Research groups all over the world used different physical and chemical techniques to obtain good quality of ZnO thin films. Some of the research papers referred during the period of present research work are briefly explained as follows.

Craciun *et al* (1994) studied the ZnO thin films deposited on glass and silicon substrates by the pulsed laser deposition technique employing a KrF laser. In this study the influence of the deposition parameters, such as substrate temperature, oxygen pressure, and laser influence on the properties of the grown films has been studied. All obtained films in this study are found to be optically transparent, electrically conductive and highly c-axis oriented.

Structural, optical and electrical properties of sputtered ZnO films is studied by Bachari *et al* (1999). In this study ZnO thin films were deposited by rf magnetron sputtering. In the reported results of this study it has been shown that the crystallinity of the films is found to increase with kinetic energy of sputtered particles. Infrared investigations have shown that zinc atoms stay tetrahedrally co-ordinated even though oxygen zinc atomic ratio changes from 0.95- 1.06.

Gong *et al* (2002) studied the effect of deposition conditions on the structural properties of R.F sputtered ZnO thin films. In this study the deposition was done on glass substrate and under different deposition ratio of argon and oxygen. The study was also carried out by changing the substrate temperature. In this study it has been shown that the pressure ratio has no effects on the orientation of the films.

The electrical properties of sputtered zinc oxide thin films deposited on silicon substrate using zinc target is studied by Ndong *et al* (2003). In this study the frequency dependence of both the AC conductivity and dielectric constant of ZnO thin films

have been investigated. It has been reported that the hopping is the predominant conduction process and dielectric constant of the film is nearly frequency independent at room temperature.

Influence of deposition temperature, rate of air flow and precursors on the cathodoluminescence properties of ZnO thin films obtained by spray pyrolysis method is studied by Hichou *et al* (2005). This study proved the critical dependence of cathodoluminescence property of ZnO thin film on spray rate and substrate temperature.

ZnO thin films were deposited at low temperature on polyethylene terephthalate by Banerjee *et al* (2006). The electrical conductivity of these films is measured and compared with that obtained by depositing on glass substrates. This report provided newer applications of ZnO thin films in flexible display technology.

Aida *et al* (2006) studied annealing and oxidation mechanism of evaporated zinc oxide thin films obtained by evaporating zinc oxide powder. This study showed a systematic investigation on influence of annealing temperature on the film composition and structural and optical properties by using Rutherford Back Scattering (RBS) analysis, X-ray Diffraction (XRD) and UV-visible transmission respectively.

Effect of annealing on the optical properties of thermally evaporated ZnO thin films is studied by Aly *et al* (2001). This study reported the dependence of absorption coefficient and the refractive index on wavelength before and after post-deposition heat treatment. This result demonstrated the application of ZnO thin film as an anti-reflection coating.

Rusu *et al* (2007) obtained ZnO thin films by the thermal oxidation of pure zinc film. This research group studied the structural changes that takes place during the process of evaporation. The microstructural changes that Zn thin film will undergo in the stage of changing from Zn to ZnO is investigated.

Characterization of sputtered ZnO thin film as sensor and actuator for diamond AFM probe is studied by Shibata *et al* (2002). In order to develop a diamond atomic force microscopy (AFM) probe with a piezoelectric sensor and actuator. The research group fabricated piezoelectric ZnO thin film and measured its piezoelectric constant. Finally in this study they achieved ZnO thin film with high piezoelectric constant of -3.5 pC/N. Using this value, properties of the diamond cantilever AFM probes of various dimensions and of 5 mm in thickness with a ZnO sensor and actuator of 1 mm in thickness is calculated.

Effects of the annealing treatment on electrical and optical properties of ZnO transparent conducting films by ultrasonic spray pyrolysis is studied by Lee *et al* (2004). This study showed the reduction in the resistivity and band gap of the film with increase in the deposition temperature. An improvement in the electrical conductivity of the films due to the annealing treatment is also observed and ZnO films with lowest resistivity of $1.6 \times 10^{-1} \Omega \text{ cm}$ are obtained.

Tellier *et al* (2010) obtained transparent, amorphous and organics free ZnO thin film by chemical solution deposition method. In this case the films were deposited on SiO_x/Si, soda-lime glass and polymer substrates. It was shown that the the films coated on glass and polymer substrates were amorphous in nature, but films coated on SiO_x/Si substrates which were then additionally heated for 450°C found to be crystalline consisting of randomly oriented grains.

Recently research groups are much interested in doping of ZnO thin films and improving its electrical properties with out disturbing its transparency. ZnO thin film can be doped either as p-type or n-type. Since basically ZnO is an n-type semiconductor, n-type doping is much easier, and properties are stable and reproducible. Different research groups have been succeeded in doping ZnO thin films with n-type donors using different deposition techniques.

Gomez *et al* (2005) obtained gallium doped ZnO thin films by spray pyrolysis technique. The study was carried out by changing the [Ga]/[Zn] ratio with substrate

temperature and post deposition heat treatment. The films were of n-type conductivity with an electrical resistivity in the order of $8 \times 10^{-3} \Omega \text{ cm}$ and optical transmittance higher than 80% in the visible region.

Aluminum doped ZnO thin films were obtained by Musat *et al* (2004). In this method ZnO thin films were doped with Al using sol-gel technique using zinc acetate. The film was doped with 2 wt % Al using aluminum chloride as the source of dopant. In this study it was reported that the films obtained have a transmittance of up to 85% to 90%, with reduction in the resistance of up to $1.3 \times 10^{-3} \Omega$.

Dghoughi *et al* (2010) also doped ZnO thin film with aluminum. In this study the research group varied atomic % of Al and then finally showed that films deposited with the $[\text{Al}]/[\text{Zn}]$ ratio equal to 0.05 had high transmittance of about 80% and 95% in the visible and near infra-red regions respectively and minimum resistivity of $1.4 \times 10^{-3} \Omega \text{ cm}$. The chemical composition analysis (EPMA) showed that this film was nearly stoichiometric with a slight oxygen deficiency.

Prasada and Santhosh (2010) obtained Ga doped ZnO thin films using spray pyrolysis technique. In this study the physical properties of the films are studied as a function of increasing Ga dopant concentration from 1% to 9 %. It has been reported that at 3 at% Ga doping, the film has lowest resistivity of $6.8 \times 10^{-3} \Omega \text{ cm}$.

Indium doped ZnO thin films were obtained by Hafdallah *et al* (2012) using spray pyrolysis technique. In this study indium chloride is used as the source of dopant. The study was carried out by varying the concentration of dopant from 2% to 8%. In this study it is observed that the grain size increased with indium doping.

Effect of target properties on transparent conducting Al-doped and Ga - doped ZnO thin films deposited by DC magnetron sputtering is studied by Minami *et al* (2010). Both Al-doped and Ga-doped ZnO (AZO and GZO) thin films were deposited on glass substrates using a dc-magnetron sputtering apparatus with various high-density sintered AZO or GZO disk targets. From this study it was observed that

the oxygen content in deposited thin films decreased as the oxygen content of the target used in the deposition was decreased. Thus in this paper it is concluded that as the dc-magnetron sputter deposition of transparent conducting impurity-doped ZnO thin films suitable for LCD applications requires the preparation of significantly reduced AZO and GZO targets with low oxygen content.

Chakraborty *et al* (2008) studied the effects of aluminum and indium incorporation on the structural and optical properties of ZnO thin films synthesized by spray pyrolysis technique. In this study aluminum chloride and aluminum nitrate were used as the source of dopants with zinc nitride and the concentration ratio of [Al]/[Zn] or [In]/[Zn] was kept at 1 at.%. The changes in the structural properties of the film with different dopants and different dopant sources is studied in detail.

Shelke *et al*(2012) studied the electrical and optical properties of transparent conducting tin doped ZnO thin films using sol-gel method. The study was carried out by varying the concentrations of the of the dopant using zinc acetate dehydrate and stannous chloride as source of zinc and tin respectively. Finally the paper reported a minimum resistance value of 3.11 Ωcm for tin doping concentration of 4 at%.

Chang *et al* (2002) obtained aluminum doped ZnO thin films deposited onto SiO₂/Si substrates by rf magnetron sputtering, which can be used as carbon monoxide gas sensor. In this study the dependence of the thin film thickness on CO gas sensing properties was investigated, where the film thickness was varied by controlling the deposition time. In this study it was concluded that the CO gas sensing properties were relative to the structural characteristics where the maximum sensitivity of 61.6% was obtained at 65 nm film thickness for the operation temperature of 400°C.

It is very difficult to obtain p-type doping in wide band gap semiconductors, such as GaN, ZnSe and ZnO. The difficulties can arise from a variety of causes like dopants may be compensated by low-energy native defects, such as Zn_i or V_0 , or background impurities like hydrogen. Low solubility of the dopant in the host material is also another possibility (Özgür *et al* 2005). While a number of research groups have

reported achieving p-type ZnO, there are still problems concerning the reproducibility of the results and the stability of the p-type conductivity. Some of the reports on p-type ZnO thin films are as follows.

Ye *et al* (2003) reported the preparation and characterization of p-type ZnO thin film. In this report the deposition of the film was done by dc-magnetron sputtering and in this case nitrogen is used as the dopant. Here nitrogen was incorporated in to the film in the form of ammonia gas. The study was carried out by changing the ammonia concentration from 0% to 67%. The report showed that the films with ammonia concentration 50% showed very good p-type conductivity with minimum resistance of 35 Ωcm and visible region transmittance of above 90 %.

Kim *et al* (2003) obtained p-type ZnO thin films by phosphorus doping. In this method ZnO films were prepared on a sapphire substrate using P_2O_5 as a phosphorus dopant. Phosphorus was doped in ZnO thin films using the ZnO target mixed with 1 wt% P_2O_5 . Obtained films are reported to show a low resistivity of 0.59 - 4.4 Ωcm .

Wang *et al* (2003) obtained p-type ZnO thin films by the oxidation of zinc nitride thin films. In this method zinc nitride thin films were deposited by reactive DC magnetron sputtering of zinc in argon and nitrogen mixture atmosphere. It is reported that in this method by controlling the oxidation temperature, p-type ZnO films with various hole concentrations can obtained but when the oxidation temperature was higher than 500⁰C, the ZnO film is n-type because of not enough nitrogen in the film.

1.4 Scope and objectives of the present work

From the literature survey it is noted that the ZnO thin films have been deposited by using wide variety of physical and chemical techniques. It is possible to tailor the properties of ZnO thin films by controlling the preparation conditions, which in turn make these films suitable for a particular applications. Therefore the preparation technique play a vital role. Depending on the type of devices, geometry and expected performance, one can employ an appropriate preparation technique.

Despite of the interest in ZnO thin film, very less importance has been given to its preparation by vacuum (thermal) deposition technique. Much of the previous studies on ZnO thin films deposited by thermal evaporation technique concentrated on the effect of annealing and the study of oxidation mechanism of the films (Aida *et al* 2006, Aly *et al* 2001). More over not much reports have been observed on the study of electrical and structural properties of thermally evaporated ZnO thin films.

Vacuum deposition technique is basically a less expensive and economical method to obtain ZnO thin film. This method involves a simple evaporation and condensation principle. Control over the deposition parameters in this method is relatively easy and it does not require any catalyst. The temperature of annealing for further oxidation of these films is also moderate enough to be easily applied in thin film technology.

In the present work ZnO thin films were deposited on glass substrates using both molybdenum (Mo) and tungsten (W) evaporation sources (boats). Then the films obtained were subjected to detailed structural characterizations using X ray diffractometer (XRD), and scanning electron microscopy (SEM). The compositional analysis of these films was done using energy dispersive analysis by X-ray (EDAX) and X ray photon spectroscopy (XPS). Optical properties of the films were studied using UV visible spectrophotometer and electrical characterizations were carried out with the help of computer assisted Keithley source meter set up. The optimum deposition and annealing conditions required to achieve highly transparent and conducting ZnO thin films are investigated.

Further an attempt was made to improve the n-type conductivity of these films by doping III group dopants. Role of third group dopants in the form of pure metal and metal oxides is studied by considering an example of indium (In) and indium oxide (In_2O_3) and also the modulations in the structural, optical and electrical properties of the film after doping with indium and indium oxide is studied in detail. The films were further doped with gallium oxide (Ga_2O_3) and aluminum oxide (Al_2O_3) and subjected for detailed structural, optical and electrical characterizations. Modifications in properties of the ZnO thin film with different third group oxide dopants is studied in detail.

Chapter 2

Growth and characterization

2.1 Growth technique

From the previous sections we have come to know that ZnO thin film has been obtained by different and almost all well known deposition technologies. The selection of a particular deposition method depends on various factors like quality of the films that can be produced by this method, ease of operation and maintenance, cost of production etc.

Despite of the interest in ZnO thin film and its research, not much attention has been paid towards its preparation by vacuum (thermal) evaporation technique. The research works already reported on the deposition of ZnO thin films by vacuum evaporation technique mainly concentrated on the effect of annealing on the optical properties and oxidation mechanism of the films (Aida *et al* 2006, Aly *et al* 2001, Bouhssira *et al* 2006). To the best of our knowledge not much work has been done on the detailed study of structural, compositional, electrical and optical properties of vacuum evaporated ZnO thin films.

By vacuum deposition technique ZnO thin film can be obtained either by evaporating pure zinc metal and then oxidizing it or by evaporating pure ZnO powder. The later also requires post deposition annealing process since ZnO undergoes decomposition during the process of annealing.

In our present work we have obtained ZnO thin films by vacuum evaporating pure ZnO powder using two different evaporation sources namely tungsten (W) and molybdenum (Mo). Vacuum evaporation method is proved to be one of the simple and low cost technique. It does not require any catalyst or high temperature growth and the temperature of further oxidation of ZnO thin films obtained by this method is also moderate enough to be easily applied in thin film technology.

An evaporation system is shown schematically in figure.2.1. The essential parts are: the vacuum enclosure, which provides a suitable environment for the evaporation process; a evaporation source, where the material to be evaporated can be held and heated; the substrates, which are to be coated with evaporant; and substrate holder and heater. Inside the vacuum chamber a residual pressure of the order of 10^{-5} torr to 10^{-6} torr is maintained with the help of vacuum pumps. In most of the cases combination of diffusion pump and rotary pump is used to reduce the pressure inside the chamber and in highly sophisticated vacuum evaporation systems turbo-molecular pump with rotary pump will be used.

The growth of thin film by vacuum evaporation process mainly involves three major steps described as follows.

i. Transition of source material from condensed phase to gaseous phase

In this stage the charge to be evaporated, which is kept in the source material is melted by heating the source material. In the case of charge materials which will undergo sublimation on heating, direct evaporation of the charge takes place and evaporants will get condensed on the substrate. Here evaporation source is chosen carefully so that it does not react chemically with the evaporant at high temperature.

The melting point of ZnO powder is 1975°C . Previous reports on the study of vacuum evaporated ZnO thin films have mentioned “Mo” and “W” as the suitable sources for evaporation (Aida *et al* 2006, Aly *et al* 2001, Bouhssira *et al* 2006). In our study we have used both Mo and W evaporation sources for the deposition of ZnO thin films.

ii. Vapor traversing the space between the evaporation source and substrate at reduced pressure

It is important to operate the process of evaporation at reduced pressure for two reasons.

- First, reducing pressure ensures that the concentration of residual gas molecules is small enough to minimize the possible oxidation.
- Secondly, coating uniformity is enhanced at a higher vacuum. In high vacuum the mean free path of the evaporated atoms increases. When the mean free path exceeds the dimensions of the chamber, vapor atoms will strike the substrate before hitting another atom which could lead non-uniform depositions.

iii. Condensation of the vapor upon arrival on the substrate

The vapor atoms impinging on the substrate may lose their kinetic energy and become adsorbed on the surface as ad-atoms. However if the initial kinetic energy of the atom is too high, it may re-evaporate after a finite time or even bounce off immediately. Thus condensation is necessarily a result of an equilibrium between adsorption and desorption process. The movement of ad-atoms depend on particularly the energy of vapor atoms, the rate of impingement, the adsorption and desorption activation energy, the topography and chemical nature of substrate and substrate temperature. The critical requirement for condensation to occur is that the partial pressure of the film material in the gas phase be equal to or larger than its vapor pressure in the condensed phase at that temperature.

Condensation is initiated by the formation of small but highly mobile clusters or islands through the combination of several ad-atoms. The clusters are called nuclei and the process of cluster formation is called nucleation. The nuclei further incorporate impinging atoms and sub-critical clusters and grow in size while the island density rapidly saturates. The next stage involves merging of the islands by coalescence phenomenon. Coalescence decreases the island density, resulting in local denuding of the substrate where further nucleation can occur. Crystallographic facets and

orientations are frequently preserved on islands and at interfaces between initially disoriented, coalesced particles. Coalescence continues until a connected network with unfilled channels in between develops. With further deposition the channels fill in and shrink, leaving isolated voids in between. Finally even the voids fill completely and the film is said to be continuous. This collective set of events occur during the early stage of deposition, typically accounting for the first few hundred angstroms of film thickness. The critical thickness on which the film becomes continuous depends mainly on nucleation site and substrate temperature.

The selection and preparation of substrates is also very important. The substrates not only provide mechanical strength but also crystal structure and orientation of the films. Ideally substrate should have no chemical interaction with the film except providing sufficient adhesion. Some desirable properties of the substrates are automatically smooth surface, perfect flatness, non porosity, good mechanical strength, thermal coefficient of expansion nearly matching with that of the film, high thermal conductivity, thermal and chemical stability and low cost.

A variety of substrate materials are used for vacuum deposition. In the present study commercially available soda lime glass slides were used as the substrates. Glass substrates are very cheap, chemically inert and provide good mechanical support for the films. They can also bare reasonably high deposition and annealing temperature. Since glass is amorphous it normally does not influence the crystal structure of the films deposited on it. Adhesion of the deposited films to the glass substrates depend on the film material. Glass substrates are some times treated with the chromic acid prior to the deposition in order to improve the adhesion of the films. Chromic acid corrodes the glass surface and makes it slightly rough. This would result in the better adhesion of the film to the glass surface.

The substrates must be cleaned properly prior to the deposition. Usually the substrates are cleaned in distill water to remove water soluble contaminants. Organic solvents such as acetone, alcohol can be used to remove contaminants which are insoluble in water.

In the present study the depositions were carried out in a vacuum coating unit (HIND HIVAC 12A4D) provided with 12 inch vacuum chamber and a diffusion pump of 4 inch diameter backed by an oil sealed rotary pump. The photograph of the unit is given in figure 2.2. Aly *et al* (2001) obtained thermally evaporated ZnO thin films using Mo as evaporation source, whereas Aida *et al* (2006) and Bouhssira *et al* (2006) evaporated pure ZnO powder using W as evaporation source. In the present work we have used both W and Mo evaporation sources for the evaporation of pure ZnO powder and the suitable evaporation source for further study is chosen after characterizing these films, structurally, compositionally and optically.

Highly pure zinc oxide powder (99.99%) supplied by Alpha Aesar were evaporated using both W and Mo evaporation sources separately by resistive heating. The glass substrates used for deposition were first thoroughly cleaned with soap solution (Laboline) and then dipped in a weak solution of chromic acid for nearly 24 hours. The substrates were then rinsed with distilled water and dipped in acetone for 10 minutes. After drying, the substrates were placed immediately inside the chamber. The source substrate distance was about 14 cm. The deposition was carried out under a residual pressure less than 10^{-5} torr. The substrates were maintained at room temperature during the process of deposition. Films obtained were found to be uniform and had good adhesion to the substrate.

The main challenge that one has to confront during the vacuum deposition of the compound materials is of achieving stoichiometry in the deposited films due to the possible dissociation of the compounds, during evaporation and the difference in vapor pressure of the constituent elements in the compound. The resulting films usually have a composition different from that of the source material. However this problem can be solved to a large extent by selecting a suitable substrate temperature or by subjecting the film to post deposition heat treatment. In the present study during the process of evaporation ZnO decomposes in to zinc and atomic oxygen as in equation (2.1.1) (Boris *et al* 2004).



During the process of evaporation oxygen will be released as the primary by-product and escapes out as gas. Hence the vacuum evaporated ZnO thin films in the as deposited condition expected are to be zinc rich and oxygen deficient. The films in the as deposited condition are found to be dark brown in color and opaque in nature. These films are then subjected to post deposition annealing process until the stoichiometry of the film is regained and film becomes transparent. The appearance of the film in the as deposited condition and after post deposition heat treatment are shown in the figure 2.3.

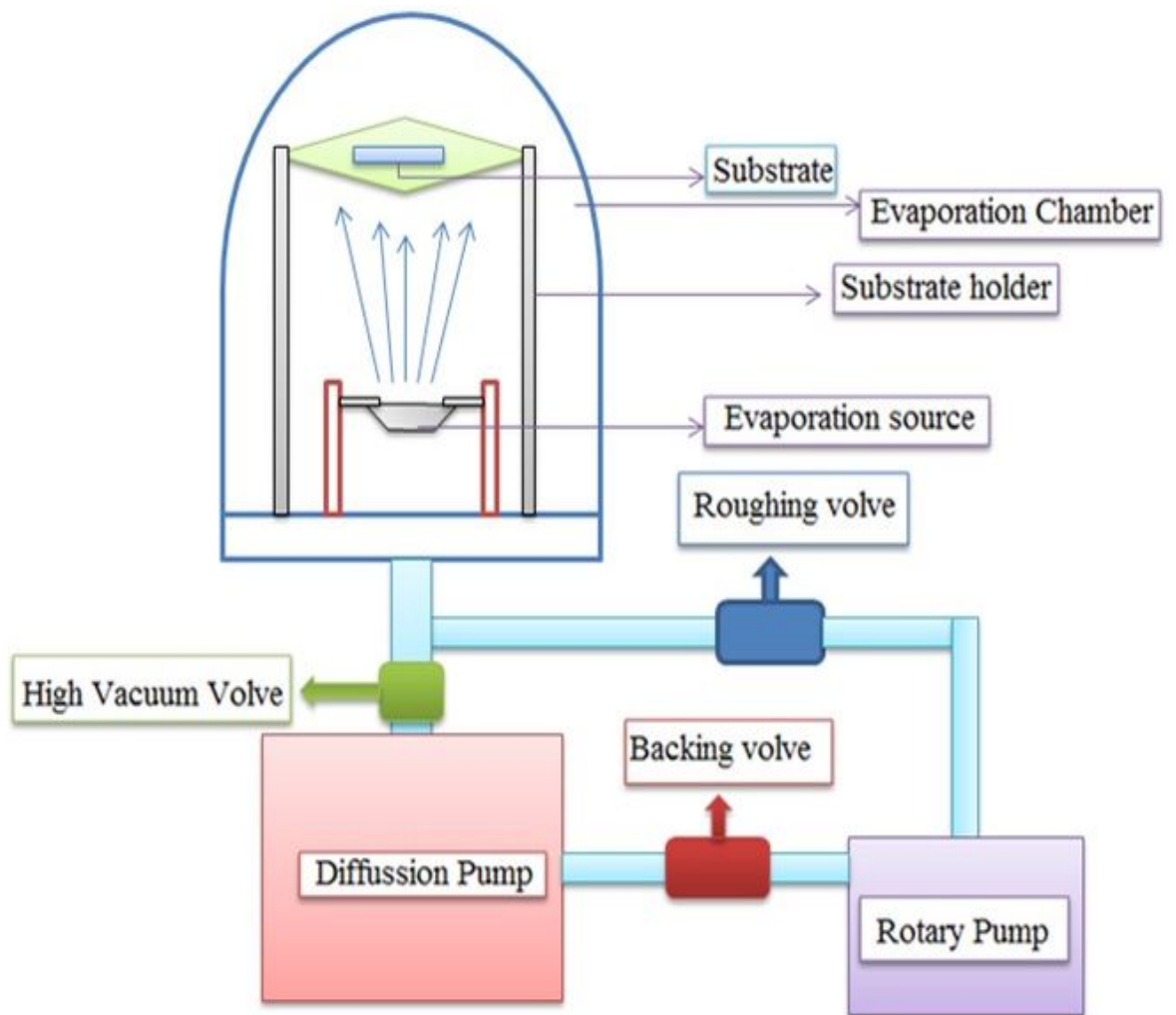


Figure 2.1: Schematic diagram of vacuum coating unit



Figure 2.2: Vacuum coating unit (HIND HIVAC 12A4D) used in the present work

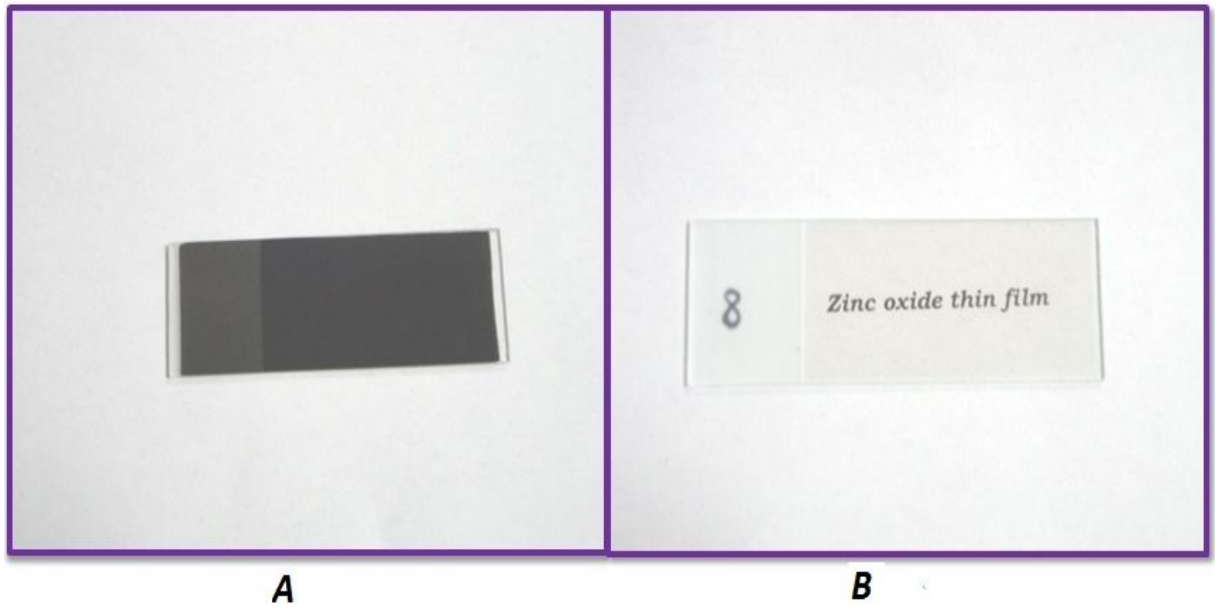


Figure 2.3: Appearance of ZnO thin film in the (A) as deposited condition and (B) after annealing

2.2 Thickness measurement methods

Thickness is defined as the distance, perpendicular to the surface, from a point on one boundary surface, through the film, to the other boundary surface. If the boundary surfaces are rough or non parallel, the thickness is not well defined. Fortunately, most vacuum deposited films have smooth and parallel, or nearly parallel, boundary surface. Resistivity and light transmittance are the examples of thin film properties which depend on film thickness. Thus to characterize films it is often necessary to measure their thickness. Although direct measurement of thickness is preferred, it is sometimes easier to measure some film parameter which is related to the thickness. The thickness is then calculated from this parameter or the parameter itself is used to control the deposition process.

Many techniques are available for the thickness measurements of the films. Some of these techniques are destructive and require special sample preparation. The precision and range of measurement vary from method to method. The measurement techniques described in this section are limited to those which are commonly applied after the substrate is removed from the vacuum system. Some of the major techniques required for thickness measurements are as follows.

A. Gravimetric method

In this method the mass of the film is determined by weighing. The thickness is then calculated, usually assuming the bulk density. If A is the area, t is the thickness, ρ is the density and m is the mass of the film then,

$$tA\rho = m \tag{2.2.1}$$

or

$$t = \frac{m}{A\rho} \tag{2.2.2}$$

Then m can be determined by weighing the substrates before and after deposition and A can be measured. By considering the bulk density thickness of the film can

be calculated with the help of equation 2.2.2. The substrates are commonly removed from the vacuum after deposition and are weighed. Because the freshly deposited film on the substrate may absorb gases such as water vapor, upon exposure to the atmospheric conditions, the change in weight due to sorption can be easily be one or two orders of magnitude greater accuracy of this method. Another limitation of the weighing method is that determination of thickness distribution on a single substrate is not possible, since an average thickness is obtained for entire area weighed.

B. Stylus

In principle this method consists only of measuring the mechanical movement of stylus as it traverses film substrate step. The stylus traverses a substrate film step, and the vertical motion of the stylus relative to the reference plane is converted to the electrical signal which is amplified and recorded on rectilinear paper. Thus, a profile graph is produced which represents a cross section of the film step as well as substrate surface irregularities.

Factors which limit the usefulness and accuracy of this instrument are:

- The diamond stylus may penetrate and scratch a groove in soft films, such as tin. This will destroy the films or introduce large error.
- Substrate roughness may introduce “noise” which causes because of uncertainty in the position of substrate and film surface.

C. Multiple beam Fizeau fringes method

This method, developed by Tolansky (Tolansky 1950), requires a sharp step in the film down to the substrate plane which can be made either by using a mechanical mask during deposition or by etching the film after deposition. A neighboring pair of light rays reflected from the film-substrate will travel different lengths and interfere by an amount dependent on the step height which is nothing but the thickness of the film itself. Both the film and substrate surfaces must be highly reflective. This is accomplished by evaporating a metal such as silver or aluminum over both film and substrate. Interference fringes are generated by placing a reflective, but

semitransparent, optically flat reference plate very close to the step region. At small distance between the two plates, multiple beam interference fringes appear with a spacing x . In the region of sharp step, fringes are shifted by a distance Δx . The thickness t of the film is then given by,

$$t = \frac{\Delta x}{x} \times \frac{\lambda}{2} \quad (2.2.3)$$

where λ is the wavelength of the light.

D. X-Ray fluorescence

When a thin film or any other target is bombarded with X-rays of proper energy, it absorbs some of these primary X-rays and emits secondary X-rays of wavelength characteristic of the target material. Thus the film becomes source for secondary X-rays. The intensity of the emerging secondary X-rays depends on the type and amount of film material, because these factors affect the amount of primary X-rays absorbed and the attenuation of the secondary X-rays as they emerge from the film.

Advantages of X-rays include;

- The technique is non destructive test.
- For most of the substrates the quantities measured are independent of the the substrate materials.
- Absolute values of mass per unit area can be obtained without comparison of standards of known thickness.

Disadvantages of this method are;

- Thickness is not obtained directly (calibration against standards or an assumption of the density of the films is necessary).
- Equipment is most expensive of any discussed.
- Thickness obtained is an average thickness of small area (Robert *et al* 1968).

In the present work thickness of the vacuum evaporated ZnO thin films obtained using both Mo and W evaporation sources were determined by gravimetric method. In this study films of thickness ranging from 200 nm to 500 nm were prepared. For structural and compositional analysis films of thickness 500 nm were used and for optical and electrical analysis films of thickness 200 nm were used .

2.3 Characterization

Vacuum evaporated ZnO thin films obtained in the present investigations were characterized using appropriate techniques to evaluate the physical properties like structure, composition, optical and electrical properties. The details of different instruments, techniques, procedures and principles used for this purpose are given in the following section.

2.3.1 Structural characterization

The microscopic properties of a material whether bulk or thin film form are determined by the arrangement of atoms or molecules in the material. Most of the solid materials have regular and periodic arrangement of atoms, or in other words a crystalline structure. Since the crystal structure of a material plays very important role in deciding its physical, optical and electrical properties, a thorough investigation of the crystal structure is highly desirable in material characterization. The crystal structure of thin films largely depend on the deposition conditions and in case of vacuum deposition even the composition of the film is affected by them. The structure and composition of the films further affect their optical and electrical properties. Hence it is also necessary to understand the influence of various deposition parameters on the structure and composition of the films. Besides, crystal structure and composition, the study of surface topography of the films is also of considerable interest. High magnification images of the film surface may provide information about the presence of any impurities or holes in the film.

A. X-ray diffraction technique

For most of the solids crystalline state is natural one since the energy of a regular arrangement of atoms is less than that of regular packing of atoms. However when atoms are not given an opportunity to properly arrange themselves by inhibiting their mobility, amorphous materials may be formed. This situation is frequently encountered during deposition of thin films. Due to the finite rate of deposition and limited mobility of atoms impinging on the substrate the resultant film may often

become amorphous. In the polycrystalline state the film contains a large number of small crystals which are often referred as grains. These grains are randomly oriented. The size of the grains may be controlled to some extent by varying the deposition parameters and post deposition heat treatment. Except for epitaxial techniques, almost all deposition techniques produce either polycrystalline or amorphous films.

X-ray diffraction is a versatile, non destructive technique that reveals detailed information about the crystallographic structure and hence chemical composition of natural and manufactured materials. From a powder diffractogram, important information about the crystallographic structure of the phase(s) present in the sample can be detected. A crystal lattice is a regular three dimensional distribution of atoms in space. These are arranged so that they form a series of parallel planes separated from one another by a distance “d” which varies according to the nature of the material.

Figure 2.4 shows the X-ray diffraction arrangement used in the present study. This consists of an X-ray tube and detector. These are positioned so that the focal spot of the source, the center orienter system and center of the detector aperture all lie in the plane accurately perpendicular to the 2θ axis. The detector mounted on 2θ circular scale, moves around the specimen at a speed of $2\theta^\circ/\text{min}$ while the sample moves θ°/min . In this way the incident and diffracted beams always make equal angles with specimen surface. With the goniostat (orienter), the specimen could also be tilted through ϕ , χ angles, to bring the diffraction beam in to the horizontal plane. The axes of the rotation ϕ and χ intersect at a known point. If the X- ray beam is made to strike the specimen at this point the crystal will not be displaced from the beam during tilting. The wavelength is controlled by using a characteristics line of the chosen target material and the absorption edge of a specific filter material.

In addition to the elements described above, the complete diffractometer normally includes a scaler for counting the pulses from the detector and usually a rate meter, which smooths the pulse to a steady current, so that the average intensity can be read on a meter or fed to a chart according to the continuous scanning of a pattern.

In the present investigation we have used JEOL X- ray diffractometer with $\text{CuK}\alpha$ radiation (1.54056 \AA) in $2\theta^\circ$ range of 20° to 80° . The scanning rate was maintained to be $1^\circ/\text{min}$.

B. Scanning electron microscopy (SEM)

SEM provides a convenient method for studying surface structure and exploring certain material vibrations. It is also capable of examining very small objects. The SEM images have resolutions of the order of few tens of nanometer. The studies provide the nature of the surface (about the uniformity, smoothness and cracks) and the nature of the grains (shape, particulate, interconnected crystallites and the grain size). It can be used to examine thick samples. Scanned images are particularly useful for examining the morphology of metal alloys, thin films, nano structures and crystalline materials.

The important feature of SEM image is the three dimensional information of the samples. The samples can be focused to the large depth. The convenience of the SEM also lies in the large working distance between the field lens and sample surface. The probe size available in the specimen is controlled by the diameter of the final aperture which determines the depth of the field of SEM. The large depth of the field associated with SEM image is due to small convergence angle at the specimen which is smaller than the corresponding angle in optical instruments. A very large value of the depth field is required for high resolution and high magnification of SEM images of rough surface. It provides much information of the specimen than that could be obtained from any other technique if depth of the focus is high.

The types of signals that can be used in SEM include secondary electrons, back scattered electrons, characteristic X-rays and light emission (cathodo-luminescence). The signals come from the beam of electrons scattering, striking the surface of the specimen and interacting with the sample at or near its surface.

In its primary detection mode, upon secondary electron imaging, the SEM can produce very high resolution image of a sample surface, revealing details about

1 to 5 nm in size. Due to the way these images are created, SEM micrographs have a very large depth of focus yielding a characteristic three dimensional appearance useful for understanding the surface structure of a sample. Characteristic X- rays are the second most common imaging mode for an SEM. X- rays are emitted when the electron beam removes an inner shell electron from the sample, causing higher energy electron to fill the shell and give off energy. These characteristic X- rays are used to identify the elemental composition of the sample.

Scanned images are particularly useful for examining the morphology of the metal alloy, thin film samples and crystalline materials. JEOL model 6380 SEM which is capable of taking highly magnified pictures of solid, dry conducting and non conducting which make up metallurgical, biological and chemical samples has been used in the present investigation.

i. Scanning process and image formation

Figure 2.5 shows the schematic diagram of scanning electron microscope. In a typical SEM, electrons are thermionically emitted from a tungsten filament cathode and are accelerated towards anode. Tungsten is normally used in thermionic electron guns because it has the highest melting point and lowest vapor pressure among all metals, thereby allowing it to be heated for electron emission. Other electron sources include (LaB₆) cathode which can be used in the place of standard tungsten filament in SEM if the vacuum system is upgraded. Electrons can also be emitted using field emission gun (FEG) which may be of the cold cathode type or thermally assisted Schottky type.

The electron beam which typically has an energy ranging from a few hundred eV to 40 keV is focused by one or two condenser lenses into a beam with very fine focal spot sized 0.4 nm and 5 nm. The beam passes through pairs of scanning coils or pairs of deflector plates in the electron column, typically in the final lens, which deflects the beam horizontally and vertically, so that it scans in a raster fashion over a rectangular area of the sample surface.

When the primary electron beam interact with the sample, the electrons lose energy by repeated scattering and absorption within a tear drop volume of the specimen known as the interaction volume, which extends from less than 100 nm to around 5 μm in to the surface. The size of the interaction volume depends on the electron landing energy, the atomic number of the specimen and the specimen density. The energy exchange between the electron beam and the sample results in the reflection of high energy electrons by elastic scattering, emission of secondary electrons by inelastic scattering and the emission of electromagnetic radiation which can be detected to produce a image as described below.

Electronic devices are used to detect and amplify the signals and display them as an image on a cathode ray tube in which the raster scanning is synchronized with that of the microscope. The image displayed is therefore distribution map of the intensity of the signal being emitted from the scanned area of the specimen. The image may be captured by photography from high resolution cathode ray tube. But in modern machines is digitally captured and displayed on computer monitor.

ii. Magnification

Magnification in SEM can be controlled over a range of about 5 orders of magnitude from 25X to 250,000X or more. Unlike optical and transmission electron microscope, image magnification in the SEM is not function of the power of the objective lens. SEMs may have condenser and objective lenses but their function is to focus the beam to a spot, and not to image the specimen. In SEM magnification results from the ratio of the dimensions of the raster on the specimen and rather raster on the display device. Assuming that the display screen has a fixed size, higher magnification results from reducing the size of the raster on the specimen, and vice versa. Magnification is therefore controlled by the current supplied to the x, y scanning coils, and not by objective lens power.

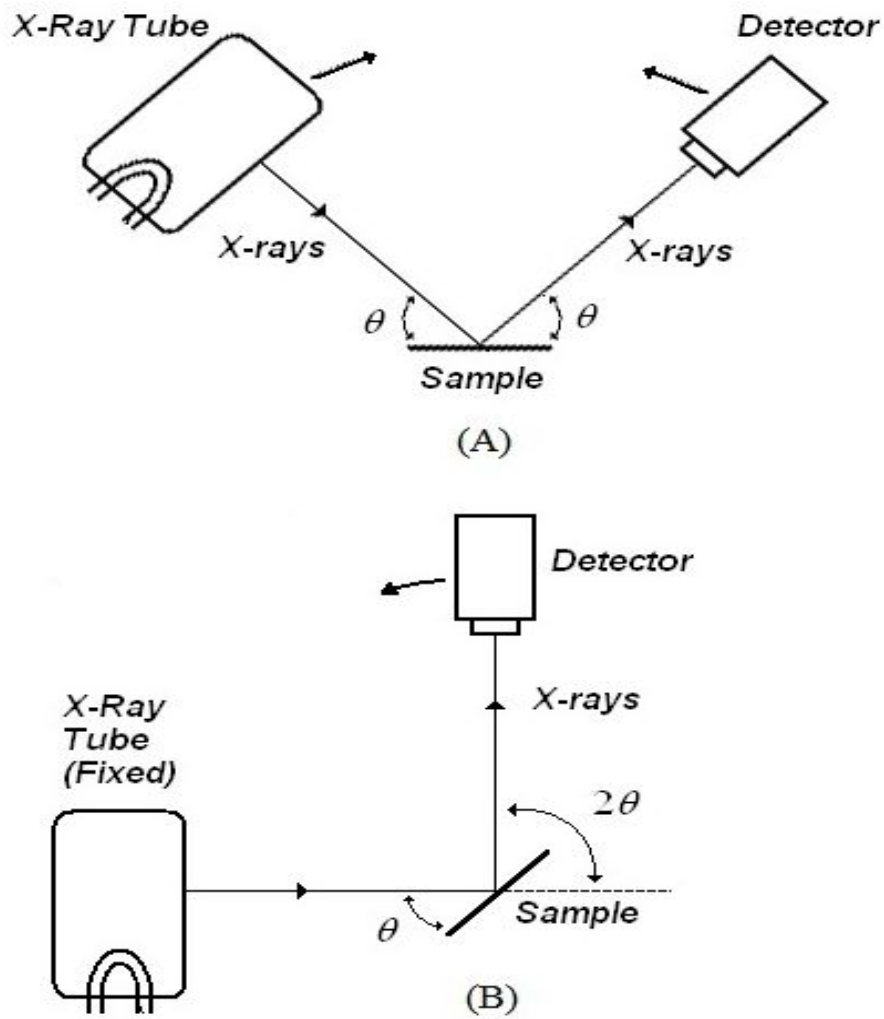


Figure 2.4: Schematic representation of X-Ray diffractometers: (A) $\theta - \theta$ - type (b) $\theta - 2\theta$ type

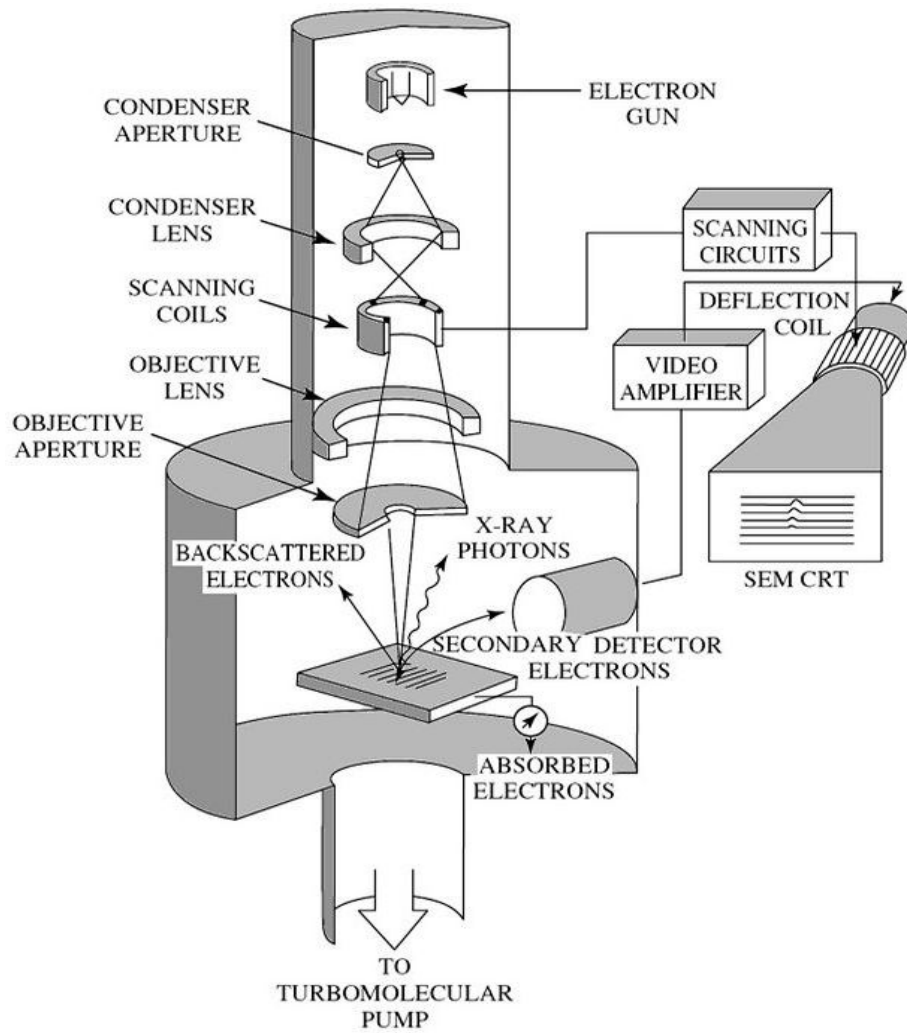


Figure 2.5: Schematic diagram of scanning electron microscope *Ref: Schroder (2005)*

2.3.2 Compositional characterization

A. Energy dispersive X- ray analysis (EDS/EDAX)

It is an analytical technique used for the elemental analysis or chemical characterization of the sample. As a type of spectroscopy, it relies on the investigation of samples through interaction between electromagnetic radiation and matter, analyzing X-rays emitted by the matter in response to being hit with the charged particles. Its characterization capabilities are due in large part to the fundamental principle that each element has a unique atomic structure allowing x-rays that are characteristics of an elements atomic structure to be identified uniquely from each other.

To stimulate the emission of characteristic X-rays from a specimen a high energy beam of charged particles such as electrons or protons or a beam of X-rays is focused on to a sample being studied. At rest an atom within the sample contains ground state (or unexcited) electrons in discrete energy levels or electrons bound to the nucleus. The incident beam may excite an electron in an inner shell, ejecting it from the shell while creating vacancy where the electron was. An electron from an outer, higher energy shell then fills the vacancy, and the difference in energy between the higher energy shell and lower energy shell may be released in the form of X-ray. The number and energy of the X-ray photon emitted from a specimen can be measured by an energy dispersive spectrometer. As the energy of X-rays is the characteristic of the difference in energy between two shells, and of the atomic structure of the element from which they were emitted, this allows the elemental composition of the specimen to be measured.

The set of X-rays emitted from these electron interactions is the characteristic with respect to both energy and wavelength for each element.

The energy and wavelength are related by the equation

$$\lambda = \frac{12.396}{E} \quad (2.3.1)$$

where λ is the wavelength in angstroms and E is the energy in keV.

There are two types of spectrometers used in electron micro-probes, The wavelength dispersive or electron probe microanalysis spectrometer (WDS/EPMA) or energy dispersive spectrometer (EDS/EDAX). The WDS is used for highly qualitative analysis. The EDAX (or EDS) utilizes solid state detector to analysis all X-ray photon energies simultaneously. Thus EDAX is a method of elemental analysis by scanning bulk scattered X-rays from high voltage electron bombardment usually in SEM characteristic emission peaks which enables identification of most of the elements. This can be made quantitative by comparing with standards.

B. X-ray photoelectron spectroscopy (XPS)

X-ray photoelectron spectroscopy is one of a number of surface analytical techniques that bombard the sample with photons, electrons or ions in order to excite the emission of photons, electrons or ions. It is a quantitative technique in the sense that the number of electrons recorded for a given transition is proportional to the number of atoms at the surface. Instead of impinging the sample surface with an electron beam, XPS utilizes a monoenergetic X-ray beam to cause electrons to be ejected, usually two to twenty atomic layers deep. In XPS, the sample is irradiated with low-energy (~ 1.5 keV) X-rays, in order to provoke the photoelectric effect. The energy spectrum of the emitted photoelectrons is determined by means of a high-resolution electron spectrometer. The sample analysis is conducted in a vacuum chamber, under the best vacuum conditions achievable, typically $\sim 10^{-10}$ torr. This facilitates the transmission of the photoelectrons to the analyzer but more importantly minimizes the re-contamination rate of a freshly cleaned sample. This is crucial because XPS is very surface-sensitive, with a typical sampling depth of only a few nanometers.

In practice, however, to produce accurate atomic concentrations from XPS spectra is not straight forward. The precision of the intensities measured using XPS is not in doubt; that is intensities measured from similar samples are repeatable to good precision. What may be doubtful are results reporting to be atomic concentrations for the elements at the surface. An accuracy of 10% is typically quoted for routinely performed XPS atomic concentrations. For specific carefully performed and characterized measurements better accuracy is possible, but for quantification based on standard relative sensitivity factors, precision is achieved not accuracy. Since many problems involve monitoring changes in samples, the precision of XPS makes the technique very powerful.

The basic mechanism behind an XPS instrument is illustrated in figure 2.6. Photons of a specific energy are used to excite the electronic states of atoms below the surface of the sample. Electrons ejected from the surface are energy filtered via a hemispherical analyzer (HSA) before the intensity for a defined energy is recorded by a detector. Since core level electrons in solid-state atoms are quantized, the resulting

energy spectra exhibit resonance peaks characteristic of the electronic structure for atoms at the sample surface. While the x-rays may penetrate deep into the sample, the escape depth of the ejected electrons is limited. That is, for energies around 1400 eV, ejected electrons from depths greater than 10 nm have a low probability of leaving the surface without undergoing an energy loss event, and therefore contribute to the background signal rather than well defined primary photoelectric peaks.

In principle, the energies of the photoelectric lines are well defined in terms of the binding energy of the electronic states of atoms. Further, the chemical environment of the atoms at the surface result in well defined energy shifts to the peak energies. In the case of conducting samples, for which the detected electron energies can be referenced to the Fermi energy of the spectrometer, an absolute energy scale can be established, thus aiding the identification of species.

When an electron is emitted from the initial state due to the absorption of a photon, the electrons emerge with kinetic energies characteristic of the final states available to the electronic system and therefore XPS peaks represent the excitation energies open to the final states. Since these final states include electronic sub-shells with unpaired electrons, the spin-orbit coupling of the orbital and spin angular momentum results in the splitting of the energy levels which were otherwise identical in terms of common principal and orbital angular momentum. Thus, instead of a single energy level for a final state, the final state splits into two states referred to in XPS as doublet pairs.

To differentiate between these XPS peaks, labels are assigned to the peaks based on the hole in the final state electronic configuration. Since these final states, even when split by spin-orbit interactions, are still degenerate in the sense that more than one electronic state results in the same energy for the system, three quantum numbers are sufficient to identify the final state for the X-ray excited system. Specifying the three quantum numbers in the format nl_j , both uniquely identifies the transition responsible for a peak in the spectrum and offers information regarding the degeneracy of the electronic state involved. The relative intensity of these doublet pair

peaks linked by the quantum numbers nl is determined from the $j = l \pm \frac{1}{2}$ quantum number. Doublet peaks appear with intensities in the ratio $2j_1+1 : 2j_2+1$. Thus p-orbital doublet peaks are assigned j quantum numbers $1/2$ and $3/2$ and appear with relative intensities in the ratio $1:2$. Similar intensity ratios and differing energy separations are common features of doublet peaks in XPS spectra. Final states with s symmetry do not appear as doublets, e.g. O 1s (CASA-XPS 2011) .

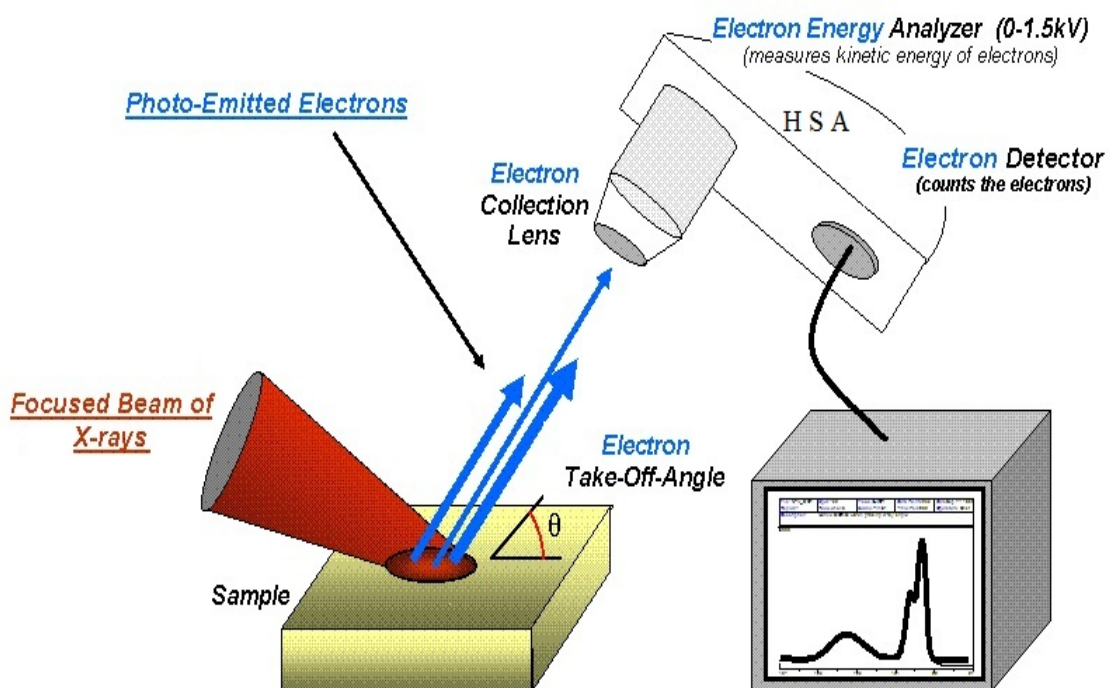


Figure 2.6: Schematic diagram of a XPS mechanism

2.3.3 Optical characterization

One of the simplest methods to analyze the band structure of semiconductor materials is the study of their interaction with light. When light falls on a material some part of the incident light may get reflected, some part may get absorbed and the remaining part may get transmitted. The amount of reflected, transmitted or absorbed light energy depends on the energy of the incident photons and the band structure of the material. The transmission or absorption measurements would, therefore, reveal valuable information about the band structure of the material. In general the optical absorption in a semiconductor may take place due to several mechanisms and each of these contributes to total absorption (Yokobi 2004, Mishra and Singh 2008).

These mechanisms include

- fundamental absorption process (band-to-band)
- absorption due to dopants and imperfections
- absorption due to intraband transitions
- free carrier absorption.

The most important among all the above mechanisms is the fundamental absorption process resulting from band-to-band transition. The remaining mechanisms are significant only when the incident light energy is less than the band gap energy of the material. The absorption due to dopants occurs because of the transitions from donor level to conduction band or valence band to acceptor level. These transitions usually result in the absorption in far-infrared region. Absorption may also occur due to the imperfections (such as point defects, impurities, grain boundaries etc) that introduce localized energy levels in the energy gap of a semiconductor. In this case, transitions may occur from occupied imperfection levels to the conduction band or from the valence band to the unoccupied imperfection levels. The intraband transitions take place, in many semiconductors, due to the transitions between light-hole and heavy-hole bands in the valence band while free carrier absorption results from the transitions to higher energy levels within the same energy band.

In the fundamental absorption process, the incident photon excites an electron from valence band to conduction band. During such transition both energy and momentum must be conserved. The conservation of energy implies that the final energy E_f of the electron must be equal to the sum of initial energy E_i and photon energy $h\nu$. i.e.,

$$E_f = E_i + h\nu \quad (2.3.2)$$

Since the minimum energy difference between conduction band and the valence band is the bandgap energy E_g , the incident photon energy must be larger than the bandgap energy. The conservation of momentum requires the effective momentum k of the electron-photon system to be same before and after the transition. Since the k -value of the photon, given by,

$$k = \frac{2\pi}{\lambda} \quad (2.3.3)$$

is negligibly small compared to the k -value of the electron, the transition can take place only if the k -value of the electron remains same before and after the transition. Thus for the fundamental absorption process only transitions which are vertical in k are allowed as shown in figure 2.7(a).

If the minimum of the conduction band and maximum of the valence band of a semiconductor occur at the same value of k (figure 2.7(b)) then the semiconductor is said to be direct band gap semiconductor. In such semiconductors the most likely transitions are across the minimum-energy gap, between minimum of the conduction band and the maximum of the valence band. ZnO and other II-VI semiconductors are direct band gap semiconductors. If the minimum of the conduction band and maximum of the valence band do not occur at same k -value then the material is said to be indirect band gap semiconductor (figure 2.7(c)). The most widely used semiconductors Si, Ge are indirect band gap semiconductors. The band-to-band transitions in indirect band gap semiconductors essentially require the participation of phonons in order to conserve momentum. The probability of such a transition is very low and hence the optical transitions near the band edges are very weak.

The process of absorption is characterized by absorption co-efficient , which can be defined as the relative decrease in the intensity $I(h\nu)$ of the light in its path of propagation in the material.

$$\alpha = \frac{1}{I(h\nu)} \times \frac{d[I(h\nu)]}{dx} \quad (2.3.4)$$

The absorption co-efficient of a material can be determined by the transmission measurements. If I_0 is the incident light intensity, I is the transmitted light intensity, and R is the reflectivity, then transmittance $T = I/I_0$ is given by,

$$T = \frac{(1 - R)^2}{1 - R^2} \times \frac{\exp(-\alpha t)}{\exp(-2\alpha t)} \quad (2.3.5)$$

where t is the thickness of the material.

For large values of αt and negligible reflectance equation (2.3.5) reduces to,

$$T = \frac{I}{I_0} = \exp(-\alpha t) \quad (2.3.6)$$

The transmittance T is related to absorbance A by the equation,

$$A = -\ln(T) = \alpha t \quad (2.3.7)$$

Thus α can also be defined as absorbance per unit thickness.

In the case of direct band gap semiconductors, α is related to band gap energy E_g by the equation,

$$(\alpha h\nu)^2 = B(h\nu - E_g) \quad (2.3.8)$$

where B is a constant (10^4). A plot of $(\alpha h\nu)^2$ against $h\nu$, called Taucs plot, shows a linear portion; which, when extrapolated, meets the x-axis at $h\nu = E_g$.

The phenomenon of optical transmission or absorption in a thin film can be studied by the help of a spectrophotometer (Schroder 2005). For wide- bandgap materials like ZnO the absorption edge is located in the UV region of the electromagnetic spectrum. Hence a UV-Visible spectrophotometer is normally preferred for such

materials. Although many variations of UV-Visible spectrophotometers are available, the basic setup and working principle are same for all of them.

The schematic diagram of a typical UV-Visible spectrophotometer is shown in figure 2.8. The functioning of the instrument is relatively straightforward. A beam of light from a visible and/or UV light source is separated into its component wavelengths by a prism or diffraction grating. Each monochromatic beam in turn is split into two equal intensity beams by a half-mirrored device. One beam, the sample beam, passes through the film sample being studied. The other beam, the reference, passes through a reference specimen of the substrate which is used to deposit the films. The intensities of these light beams are then measured by electronic detectors and compared. The intensity of the reference beam, which should have suffered little or no light absorption, is defined as I_0 . The intensity of the sample beam is defined as I . Over a short period of time, the spectrometer automatically scans all the component wavelengths in the manner described. The ultraviolet (UV) region scanned is normally from 200 to 400 nm, and the visible portion is from 400 to 800 nm. If the sample compound does not absorb light of a given wavelength, then $I = I_0$ for that wavelength. However, if the sample compound absorbs light then I is less than I_0 . Absorption is usually presented as transmittance ($T = I/ I_0$) or absorbance ($A = \ln (I_0/I)$). If no absorption has occurred, $T = 1.0$ and $A = 0$.

Since ZnO is a well known transparent oxide in the present investigation the major priority is given to study the transmittance of obtained ZnO film. Further optical band gap of ZnO and its variation under different conditions is also studied. In the present work transmittance and absorbance measurements of ZnO thin films were carried out relative to the uncovered substrate at normal incidence in a spectral range of 250 - 850 nm using Ocean Optics Inc SD 2000 UV-VIS spectrometer .

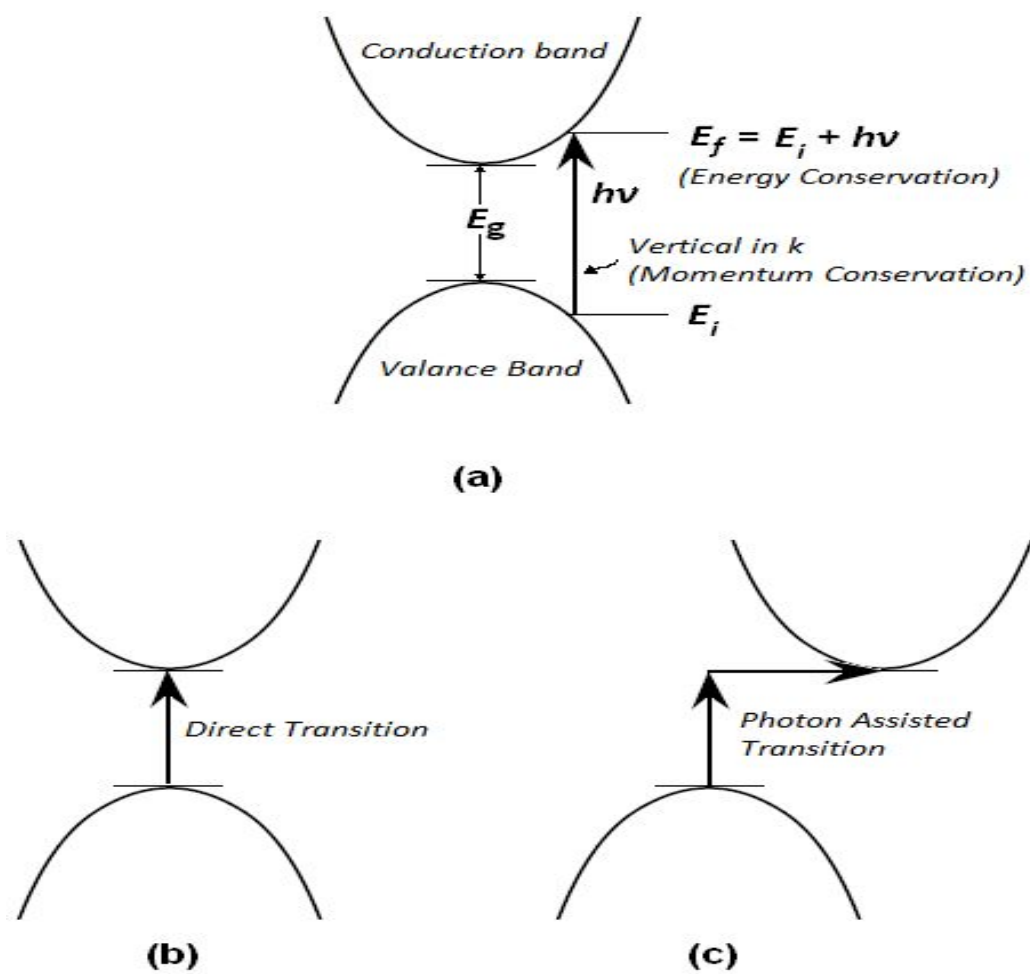


Figure 2.7: The optical absorption phenomenon: (a) Conservation of energy and momentum, (b) Transition in direct bandgap material (c) Transition in indirect bandgap material

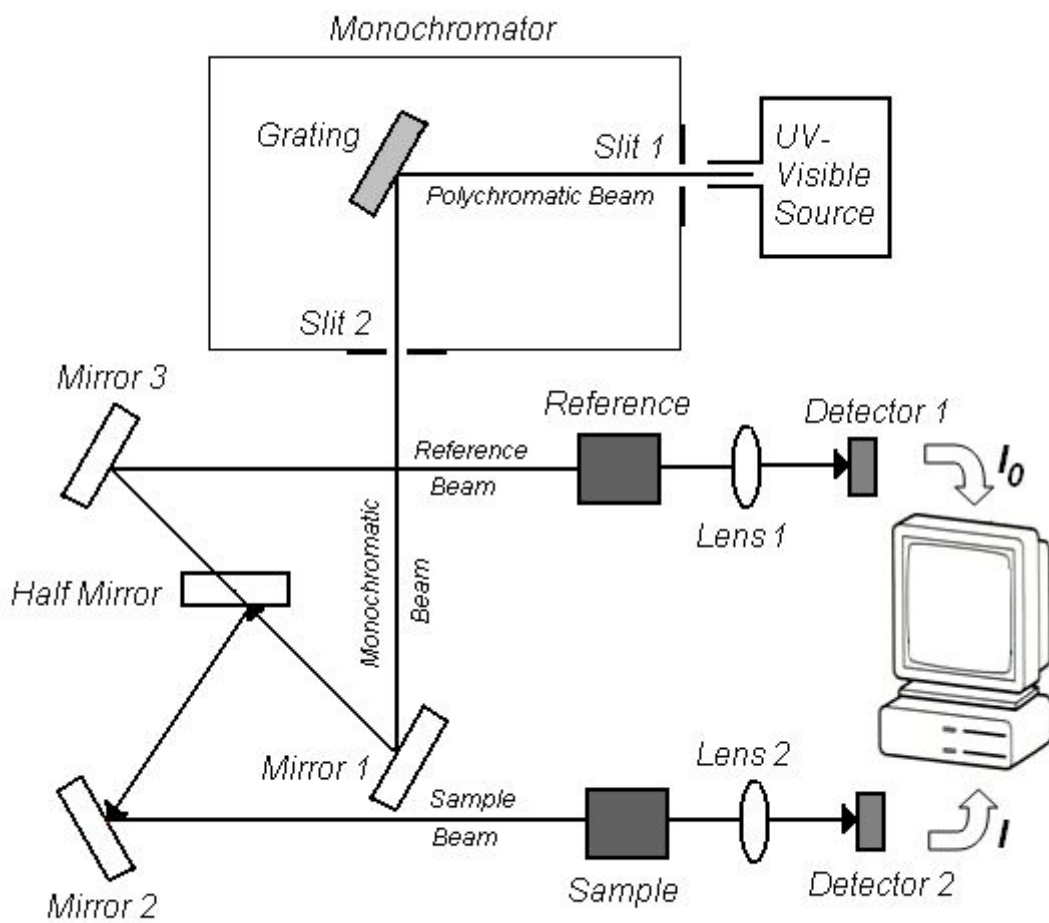


Figure 2.8: Schematic diagram of a typical spectrophotometer

2.3.4 Electrical characterization

Utilization of thin films in any sort of device fabrication essentially requires a rigorous study and thorough understanding of their electrical properties. The structure and composition of the films have a strong bearing on their electrical properties. Investigations of such correlations would not only provide a better understanding of the electrical properties of the films but also help to control and improve their performance as active devices.

The presence of donor or acceptor type impurities in a semiconductor material gives rise to the donor or acceptor levels in the forbidden energy gap of the material (Kittel 1996, Sze 2006). The impurity concentration is usually very low, compared to the atomic density of the material, and the impurities are scarcely distributed within the material. Hence the resulting impurity levels are localized only near the impurities. The donor levels are usually located near the lower edge of the conduction band and acceptor levels near the upper edge of the valence band. Electrons having sufficient energy can jump from valence band to acceptor levels producing an equal number of holes in the valence band. Similarly, the electrons can jump from donor levels to conduction band. Both these processes are limited by the impurity ionization energies. The conductivity of semiconductor material will be low at very low temperatures even if it contains donor or acceptor impurities. As the temperature increases more and more donors or acceptors get ionized, contributing either electrons to the conduction band or holes to the valence band, resulting in an increase in the electrical conductivity. This electrical conduction which is largely due to the free carriers contributed by the impurities is referred as extrinsic conduction. If the temperature is increased further then a point will be reached where all the impurities get ionized and conductivity will become independent of temperature. The extrinsic conduction is said to be saturated at this point. Beyond this point the electrical conductivity of the material will remain constant with the increase in temperature until the intrinsic conduction, due to the electrons jumping from valence band to the conduction band, begins. The intrinsic conduction is limited by the forbidden energy gap, which is far higher than the activation energy, and hence takes place at relatively high temperatures. Once the intrinsic conduction begins, the electrical conductivity once again increases

sharply with the increase in temperature. The intrinsic and extrinsic conduction are not mutually exclusive, but can co-exist in the material. The extrinsic conduction dominates in the low temperature region and intrinsic conduction dominates in the high temperature region.

Electrical contacts are necessary to connect a semiconductor device to the other circuit elements such as other semiconductor devices, voltage or current sources etc. Low resistance, stable contacts are critical for the good, long term and reliable performance of a semiconductor device. The metal-semiconductor contacts are most common although semiconductor-semiconductor contacts are also used in some devices. In most of the semiconductor devices it is highly desirable for the metal-semiconductor contact to have a linear I-V behavior. Such type of contact is called ohmic contact. If the I-V curve is non-linear and asymmetric then the contact is said to be blocking or rectifying contact. The contacts must be able to supply the necessary device current, and the voltage drop across the contact should be small compared to the voltage drops across the active device regions. An ohmic contact should not degrade the device to any significant extent, and it should not inject minority carriers.

The behavior of metal-semiconductor interface was well explained by Schottky (Rhoderick 1988). Before the formation of a contact the metal and semiconductor may have different Fermi levels and hence different work functions denoted by Φ_m and Φ_s respectively. When the two materials are placed in contact, electrons will flow from the one with the lower work function until the Fermi levels equilibrate. As a result, the material with the lower work function will take on a slight positive charge while that with the higher work function will become slightly negative. This will result in an electrostatic potential called the built-in field designated by V_{bi} . The built-in field causes band-bending in the semiconductor near the junction. In order to move from semiconductor to metal region, or vice versa, the carriers must have sufficient energy to surmount the barrier. This barrier- surmounting energy Φ_B is the sum of the built-in potential and the offset between the Fermi level and the conduction band. For n-type semiconductors Φ_B is given by

$$\Phi_B = \Phi_m - \chi_S \quad (2.3.9)$$

where χ_S is the electron affinity of the semiconductor.

For p-type semiconductor,

$$\Phi_B = E_g - (\Phi_m - \chi_S) \quad (2.3.10)$$

where E_g is the bandgap energy of semiconductor material. The above expressions imply that the metals with high work functions form the best contacts to p-type semiconductors while those with low work functions form the best contacts to n-type semiconductors. However the above prediction is not always applicable. It has been observed that in many semiconductor materials, like Si, Ge, GaAs etc., the barrier height is almost independent of the work function of the metal. This behavior can be attributed to Fermi level pinning. Thus it is difficult to engineer the barrier height at the metal-contact region only by selecting the suitable metal. One will have to consider other options such as doping. If the semiconductor is intrinsic or very lightly doped, the excitation of the carriers over the barrier at the contact region may have to take place entirely due to thermionic emission. However in the case of heavily doped semiconductors the space charge region at the junction will be very narrow and the carriers can easily tunnel through the barrier.

The electrical characterization of ZnO films initiated with the identification of a suitable ohmic contact material. The contacts for ZnO thin films obtained during both molybdenum and tungsten boat were made by using silver on ZnO films by vacuum deposition technique. Molybdenum boats were used to evaporate pure metallic silver. Three different structures, namely bridge, planar and sandwich structure, were used to make contacts as shown in figure 2.9. The sandwich structure is particularly useful when the film is highly resistive. Bridge and planar structures, on the other hand, are simple and easy to fabricate. The ZnO films in the present study had reasonably good conductivity. Hence planar structures were used in most of the cases. The use of sandwich structure was restricted only to highly resistive films. Unless otherwise mentioned all measurements were obtained in dark condition in order to avoid light induced conduction.

The study of variation of film resistance with ambient temperature was performed by heating the film in a hot air oven and measuring the resistance at different temperatures. A copper-constantin thermocouple was placed behind the glass substrate for the measurement of ambient temperature. Resistance of the film was noted at different temperature. Then a plot of $\log(R)$ verses reciprocal of the temperature is used to estimate the activation energy of the carriers in the sample under study. The plots show two distinct region. Generally the low temperature region corresponds to the extrinsic conduction where as the high temperature region corresponds to intrinsic conduction in the film. The thermal activation energy was determined by the slope of the plots in the extrinsic region.

The conventional hot-probe technique provides a simple yet efficient way to distinguish between n-type and p-type semiconductors using a heated probe and a standard multimeter. The experiment is done by attaching a cold probe and a hot probe to a semiconductor surface. Both probes are wired to a sensitive electrometer. The hot probe is connected to the positive terminal of the meter, while cold probe is connected to the negative terminal as shown in the figure 2.10. While applying the cold and hot probes to the n-type semiconductor positive voltage readout is obtained in the meter whereas, for p-type semiconductor negative voltage is obtained. A simple explanation for this experiment is that the the thermally excited majority free charged carriers are translated within the semiconductors from the hot probe to the cold probe. The mechanism for this motion with in the semiconductor is of diffusion type since the material is uniformly doped. These translated majority charge carriers define the electrical potential sign of measured current in the multimeter (Golan *et al* 2006).

In the present work the computer assisted high precision Keithley 2000 Multimeter and Keithley 2400 Source meter were used for electrical measurements (figure 2.11.).

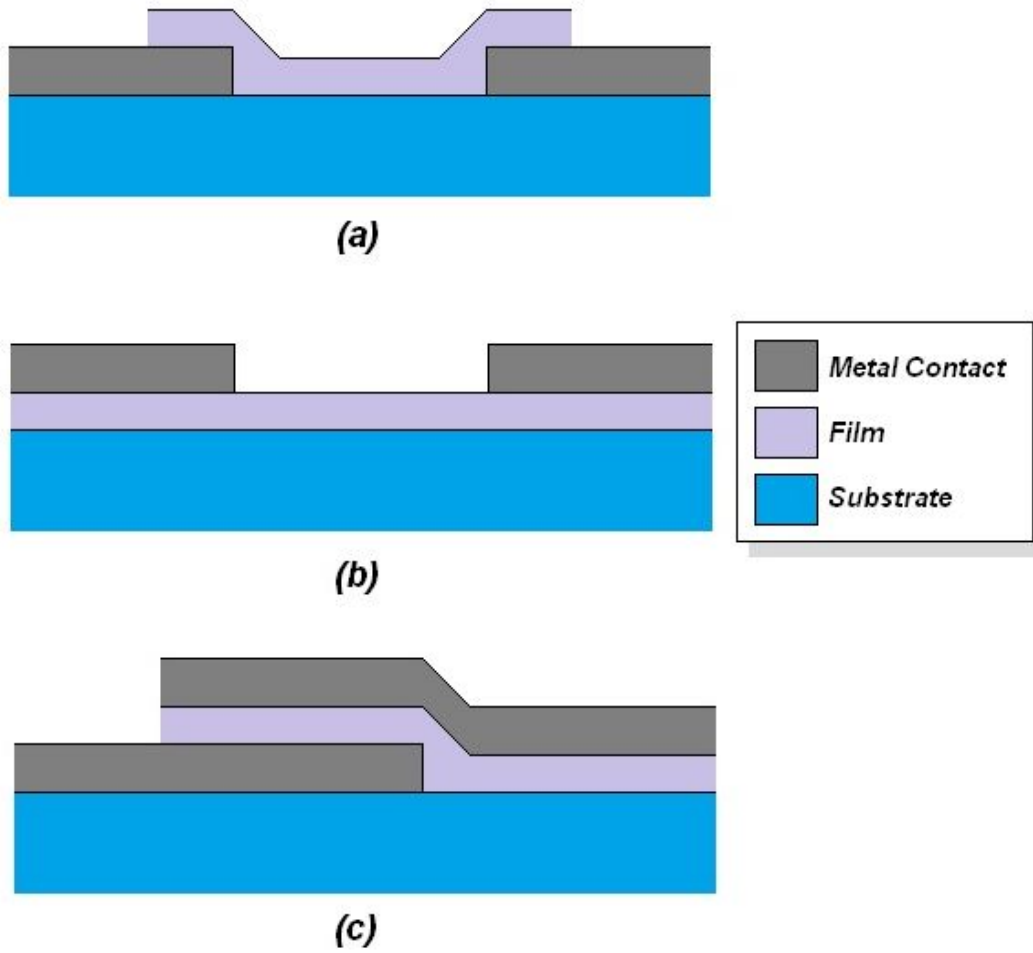


Figure 2.9: Three different structures used for making contacts to thin films. (a) Bridge structure, (b) Planar structure and (c) sandwich Structure

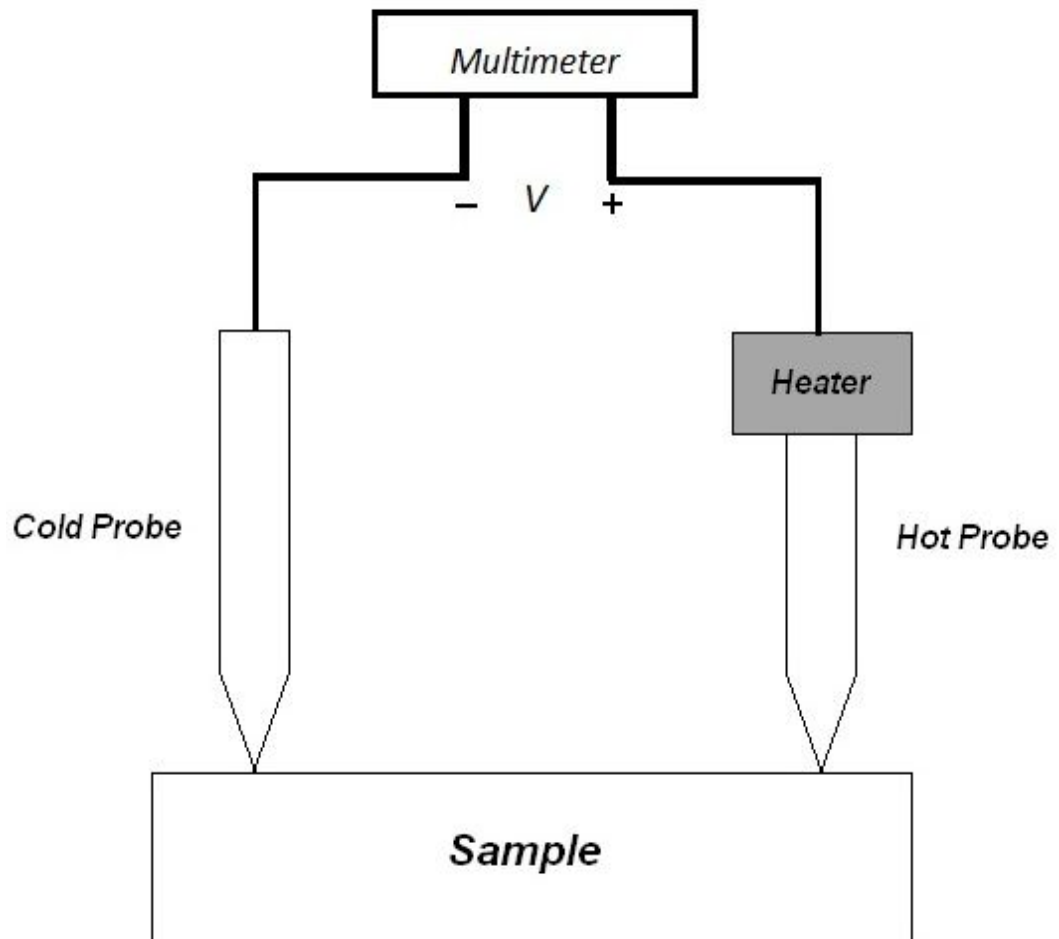


Figure 2.10: Schematic diagram of the experimental setup for hot probe technique



Figure 2.11: Keithley Multimeter (2000) and Keithley Sourcemeters (2400) used in the present study

Chapter 3

Effect of evaporation source materials

It is well known fact that the characteristics of thin films depend on the factors like deposition technique, deposition parameters/ conditions and post deposition heat treatment. Previous reports on the deposition of ZnO thin films by thermal evaporation technique have suggested molybdenum (Mo) and tungsten (W) as the suitable evaporation sources (boats) for the evaporation of pure ZnO powder (Aida *et al* 2006, Aly *et al* 2001, Bouhssira *et al* 2006). In the present investigation ZnO thin films were obtained by thermal evaporation technique using both Mo and W sources. Properties of these films were investigated by structural, compositional and optical characterizations and based on the results obtained suitable evaporation source for the deposition of ZnO thin films is selected to proceed further in the study.

In this study ZnO films of thickness 500 nm were obtained by using W and Mo evaporation sources. As mentioned in the section 2.1 ZnO films obtained using Mo and W as evaporation sources are found to be dark brown in color in the as deposited condition. These films were annealed at 400°C for 4 hours in the presence of atmospheric air. After annealing, films deposited using W source showed average visible region transmittance of up to 75%. Whereas the transmittance of films deposited using Mo source improved only up to 35%. These films on annealing at 500 °C for 4 hours showed an average transmittance of up to 70% as shown in figures

3.7 and 3.8. The structural compositional and optical characterization of these films investigated to know the effect of evaporating sources on the properties of thermally evaporated ZnO thin films is reported in the present section.

3.1 X-ray diffraction study

Most of the properties of thin films, such as physical, optical and electrical properties depend on the structure and composition of the film. Therefore complete understanding of the structural and compositional characterization of material is essential for any device application. The term structure encompasses a variety of concepts, which describe the arrangements of the building block of materials. On an atomic scale the crystal structure is defined by the crystallographic data of the unit cell. Structure of deposited films may completely differ from that of its bulk. Obviously one has to know whether the deposited film is amorphous, polycrystalline or single crystalline. The characteristics of films also depend on the orientation of the films with respect to substrate and chemical composition of the films.

In the present investigation ZnO films were characterized by X-ray diffraction with Cu-K $_{\alpha}$ radiation using JEOL Diffractometer. In order to verify the crystal structure of ZnO thin films the X-ray diffraction pattern was studied in the 2θ range of 20° to 80° . XRD pattern of ZnO thin films obtained using both W and Mo sources did not show any peak in this θ range in the as deposited condition as well as after annealing. This confirms the amorphous nature of films. The typical XRD pattern of ZnO thin films is shown in figure 3.1. It has been observed that ZnO thin films obtained using both Mo and W sources are amorphous and films did not transfer to crystalline state even after annealing.

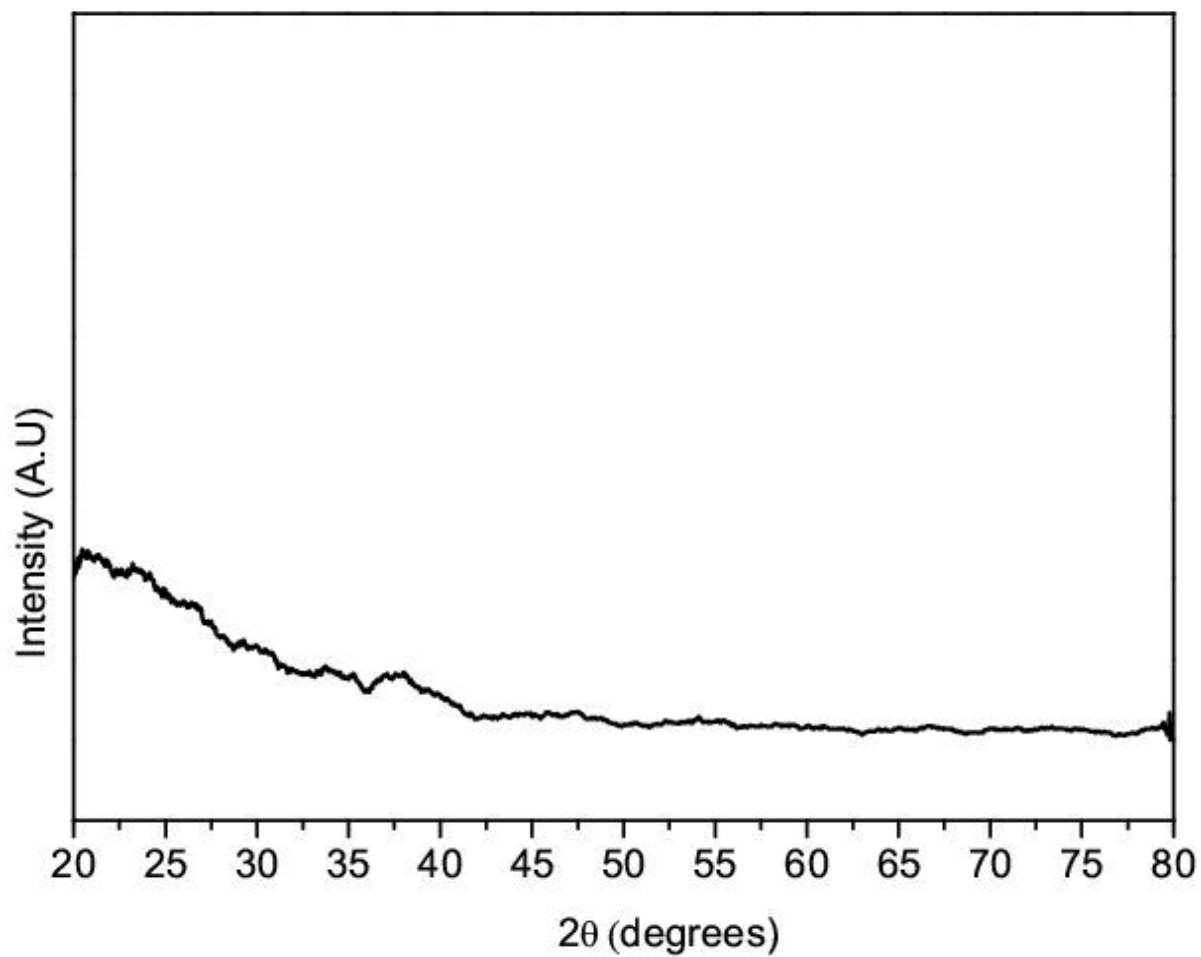
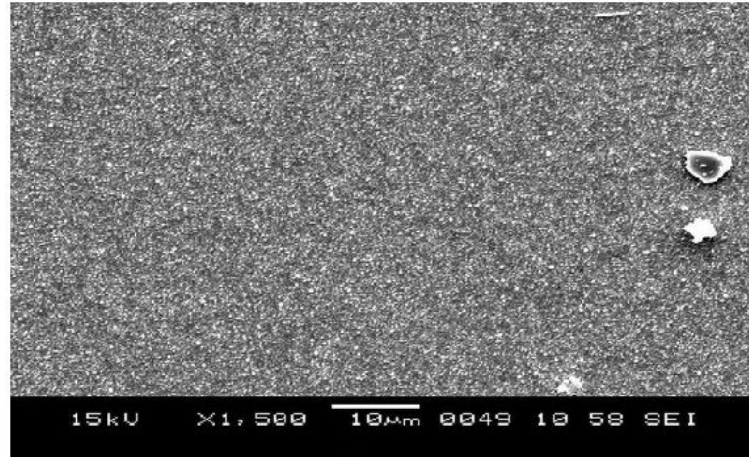


Figure 3.1: Typical XRD pattern of thermally evaporated ZnO thin films

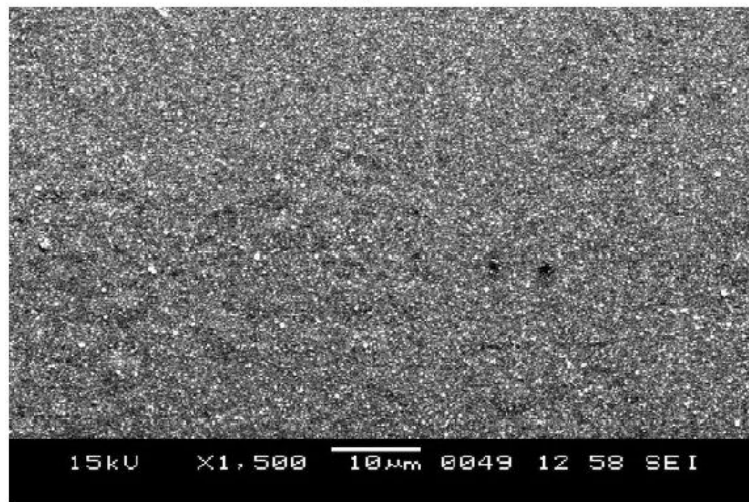
3.2 Scanning electron microscopy analysis

The surface properties of ZnO thin films obtained by using both Mo and W evaporation sources were investigated using JEOL JSM 6380 scanning electron microscope operated at 15 kV. Films were coated with gold by JEOL sputter coating unit with average coating thickness of 10 nm. Images were recorded at a magnification of 1500X.

SEM is a promising technique for the topography study of samples, as it provides valuable information regarding the growth mechanism, shape and size of particles or grains. Scanning electron micrograph of ZnO thin films deposited on glass substrates using both W and Mo evaporation sources in the as deposited condition and after annealing are shown in the figure 3.2 and 3.3 respectively. Films are observed to be uniform and well coated. The film surface in both the cases found to be smooth and continuous with out pinholes. These amorphous films with flat and smooth surface are well suited for the application of flat panel displays due to their low internal stress (Shigesato, 2010).

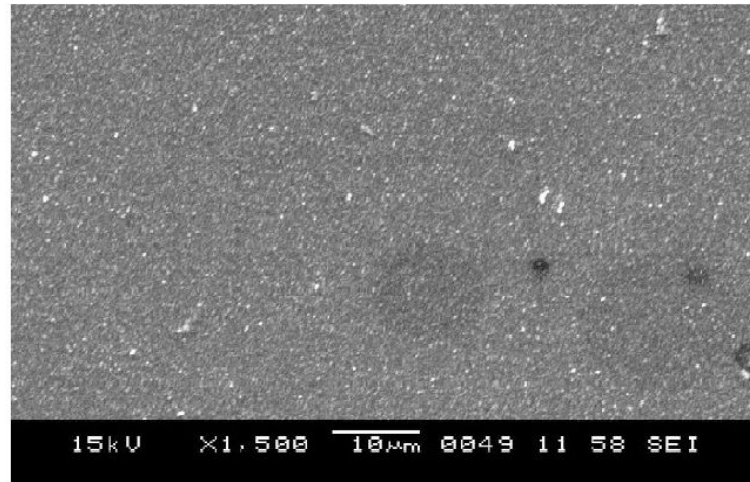


A

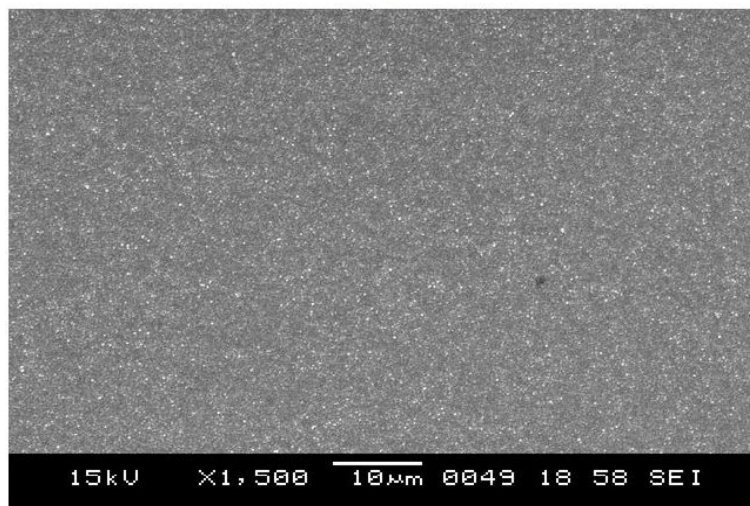


B

Figure 3.2: SEM image of ZnO thin films deposited by W source in the (A) as deposited condition and (B) after annealing at 400°C for 4 hours



A



B

Figure 3.3: SEM image of ZnO thin films deposited using Mo source in the (A) as deposited condition and (B) after annealing at 400°C for 4 hours

3.3 EDAX analysis

The compositional analysis of ZnO films obtained using W and Mo evaporation sources were studied using EDAX technique. Figures 3.4 - 3.6 shows the EDAX spectrum of ZnO thin films deposited using Mo and W sources in the as deposited condition and after annealing at different temperature. These spectra in all the cases confirm the presence of evaporation source atoms in the ZnO films. It is noted that the elements which are lighter than Na atom can not be detected by EDAX technique. Hence there are some errors in detecting the quantity of oxygen in the film.

In the as deposited condition ZnO films deposited using Mo source contained 18% of Mo atoms where as ZnO films deposited using W source contained 3% of W atoms. This incorporation of source materials in to the film can be explained considering the vapor pressure curve of Mo and W elements (Robert *et al* 1968).

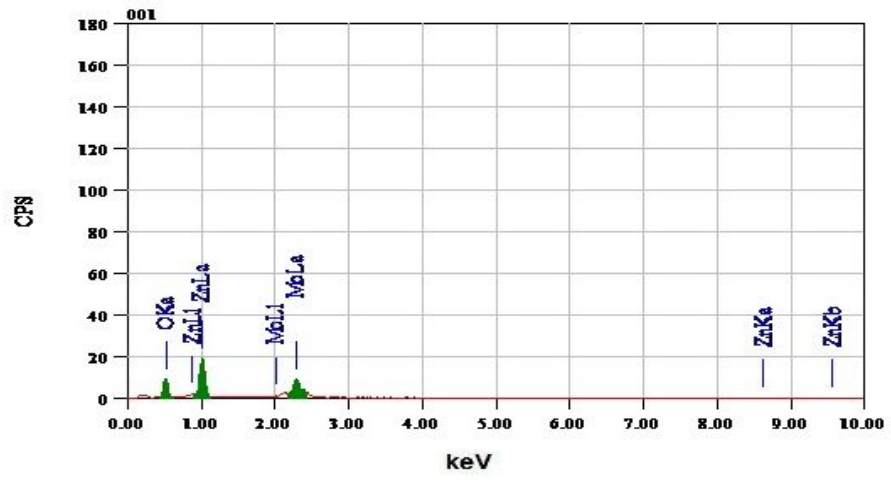
In the process of evaporation of ZnO powder a temperature of the order of 2500°C is supplied to the evaporation source which contains ZnO powder. According to vapor pressure curve of elements, at a temperature of 1900°C the vapor pressure of “Mo” element will be equal to 3×10^{-5} mbar, which is equal to the pressure maintained in the evaporation chamber. Similarly in the case of “W” element the vapor pressure will be equal to 3×10^{-5} mbar when the temperature is raised to 2400°C. Thus incorporation of these “Mo” and “W” evaporation source elements is expected in vacuum evaporated ZnO thin films. It is mentioned repeatedly that, during the evaporation of ZnO powder it decomposes in to zinc and atomic oxygen according to the kinetics of vaporization of ZnO. At temperature above 1900°C Mo atom combines with atomic oxygen to form volatile MoO. Similar conclusion can be given in the case of the incorporation of W atoms in to the films. Vapor pressure of W will be equal to 3×10^{-3} torr when its temperature is raised to 2400°C and W atom reacts with atomic oxygen to form volatile WO at a temperature higher than 2400°C (Ghoniem 1998). Since the temperature needed by the W source to evaporate is more than the temperature needed by the Mo source we find the atomic percentage of Mo in ZnO film is more compared to that of W.

When these films were annealed at different temperature, a considerable decrease in the atomic percentage of incorporated source materials was noticed. When the films deposited using Mo source were annealed at 400°C for a period of 4 hours the atomic percentage of Mo was reduced from 18% to 9.71% and on annealing these films at 500°C for 4 hours the atomic percentage of Mo was reduced to 4.16%. In the case of the films deposited using W source the atomic percentage of W was reduced from 3% to 2.5% after annealing for 4 hours at 400°C. This reduction in the atomic percentage of incorporated evaporation source atoms after annealing may be due to the re-evaporation of volatile oxides of Mo and W during annealing.

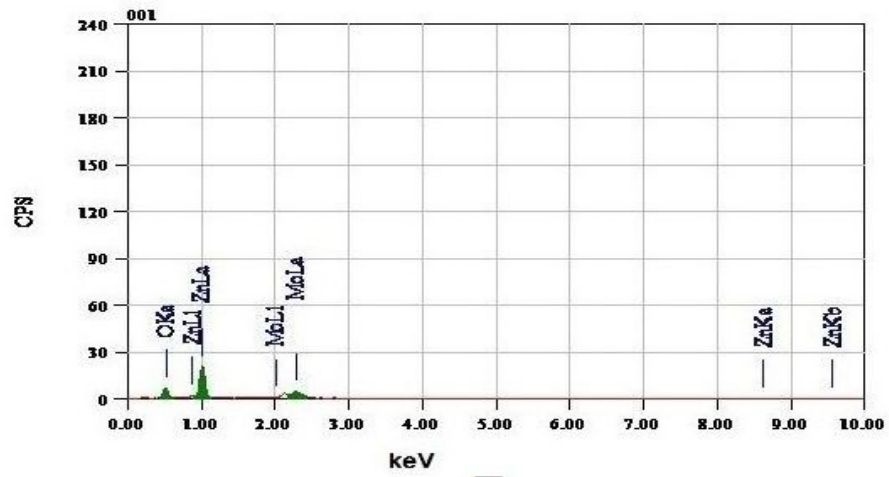
The atomic percentage of incorporated evaporation source materials in vacuum evaporated ZnO thin films and its reduction due to annealing at different temperature is summarized in table 3.1.

Table 3.1: Percentage variation of incorporated evaporation source atoms in thermally evaporated ZnO thin film with annealing

Sample	Atomic % (Mo)	Atomic % (W)
As Deposited film	18	3
After annealing at 400°C for 4 hours	9.71	2.5
After annealing at 500°C for 4 hours	4.16	—



A



B

Figure 3.4: EDAX Spectra of ZnO thin film deposited using Mo source in the (A) as deposited condition and (B) after annealing at 400°C for 4 hours

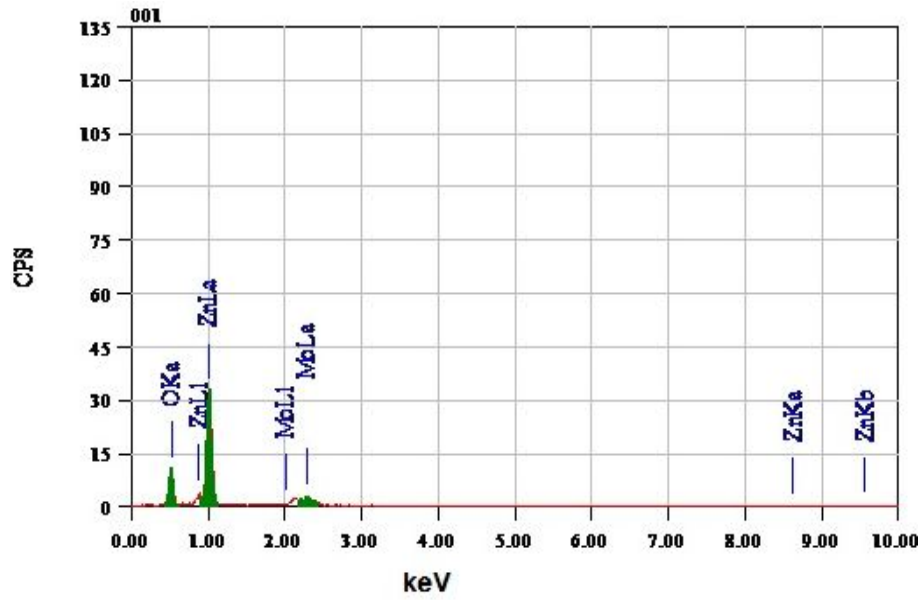


Figure 3.5: EDAX Spectrum of ZnO thin film deposited using Mo source after annealing at 500°C for 4 hours

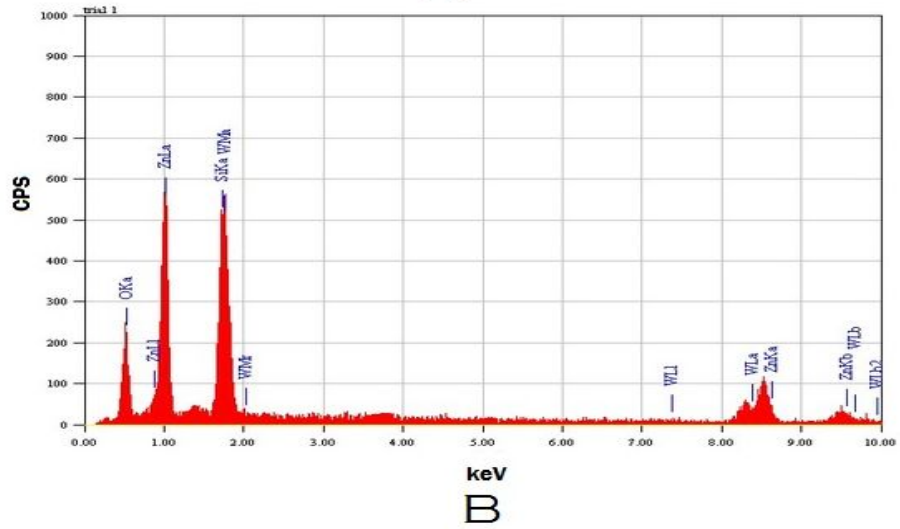
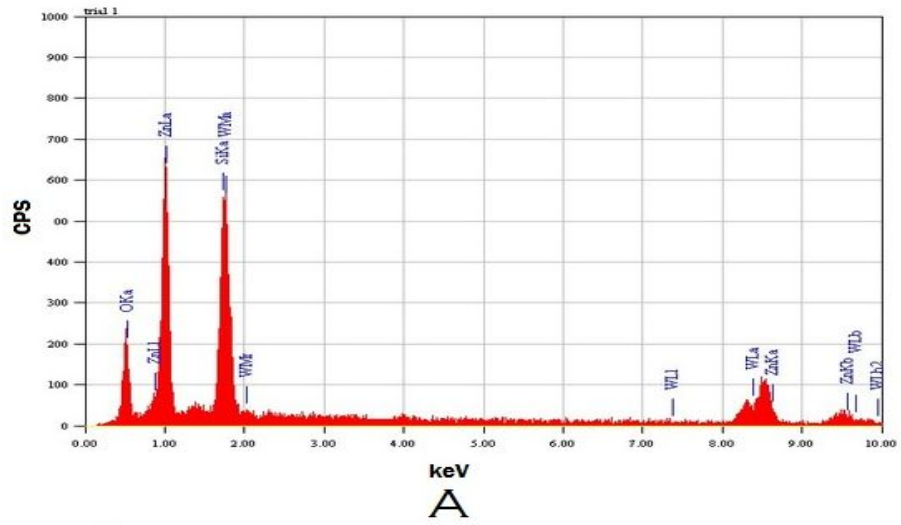


Figure 3.6: EDAX Spectra of ZnO thin film deposited using W source in the (A) as deposited condition and (B) after annealing at 400°C for 4 hours

3.4 Optical characterization

Transmittance spectra of ZnO thin films deposited using Mo source and W source were taken in the visible region of the electromagnetic radiation spectrum. Films deposited using Mo and W evaporation sources in the as deposited condition were dark brown in color and opaque in nature. But both the films after annealing showed a good transmittance in the visible region.

Films deposited using tungsten source after annealing for a period of 4 hours at 400°C showed a transmittance of up to 75% in the visible region of the electromagnetic radiation spectrum. In the same annealing condition films deposited using Mo source showed the transmittance less than 40% in the visible region. On annealing these films at 500°C for 4 hours an average visible region transmittance of up to 70% is achieved as shown in the figure 3.7 and 3.8.

The process of annealing leads to the oxidation of film. ZnO films which were Zn rich in the as deposited condition will attain stoichiometry during the process of oxidation. As the film reaches its stoichiometry or complete oxidation state it becomes transparent. There are reports, which prove the improvement in the stoichiometry of ZnO film after annealing (Aida *et al* 2006, Aly *et al* 2001, Bouhssira *et al* 2006, Rusu *et al* 2007). During the annealing process oxidation takes place due to the diffusion of oxygen atoms in to the film. Thus attainment of complete oxidation state again depends on thickness, composition and structure of the film. Since the film deposited using Mo source contains more Mo atoms than the W atoms present in the film deposited using W source, the attainment of complete oxidation state may be slower in ZnO films deposited using Mo source. The low transmittance at lower annealing temperature is again due to the considerable percentage of Mo atoms present in the film at this condition. These Mo impurities may create mid gap states, which leads to the absorption in the visible range. As the percentage of Mo atoms in the film will decrease after annealing at 500°C for 4 hours the film attained a transmittance of up to 70%.

Optical band gap of ZnO thin film deposited using Mo and W evaporation sources and the effect of annealing on the optical band gap of these films are estimated from the optical measurements carried out in the visible region of the electromagnetic spectrum. Since ZnO is a direct band gap semiconductor, allowed direct transitions can be assumed and band gap E_g can be calculated using the equation 3.4.1.

$$(\alpha h\nu)^2 = B(h\nu - E_g) \quad (3.4.1)$$

According to equation 3.4.1, when $(\alpha h\nu)^2$ is equal to 0 the corresponding $h\nu$ will be equal to E_g . Hence in the plot of $(\alpha h\nu)^2$ vs $h\nu$ the linear portion of the plot is extrapolated to 0 to find the optical band gap of the film.

It is noticed that in the case of films obtained using tungsten source, after annealing for a period of 4 hours at 400°C band gap (E_g) of around 3.3 eV is obtained in accordance with the value of band gap of bulk ZnO (3.37eV at 300K). But in the case of films obtained using molybdenum source, after annealing for a period of 4 hour at 400°C the obtained value of E_g is 2.9 eV (Figure.3.9). When these films were annealed at 500°C for a period of 4 hours the value of E_g is increased to 3.35 eV (Figure. 3.10). This may be due to the large number of Mo impurities present in the film when annealed at 400°C for 4 hours, which will absorb the photons having energy lower than the band gap value and thus reduce the band gap value.

Based on the results of investigations carried out it is concluded that “W” is the better source of evaporation for evaporating ZnO thin films. This is the special observation made in the present study and none of the previous reports on thermally evaporated ZnO thin films have mentioned the incorporation of evaporation source materials in to the film, and the reduction in the atomic percentage of these incorporated atoms on annealing.

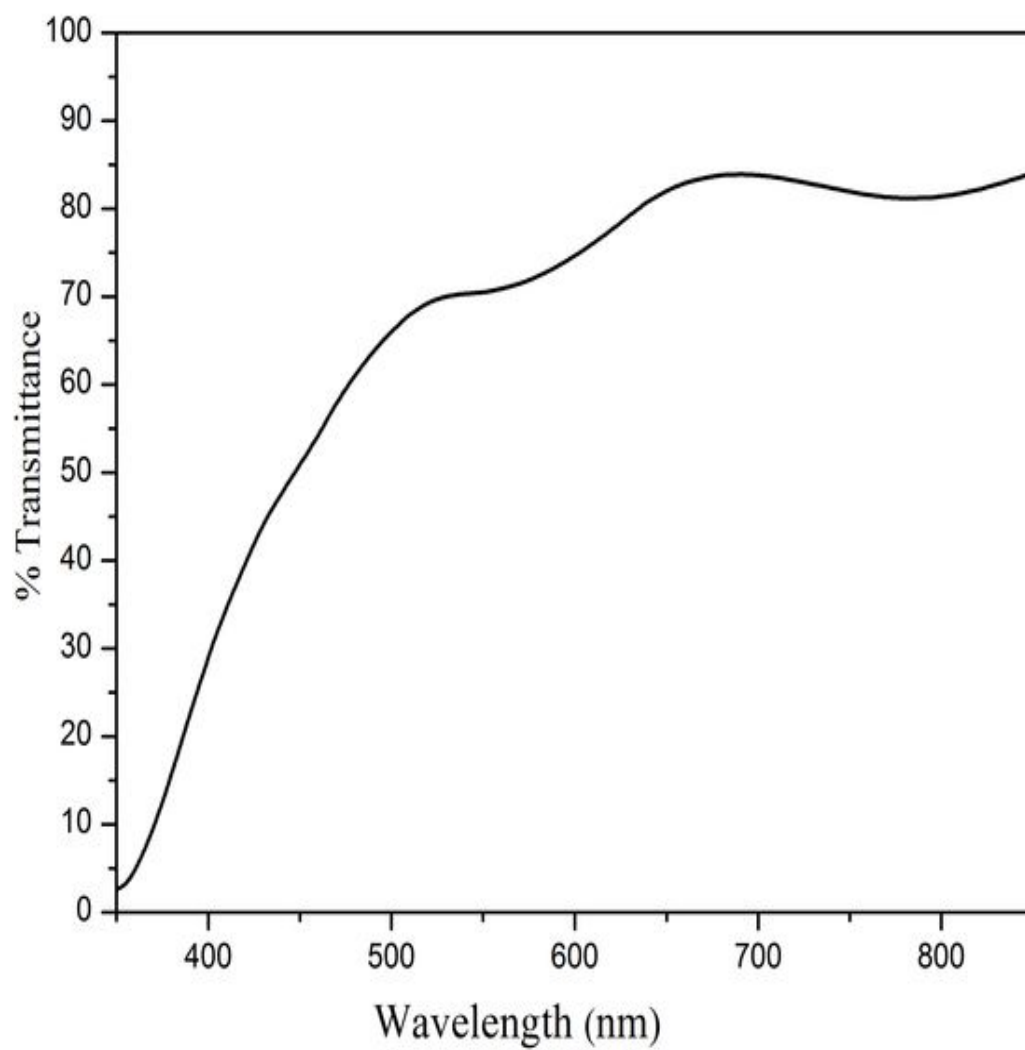


Figure 3.7: Transmittance spectrum of ZnO thin film deposited using W source after annealing at 400°C for 4 hours

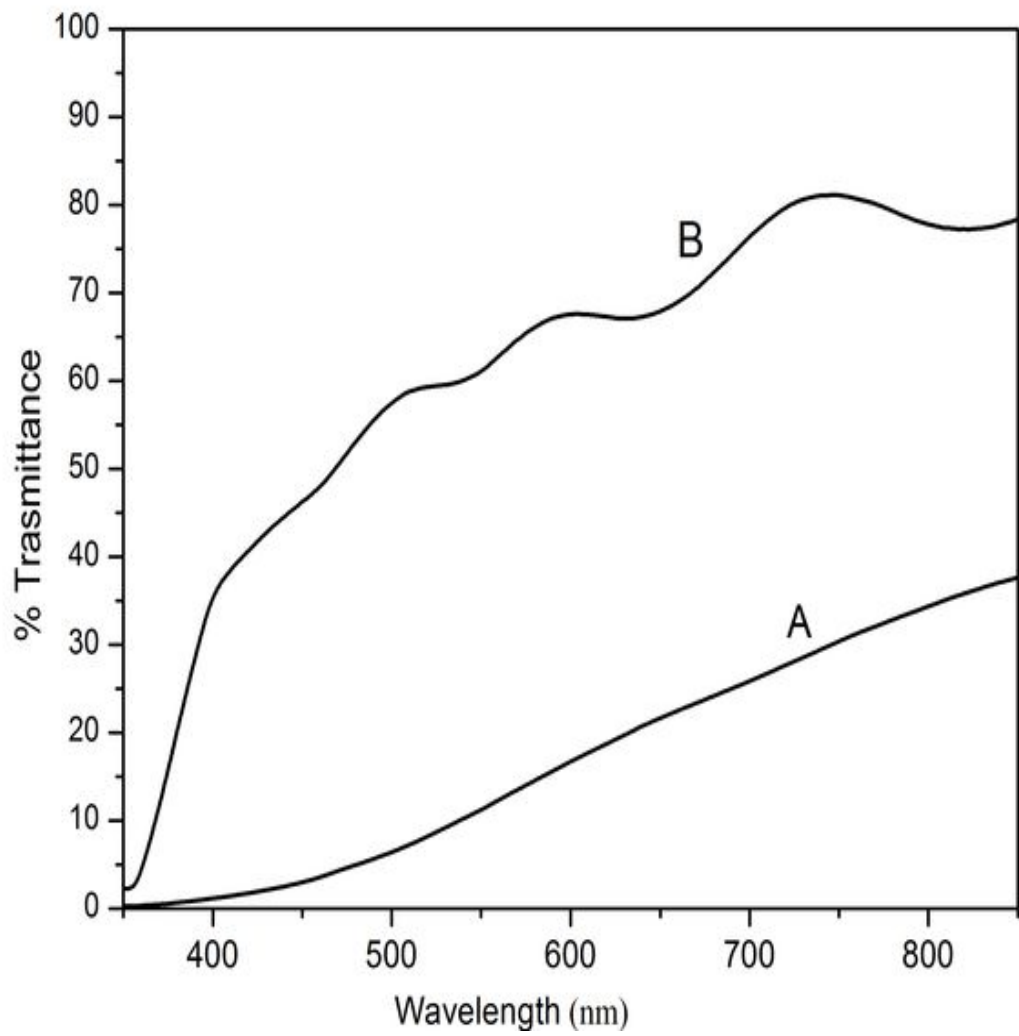


Figure 3.8: Transmittance spectra of ZnO thin films deposited using Mo source after annealing at (A) 400°C for 4 hours and (B) 500°C for 4 hours

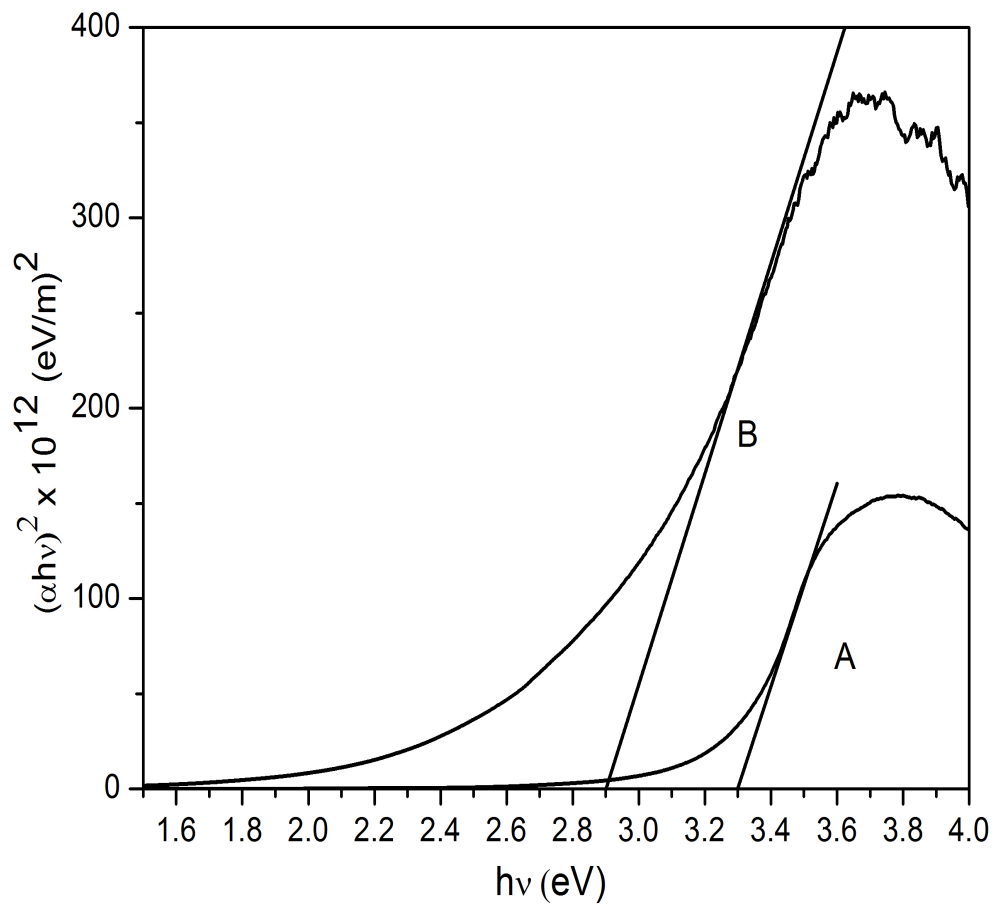


Figure 3.9: Optical Band gap calculation of ZnO thin films deposited using (A) W source and (B) Mo source, after annealing at 400°C for 4 hours

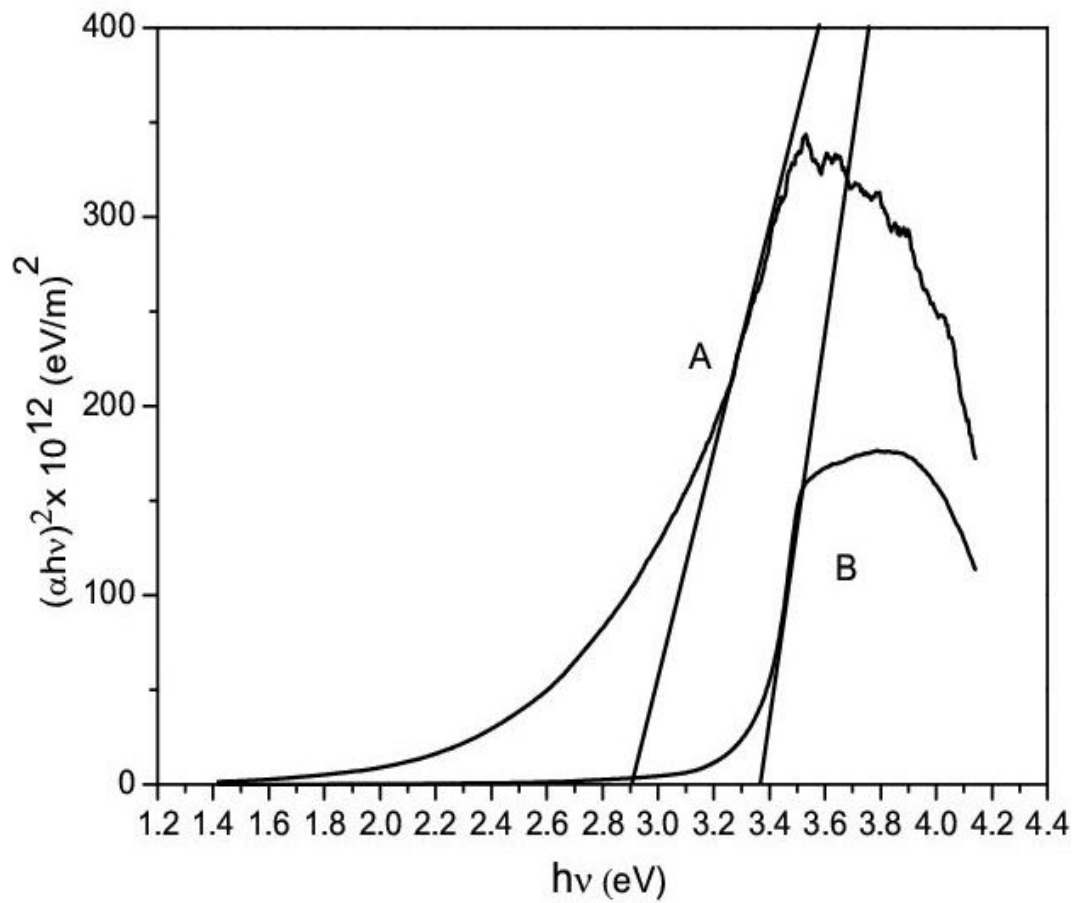


Figure 3.10: Optical band gap calculation of ZnO thin films deposited using Mo source after annealing at (A) 400°C for 4 hours and (B) 500°C for 4 hours

Chapter 4

Study of undoped ZnO thin films

With the beginning of semiconductor age after the invention of transistor, systematic investigation of ZnO as a compound semiconductor was performed. In 1960 good piezoelectric properties of zinc oxide was discovered which led to the first electronic application of ZnO as a surface acoustic wave device. Currently research on ZnO as a semiconducting material sees a renaissance after intensive period in 1950's and 1970's. The renewed interest in ZnO as an optoelectronic material has been triggered by reports on diluted ferromagnetic properties, thin film field effect transistors, and considerable progress in nano structured fabrications.

ZnO thin films can be prepared by variety of techniques such as magnetron sputtering, chemical vapor deposition, pulsed laser deposition, molecular beam epitaxy and spray pyrolysis. The first two methods also allow large area depositions making them the industrially most advanced techniques for ZnO film preparation. In the present study we have chosen vacuum evaporation method to obtain ZnO thin films. This method is one of the rarely used techniques to obtain ZnO thin films and not much attempts have been done to study the structural, electrical and optical properties of thermally evaporated ZnO thin films.

As mentioned in section 2.1 vacuum evaporation technique is one of the simple and low cost procedure used to obtain ZnO thin films. It does not require any catalyst and films can be deposited at low substrate temperature. The temperature of further oxidation of vacuum evaporated ZnO thin films is also moderate to be easily applied in thin film technology. In the present investigation it is also observed that thermal evaporation method produces the best ZnO thin film with high room temperature conductivity and good visible region transparency.

From the investigations carried out and results reported in chapter 3 it is observed that W boat is the better suitable boat for the evaporation of ZnO powder. Hence in further experiments carried out to study vacuum evaporated ZnO thin films, films were obtained by evaporating ZnO powder using only W boat. The film thickness was maintained at 200 nm in all further investigations.

4.1 Optimization of annealing duration

ZnO powder undergoes decomposition during the process of evaporation. The melting point of ZnO is 1975°C. Sublimation of ZnO occurs congruently by decomposition in to the gaseous elements according to the equation 4.1.1. In this stage the atomic oxygen may escape as gas and film is expected to be zinc rich. Hence it will lose its transparency and appear dark brown in color.



The post deposition annealing process of these films leads to the oxidation of films and helps in regaining the lost stoichiometry as well as transparency. Since oxidation is achieved by the diffusion of oxygen atoms in to film surface, thickness, composition, and structure of films are important parameters in deciding the complete oxidation temperature. It is already shown in section 3.4 that ZnO films of thickness 500 nm obtained using W evaporation source achieved a transmittance of up to 75% in the visible region after annealing at 400°C for 4 hours. For further work since thickness of film is limited to 200 nm, annealing condition was again optimized to get highly transparent films.

Thermally evaporated ZnO thin films of thickness 200 nm were annealed for 300°C for 60 mins, 90 mins and 120 mins in the presence of atmospheric air. Effect of annealing duration on the transmittance of the film is shown in figure 4.1. It is observed that as annealing duration is extended, transmittance of the film improved. Finally for a duration of 120 mins film achieved an average visible region transmittance of up to 90 %. Thus annealing temperature is fixed at 300°C and annealing duration is fixed for 2 hours.

Variation of optical band gap of the film with annealing duration is presented in figure 4.2. It is observed that as annealing duration extends the optical band gap is widened. The optical band gap of the ZnO thin film after annealing at 300°C for 60 mins, 90 mins, and 120 mins are found to be 2.73 eV, 3.07 eV and 3.27 eV respectively. The reduced optical band gap of the film at lower annealing period may be due to

the presence of oxygen vacancies in the film which act as donors and absorb photons having energy lower than the band gap value. As annealing duration is extended the number of oxygen vacancies is reduced and band gap value approached theoretical band gap value of ZnO thin films.

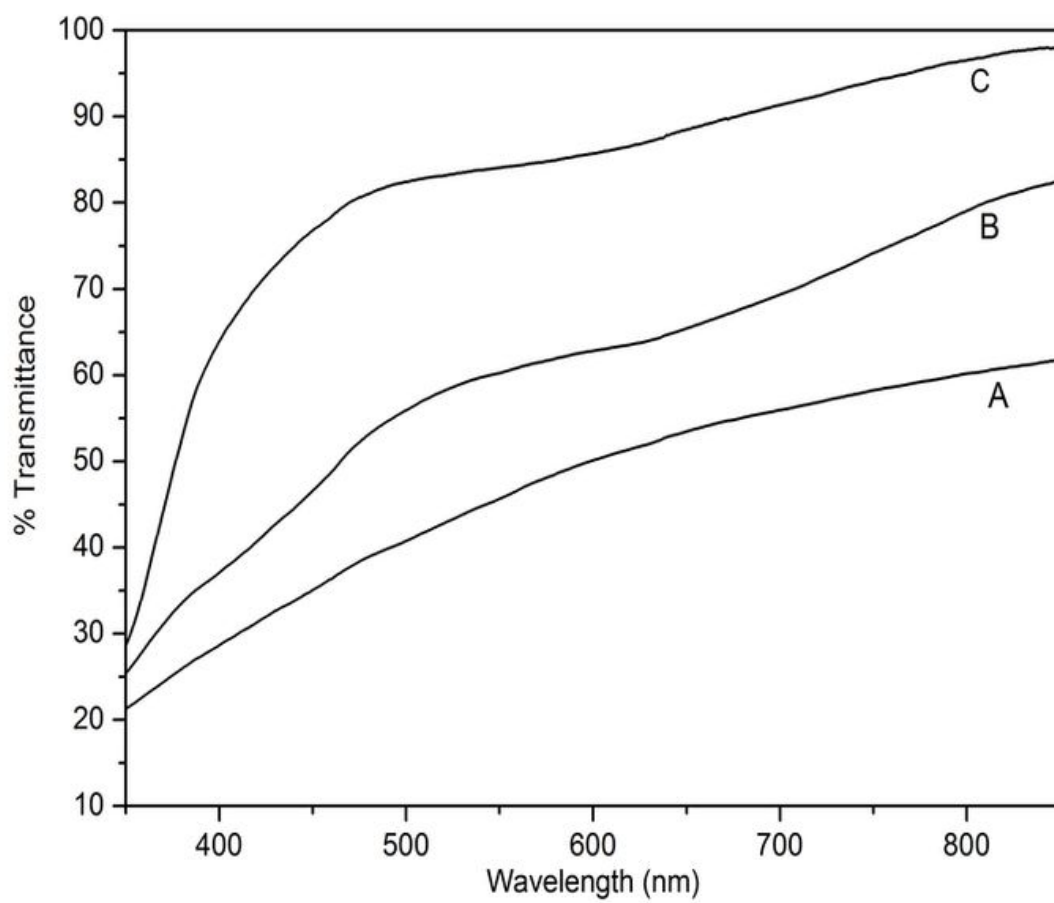


Figure 4.1: Transmittance spectra of ZnO thin films annealed at 300°C for (A) 60 mins, (B) 90 mins and (C) 120 mins

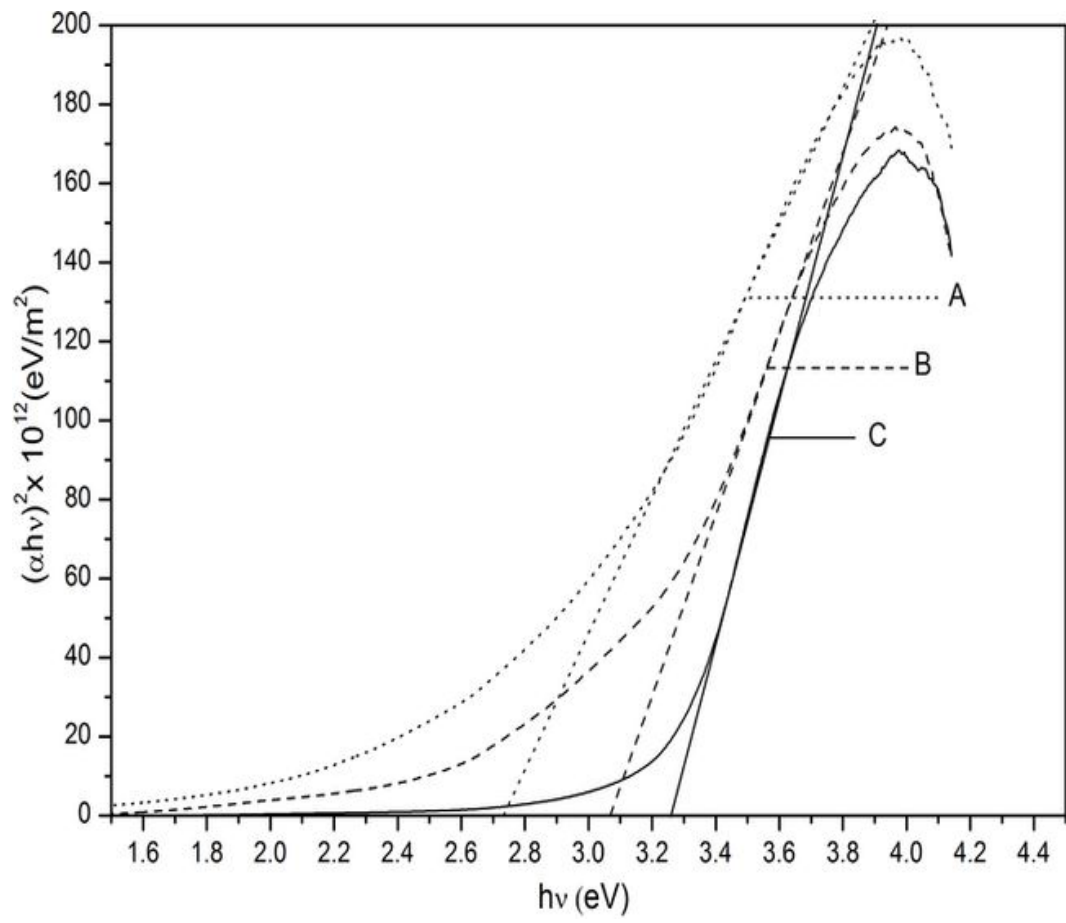


Figure 4.2: Optical band gap variation of ZnO thin films annealed at 300°C for (A) 60 mins, (B) 90 mins and (C) 120 mins

4.2 Structural characterization

The structural properties of ZnO thin film was described already in section 3.1 and 3.2. The results of these characterizations have been already confirmed that ZnO thin films obtained by thermal evaporation technique are amorphous in nature. There was no change in the structural property of the films even after annealing. The films were found to have smooth and continuous surface with absence of pin holes. Such films with flat and smooth surface and amorphous nature are proved to be well suited for the application of flat panel displays because of their flat surface and low internal stress (Shigesato, 2010).

4.3 Compositional characterization

X-ray photoelectron spectroscopy (XPS) is a material characterization technique widely used to investigate the chemical composition of the materials. The technique is based on collecting the electrons that are ejected from atoms of samples being analyzed when irradiated by X-rays. The XPS analysis do not cause any structural damage to the sample and only those photoelectrons that escape the material with out undergoing inelastic scattering are used in the analysis. This technique is non destructive and highly surface sensitive. XPS analysis provides compositional analysis of approximately the top 5 nm of the material below the studied sample surface. In the present study XPS spectra of thermally evaporated ZnO thin films after annealing at 300°C for 2 hours are analyzed to investigate the atomic percentage and chemical states of zinc and oxygen in the film.

The XPS survey spectra of annealed films were first produced before the high resolution scan of oxygen and zinc. The survey spectra of films acquired at a pass energy 75 eV are shown in the figure 4.3. The survey scan it is observed that after annealing at 300°C for 2 hours ZnO thin film is found to have 45.563 at% of zinc and 54.464 at% of oxygen. The Zn 2p core level spectrum of the film acquired at pass energy 25 eV is shown in the figure 4.4. From this spectrum it is noticed that Zn2p_{1/2} peak appeared at binding energy 1021.60 eV. This peak is attributed to Zn-O bond

rather than metallic Zn-Zn bond since the binding energy of Zn-O bond (1021.90 eV) is higher than Zn-Zn binding energy (1021.45 eV). Similarly the Zn2p_{3/2} which appeared at 1044.65 can also be attributed to binding energy of Zn-O bond (1044.78) (Aksoy *et al* 2012).

The binding states of O_{1s} spectrum belong to vacuum evaporated ZnO thin films is shown in figure 4.5. The peak could be divided into two Gaussian components one with low binding energy and other with high binding energy peaks created at 530.07 eV and 531.92 eV. Among these two peaks the peak at 530.07 eV corresponds to the oxygen bonded in metal oxides (in this case ZnO). These are surrounded by zinc atoms with full supplement of nearest neighbor O²⁻ ions. The high binding energy component can be attributed to the presence of loosely bound oxygen on the surface of nano crystals. From the spectra it is confirmed that, among the total 54.464 at% of oxygen present in the film, 74.09 at% of oxygen are bonded to zinc and rest 25.92 at% of oxygen are loosely bonded to the surface.

Thus, vacuum evaporated ZnO thin film after annealing at 300°C for 2 hours found to have 40.048 at% of oxygen bonded to the zinc, 45.563 at% of zinc and 14.389 at% of loosely bonded oxygen. This confirms the presence of oxygen vacancies in the film.

Survey_70eV-Al_afterCC

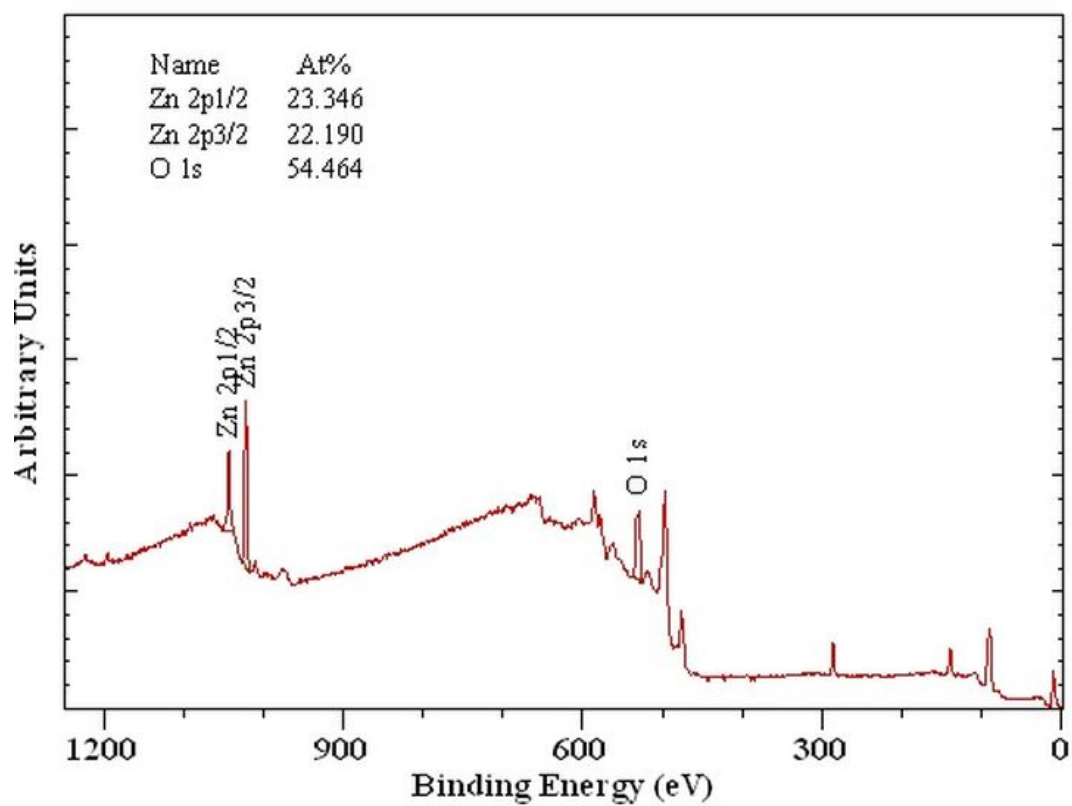


Figure 4.3: XPS Survey scan for ZnO thin film

Zn2p core level spectrum

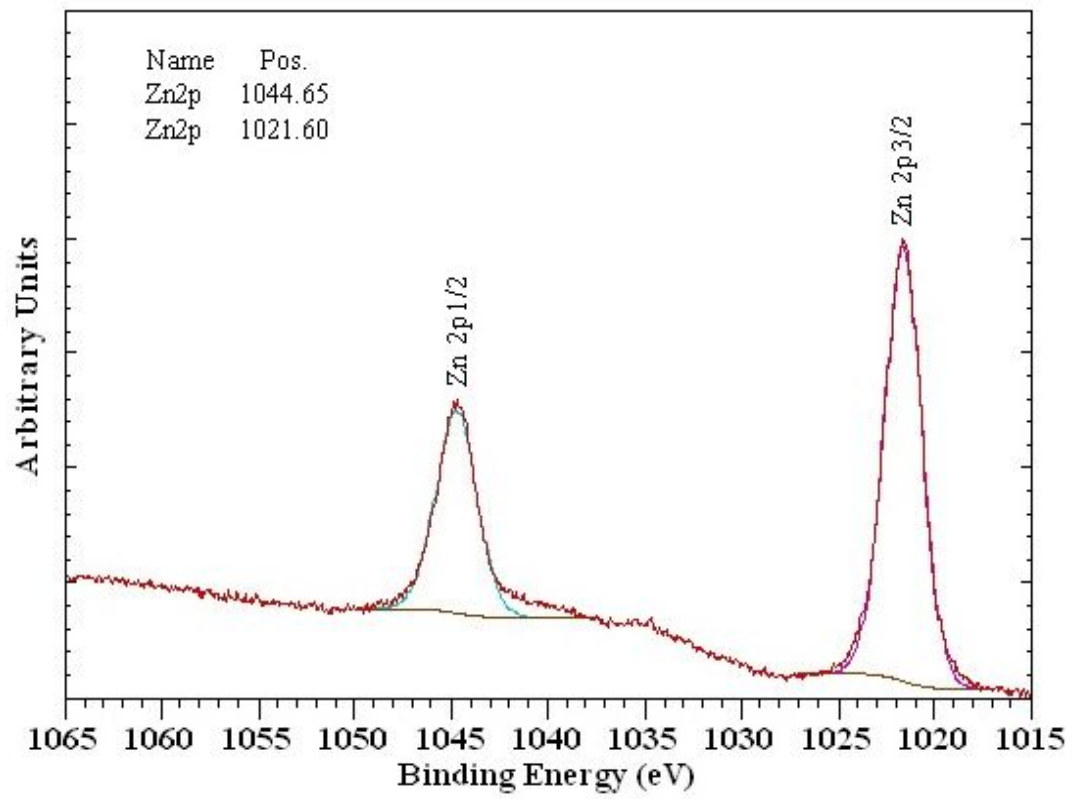


Figure 4.4: Zn2p core level spectrum for ZnO thin film

O1s core level spectrum

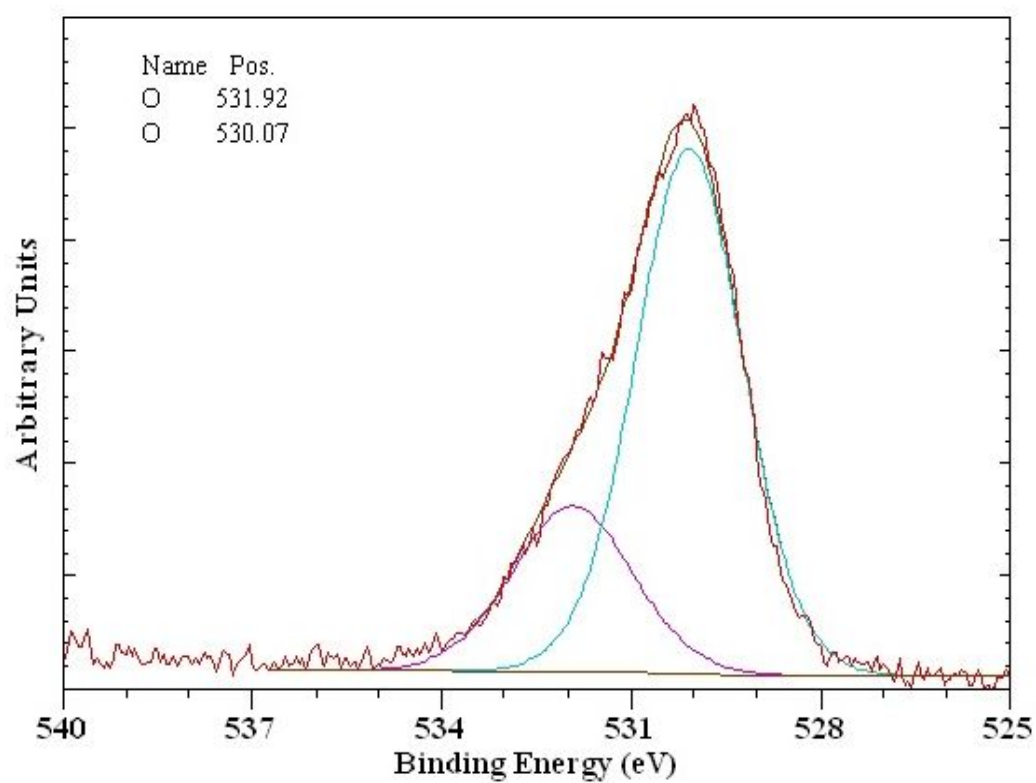


Figure 4.5: O1s core level spectrum for ZnO thin film

4.4 Electrical characterization

4.4.1 Measurement of electrical conductivity

The room temperature electrical conductivity of vacuum evaporated ZnO thin films is measured by two probe method. As mentioned in section 2.3.3 silver coating was used as the metallic contact for the film. In this technique two silver strips of thickness approximately 50 nm and a gap of 0.1 cm were coated using the mask. The conductivity of the film is calculated by using the basic conductivity formula

$$\sigma = \frac{l}{RA} \quad (4.4.1)$$

where, R = resistance of the film, l = length of the contact and A = area between the contacts.

Area between the contact can be again written as

$$A = t \times d \quad (4.4.2)$$

where, t is the film thickness and d is the gap between the contacts.

Thus, the conductivity of the film can be calculated using equation 4.4.3.

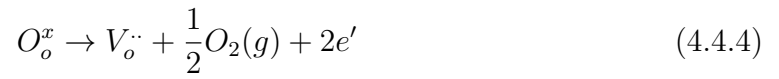
$$\sigma = \frac{l}{R \times t \times d} \Omega^{-1} cm^{-1}. \quad (4.4.3)$$

In the present work the electrical conductivity of the ZnO thin film is found to $92 \Omega^{-1} cm^{-1}$. The linear I-V characteristics of ZnO thin film is presented in figure 4.6 which shows the stability of current over a range of voltage from -5 V to 5 V. The conductivity of ZnO thin film observed in the present case is found to be very high in the case of undoped ZnO thin films as compared to the previously reported results. The conductivity and % transmittance of undoped ZnO thin films obtained from different deposition techniques compared with present results is shown in table 4.1.

Table 4.1: Conductivity and % transmittance ZnO thin films obtained from different methods reported in the literature compared with our results

Preparation method	Conductivity ($\Omega^{-1}cm^{-1}$)	Transmittance (%)
Thermal oxidation of evaporated ZnO thin films (Rusu <i>et al</i> 2007)	2	90
D.C.Sputtering (Banerjee <i>et al</i> 2006)	9.6	85
Pulsed Laser Deposition (Craciun <i>et al</i> 1994)	20	85
Thermal evaporation of pure ZnO powder (Present Work)	92	90

It is seen in table 4.1 that the conductivity of ZnO thin film obtained in the present study is considerably higher compared to the conductivity of ZnO thin films obtained by other methods. This high room temperature conductivity of the film deposited by vacuum evaporation technique may be attributed to the presence of oxygen vacancies in the film even after annealing. Oxygen vacancies present in the film will act as the defects in the film and will play a major role in improving the conductivity of the film. In binary oxides like ZnO, oxygen vacancies are responsible for the conduction electron carrier generation. The electron generation can be explained using KrögerVink notation as in the equation 4.4.4 (Kykyneshi *et al* 2010).



According to equation 4.4.4 an oxygen anion escaping from the crystal structure ($\frac{1}{2}O_2$) from the occupied oxygen site creates a doubly ionized vacancy site ($V_o^{\cdot\cdot}$) with two free electrons. Thus, multiple carriers are created from a single defect and good n-type conductivity can be obtained. Hence, low resistivity at room temperature in ZnO thin film can be achieved by the creation of intrinsic donors by lattice defects such as oxygen vacancies.

However, it has been found that such intrinsically doped films exhibit properties which are not well suited for the application of any devices because of following two reasons. First, by intrinsic doping the resistivity of the films can be reduced only up to $10^2 - 10^3 \Omega\text{cm}$ (Elmer 2010). Further more, these films are not stable at ambient conditions (especially at higher temperatures) due to the re-oxidation of the oxygen deficient films, which increases its resistivity significantly.

To know the nature of charge carriers in ZnO thin films hot probe technique is used. The experiment is done by attaching a cold probe and a hot probe to a semiconductor surface. Both probes are wired to a sensitive electrometer. In the present study hot probe is connected to the positive terminal of the meter, and cold probe is connected to the negative terminal. Positive readout is obtained in the Keithley multimeter. This confirms n-type nature of charge carriers in ZnO thin film.

4.4.2 Measurement of activation energy

To measure the activation energy of vacuum evaporated ZnO thin films, study of variation of film resistance with ambient temperature was performed by heating the film in a hot air oven and measuring the resistance at different temperatures. In the present study temperature of the film is raised up to 300°C from room temperature. The results thus obtained, are plotted as the variation of $\log(R)$ with $1/T$. Resistance of the film decreased with increased temperature indicating semiconducting nature of film. The graph shows two distinct regions. Normally low temperature region corresponds to extrinsic conduction whereas high temperature region corresponds to intrinsic conduction in the film. But in this case since temperature of films was raised only up to 300°C only extrinsic conduction predominates since ZnO has a wide band gap of the order of 3.3 eV.

Semiconducting nature of the films follows the equation 4.4.5 (Sze, 2006).

$$R = R_o \times \exp\left(\frac{E_a}{k_b \times T}\right) \quad (4.4.5)$$

where R is the resistance of the film at temperature T , R_o is a constant, k_b is Boltzmann's constant and E_a is the activation energy required for conduction.

A representative graph of variation of $\log(R)$ with the reciprocal of temperature ($1/T$) for undoped ZnO thin film is shown in figure 4.7. From the logarithmic resistance profile with respect to reciprocal of temperature, the thermal activation energy is calculated using the equation 4.4.6.

$$E_a = \frac{2.303 \times k_b \times (Slope)}{e} \quad (4.4.6)$$

where $Slope$ is the slope of the linear portion of the graph $\log(R)$ verses ($1/T$).

For undoped ZnO thin film, logarithmic resistance curve with variation in the reciprocal of temperature shows a linear behavior in two regions. This shows the presence of two donor levels below the conduction band. The first one from (1.7-2.1) $1/K$ and the other from (2.3-3.2) $1/K$. In these two ranges the activation energy is proportional to the slope according to equation 4.4.6. Undoped ZnO thin film presents first donor level with activation energy of 130 meV in the $1000(1/T)$ range (2.3-3.2 $[1/K]$) and another donor level with activation energy of 261 meV in the $1000(1/T)$ range (1.7-2 $[1/K]$).

Thus, based on the investigations carried out on undoped ZnO thin films it can be concluded that ZnO films with good combination of room temperature conductivity and visible region transmittance can be obtained by vacuum evaporation method. Structural characterization has shown the amorphous nature and smooth surface of the films, which leads to low internal stress, and compositional analysis confirms the presence of oxygen vacancies in the film. Activation energy measurements have shown that undoped vacuum evaporated ZnO thin films have two donor states below the conduction band.

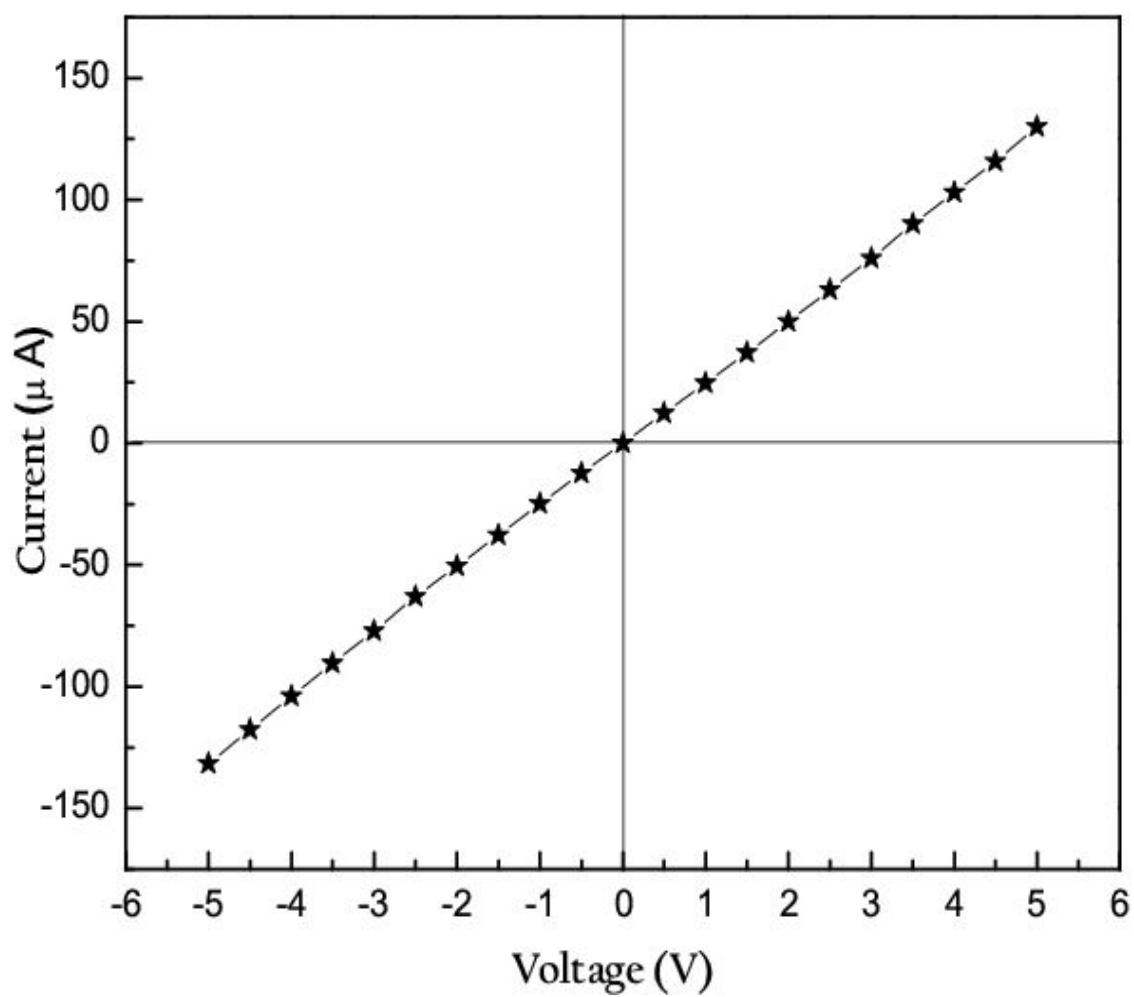


Figure 4.6: I-V Characteristics of undoped ZnO thin film

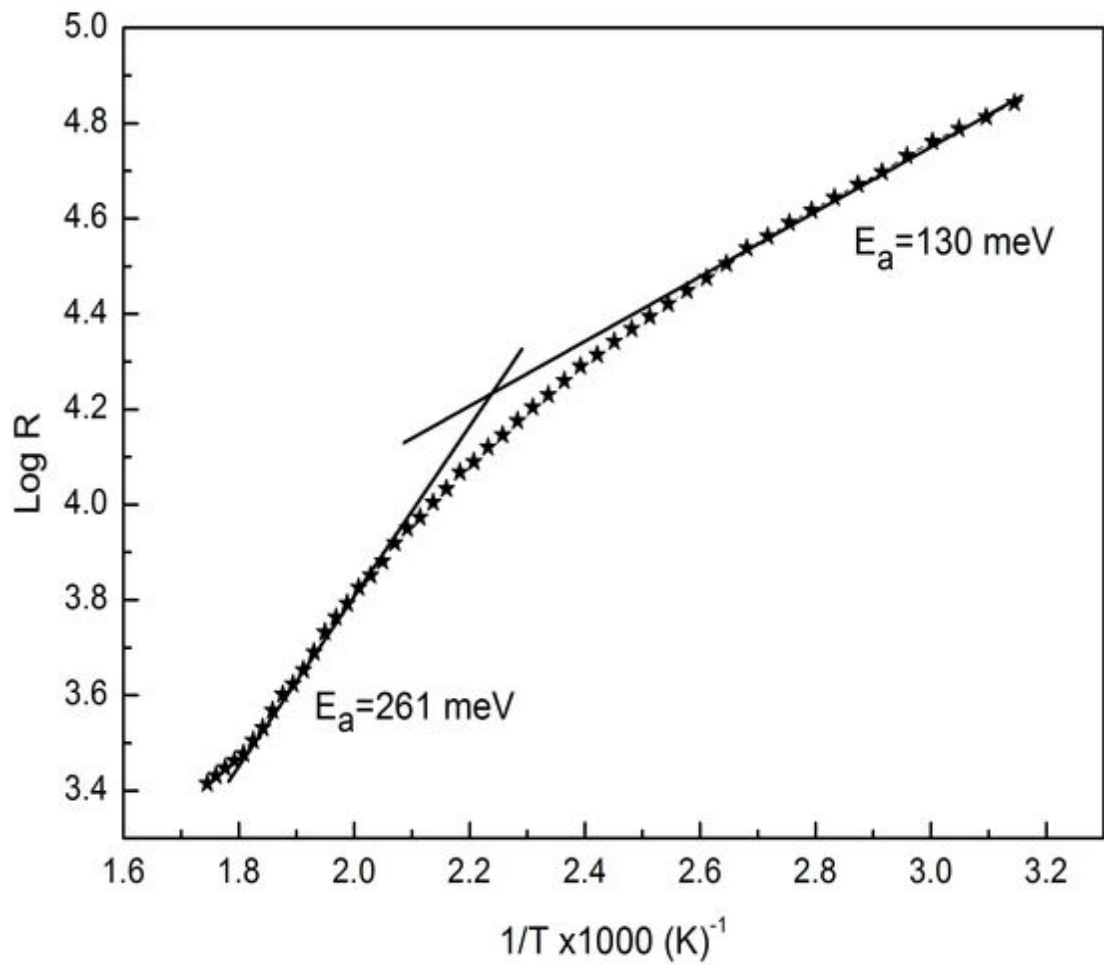


Figure 4.7: Logarithmic resistance profile of ZnO thin film with respect to reciprocal of the temperature

Chapter 5

Doping of thermally evaporated ZnO thin films

5.1 Introduction

Thin films, deposited by most of the well known deposition techniques, usually have high electrical resistivity. In the case of semiconductor films, which have potential applications in electronics or optoelectronics, it is highly desirable to increase the electrical conductivity by doping. The selection of the suitable dopant impurity is the primary requirement of doping. However mere inclusion of impurities will not suffice. To obtain good electrical conductivity, a number of requirements have to be fulfilled.

- First, an adequate concentration of doping atoms has to be incorporated into the material.
- The added dopants must produce shallow levels in the forbidden bandgap region of the material. That is the energy levels of these dopants have to be close enough to the corresponding band edge (conduction band edge for donors and valence band edge for acceptors). Only then the dopants will get easily ionized at the device working temperature (usually room temperature) providing desired quantity of free carriers in the respective bands.
- The incorporation of dopants must not provoke spontaneous formation of some

oppositely charged defects which would de-activate them, either directly, by pairing with dopants or by compensating their electrical activity from the distance. This is not a rare possibility. In fact this problem has been impeding the progress of thin film semiconductor research, especially in that of II-VI semiconductors (Desnica 1998).

Doping of the semiconductor still suffers from the considerable short comings. The mechanisms that limit the doping of semiconductors is explained as follows.

A. Self compensation of native defects

Native defects (also referred as intrinsic defects) commonly occur in semiconductors. The three basic types of point defects are vacancies (an point missing from the lattice site), self-interstitials (additional atom in the lattice) and antisites (in a compound semiconductor, when for example a cation is sitting in an anion site). For each of these type, the defects can occur either on cation site or on anion site. Because formation of native defects often require breaking or rearranging of bonds and deep levels in semiconductor bands are typically introduced. The occupation of levels determines the charge state of the defect. Depending on the location of levels in the gap and charge states they can assume, native defects can have donor character or acceptor character or even be amphoteric.

For the sake of argument, let us assume that in a semiconductor material, a donor like native defect is formed which in its neutral state has an electron residing in the level near the conduction band. If we try to dope this material p-type, we are driving the fermi level down to a position near the top of the valance band. The donor of course will become positively charged by transferring its electrons from the gap level to the Fermi level in the process of compensating electron activity of an acceptor. The amount of energy gained by this charge transfer can be the order of band gap. The net formation energy of a native defect is equal to the energy required to create a neutral defect minus energy gained by transferring the electron. The above argument indicate that in a wide band gap semiconductor the net formation energy of a compensating native defect could be very low. This would lead to the formation

of large number of native defects. This donor type defects compensate the acceptors which were introduced to make the material p-type (Van-de Walle 1997).

B. Compensation by other configurations of impurity

Suppose an impurity is incorporated in to the crystal with the goal of introducing shallow acceptor level it is necessary for impurity to be located in substitutional lattice site. But if the growth condition is such that a large number of impurity atoms are incorporated to the interstitial sites as opposed to the substitutional site significant compensation will occur.

C. Formation of complexes

In the process of doping a semiconductor there is a possibility of formation of complexes between dopant impurities and native defects. Indeed if the binding energy between native defect and dopant is large enough the formation energy of resulting complex may be lower than that of the individual defect.

D. Solubility limit

In order to dope a material, impurities that act as dopants may be introduced in to the semiconductor. In p-type material the hole concentration is obviously limited by the concentration of acceptor impurities incorporated in the lattice. If this hole concentration is limited it can lead to limitation in the achievable doping level (Van-de Walle 1997).

5.2 Doping of ZnO thin films

Zinc oxide is a typical semiconductor which can be made conductive both by intrinsic dopants (defects) as well as by extrinsic ones (foreign atoms). The low resistivity at room temperature that is degenerate doping which is acquired for the application of ZnO as transparent electrodes can be achieved in two different ways.

- Creation of intrinsic donors by lattice defects (for instance oxygen vacancies or zinc atoms on interstitial lattice sites).
- Introduction to extrinsic dopants (either metal with oxidation number three on substitutional metal lattice sites or halogens with oxidation number minus one on oxygen lattice sites).

The first possibility can be realized during deposition by carefully adjusting oxygen partial pressure and deposition rate. The other way is a reduction process of the oxide film after deposition for instance, annealing in vacuum or in atmosphere containing hydrogen. As mentioned in chapter 4 in the present investigation, the oxygen vacancy in the film is confirmed by XPS analysis which acts as intrinsic dopant and helped in achieving significantly high room temperature conductivity of the film in its undoped state.

Though the electrical properties of zinc oxide has been investigated since more than five decades it was not clear until recently which defect(s) constitute(s) dominant donor(s) in intrinsic ZnO. For a long time it was believed that the oxygen vacancy is a dominant donor which was supported by the fact that an annealing process of ZnO single crystals or thin films under reduced condition increased the carrier concentration, while oxidation process decreased the carrier concentration. But recently by comprehensive studies, researchers have assign that the zinc vacancy and oxygen interstitial as acceptors and only zinc interstitials and oxygen vacancies have shallow energetic donor positions in the band gap. Depending on the growth atmosphere different defects are most likely to form. Under zinc rich condition oxygen vacancy dominates, while zinc vacancy and oxygen interstitials are most likely defects the for oxygen rich atmosphere (Elmer 2010)

5.2.1 n-Type doping

ZnO with a wurtzite structure is naturally an n-type semiconductor because of a deviation from stoichiometry due to the presence of intrinsic defects such as oxygen vacancies “ V_o ” and Zn interstitials “ Zn_i ”. Undoped ZnO shows intrinsic n-type conductivity with very high electron densities of about 10^{21}cm^{-3} . Although it is experimentally known that unintentionally doped ZnO is n-type, whether the donors are Zn_i and V_o is still controversial. The first-principles study suggested that none of the native defects show high concentration shallow donor characteristics. First principle calculations have also suggested that the unintentionally incorporated hydrogen acts as source of conductivity and behaves as shallow donor in ZnO (Van De Walle 2000)

Attainment of intentional n-type doping of ZnO is relatively easy compared to p-type doping. As n-type dopants, group III elements B (Wenas *et al* 1991), Al (Kim *et al* 1997), Ga (Agura *et al* 2003), and In (Agne *et al* 2003), rare earth metals (group III B) Sc and Y (Minami *et al* 2000), group IV elements Si (Minami *et al* 1986), Ge (Wang *et al* 1996), and Sn (Ataev *et al* 1999) and group VII elements F (Xu *et al* 2005), Cl (Ntep *et al* 1999), and I can be used. Various deposition methods such as MBE, sputtering, PLD, and chemical vapor deposition (CVD) have been used to produce highly conductive n-type ZnO films (Myong *et al* 1997, Atev *et al* 1995, Assunçao *et al* 2003, Liu *et al* 2003, Minami *et al* 1984), where those produced particularly by MBE exhibited high crystalline quality (Kato *et al* 2002).

Group III elements Al, Ga, and In as substitutional elements for Zn are probably more suitable for n-type doping of ZnO due to their lower vapor pressures compared to group VII elements such as Cl, Br, and I substituting for O (Morkoç and Özgür 2007). Oxidation of Al source during MBE growth may also become a problem because of its high reactivity with O. Ga and In are less reactive than Al. Furthermore, Ko *et al* (2000) estimated covalent bond lengths of GaO (1.92 Å) to be slightly smaller than those of ZnO (1.97 Å), whereas the bond length of InO was estimated higher (2.1 Å), not surprisingly considering the large ionic radius of In. The bond length of Ga-O is expected to cause only small deformation of the ZnO lattice

even in the case of high Ga concentration, whereas the larger bond lengths of In-O would deform the ZnO lattice more seriously.

The motivation for n-type doping of ZnO comes from the need for transparent conducting oxides for transparent electrodes as ZnO is transparent to visible wavelengths. Carrier concentrations above 10^{21} cm^{-3} and resistivities below $10^{-4} \Omega \text{ cm}$ have been obtained for n-type ZnO films. Al-doped ZnO films prepared by photoassisted metal-organic vapor-phase epitaxy (MOVPE) were shown to exhibit a minimum resistivity of $6.2 \times 10^{-4} \Omega \text{ cm}$ (Myong *et al* 1997). For ZnO:Al films deposited on glass substrates using PLD, Agura *et al* (2003) reported a minimum resistivity of $8.54 \times 10^{-5} \Omega \text{ cm}$ and a mobility of $\sim 50 \text{ cm}^{-2} \text{ V}^{-1} \text{ s}^{-1}$ at a carrier concentration of $1.5 \times 10^{21} \text{ cm}^{-3}$ that corresponds to an Al composition of 1.8 wt%. Resistivities as low as $1.2 \times 10^{-4} \Omega \text{ cm}$ have also been reported for Ga-doped ZnO films grown by chemical vapor deposition (Atev *et al* 1995). It should be noted that the dopant concentrations in these ZnO films, which were meant to be used for transparent conductive electrodes, are relatively high.

Thus, n-type doping of ZnO is developed very well. Such films are successfully used in various applications as n-type layers in light-emitting diodes as well as transparent ohmic contacts.

5.2.2 p-Type doping

It is very difficult to obtain p-type doping in wide-band-gap semiconductors, such as ZnO, GaN and ZnSe. The difficulties can arise from a variety of causes. Attempted p-type dopants may be compensated by low-energy native defects, such as Zn_i or V_o , or background impurities (H) with propensity to n-type doping. Low solubility of the dopant in the host material and precipitate formation are also possible causes. The deep impurity level can also be a source of the doping problem causing significant resistance to the formation of shallow acceptor level.

There has been a plethora of reports of p-type behavior in ZnO, often with apparently very high hole concentrations but with low mobilities. In a few cases, the mobilities reported are unreasonably high. Even what is generally known as n-type dopants have been reported to produce p-type ZnO. Nitrogen, which is known to provide the shallowest acceptor impurity, is most likely a genuine p-type dopant. However, N has low solubility making it imperative to decrease the background donor concentration and increase solubility by co-doping. As mentioned earlier, reports are also abound with the facts that the purported p-type doping is not stable in ZnO. There have also been p-n junctions reported, but efficiency of light emission is low, the emission width is arguably wide, and the source of emission is controversial and/or not well understood (Morkoç and Özgür, 2007).

Known acceptors in ZnO include group I elements, such as Li, Na, and K, Cu, Ag, and Zn vacancies, and group V elements such as N, P, Sb, and As. However, many of these form deep acceptors and do not contribute sufficiently to p-type conduction. Zn vacancies have low formation energy in n-ZnO and can be created by high-energy (2 MeV) electrons. They were shown to be dominant acceptors in as-grown n-type ZnO using positron annihilation spectroscopy (Tumosto *et al* 2003). It is believed that the most promising dopants for p-type ZnO are the group V elements, although theory suggests some difficulty in achieving shallow acceptor level (Park *et al* 2002). Plasma sources are used for N doping, whereas conventional effusion cells can be employed for As, Sb, and P. The activation energy of P was reported to be 127 meV (Hwang *et al* 2005). Among these candidates, N has the smallest ionic radius (1.68 Å), which is

very close to O ionic radius of 1.38 Å, but as mentioned above, its solubility is low. The ionic radii for the other possible group V impurities that substitute for O in ZnO are 2.12, 2.22, and 2.45 Å for P⁻³, As⁻³, and Sb⁻³, respectively (Morkoç and Özgür, 2007).

Despite of the difficulties in p-type doping a number of groups have expended a good deal of effort in an attempt to realize p-type ZnO using different dopants. Minegishi *et al* (1997) reported the growth of p-type ZnO using chemical-vapor deposition (CVD). The NH₃ gas was simultaneously added in the hydrogen carrier gas with excess Zn. The resistivity of the resulting films was high 100 Ωcm, suggesting that the acceptor level is relatively deep with a subsequent low free-hole concentration. Ye *et al* (2003) also used NH₃ as the nitrogen source for dc reactive magnetron sputtering of p-type ZnO. Results show a hole concentration of $3.2 \times 10^{17} \text{cm}^{-3}$ and a resistivity of 35 Ω cm. Ye *et al* proposed that the excess zinc and interstitial hydrogen play an important role in p-type doping. Ohshima *et al* (2003) have attempted to synthesize p-type ZnO by PLD using various co-doping methods including the ablation of ZnO:Ga target in NO gas, and Al and N co-doping using an ion gun and a microwave ECR source. Although they could identify the presence of GaN bond in ZnO, p-type ZnO film could not be obtained.

Aoki *et al* (2000) used the PLD technique to produce phosphorus-doped p-type ZnO films using a zinc-phosphide (Zn₃P₂) compound as the phosphorus source. In this process, a Zn₃P₂ film deposited on a ZnO substrate was exposed to excimer laser radiation in high-pressure nitrogen or oxygen ambient and was consequently decomposed into Zn and P atoms which diffuse into ZnO, resulting in the formation of P-doped ZnO through the replacement of O atoms by P atoms. Ryu *et al* (2000) employed GaAs substrates as an arsenic source for p-type doping of ZnO by PLD. In this case, a p-type ZnO layer was produced at the ZnO / GaAs interface after thermal annealing.

In the present work the electrical conductivity of thermally evaporated ZnO thin films have been improved by doping them with third group metal and metal oxides namely indium (In), indium oxide (In_2O_3), gallium oxide (Ga_2O_3) and aluminum oxide (Al_2O_3). Although these metal and metal oxides have already been used to dope ZnO thin films using different deposition techniques, to the best of our knowledge not much attempts have been done to dope them in the case of thermally evaporated ZnO thin films.

Thin films can be doped by vacuum deposition technique in any of the following ways.

- Post-deposition immersion in a solution containing the dopant material. The technique relies on the diffusion of dopant from the solution into the film. It may be required to heat the solution in many cases.
- Co-evaporating a mixture of the dopant and the film material. This method is effective only if both dopant and the film material have nearly equal vapor pressures at the operating temperature.
- Co-evaporating the dopant and the film material from separate sources. This is by far the most effective technique. However it involves the difficulty of monitoring the evaporation from two separate sources simultaneously.
- Depositing the dopant and the film one after the other (Sandwiching). This technique seems to be very simple and effective and hence it has been widely used. However in this method it must be ensured that the dopant is properly diffused into the material and has not remained as a separate layer. Although annealing can produce some degree of diffusion, the dopant layer may still remain intact in some places. In such cases the electrical conduction may take place largely or entirely through the low resistance dopant film, rather than the semiconductor film, giving a false impression of improvement in electrical conductivity.

In the present work ZnO thin films were doped by evaporating a source mixture containing ZnO and dopants mixed thoroughly. In this study initially

the amount of the dopant to be added to ZnO thin film is optimized so that the conductivity is improved without disturbing the transmittance of the film. The role of third group elements as dopants in the form of pure metal and metal oxides is studied by doping the film with Indium (In) and comparing the electrical optical and structural properties of these films with indium oxide (In_2O_3) doped ZnO thin films.

Finally films were doped with two more dopants namely gallium oxide (Ga_2O_3) and aluminum oxide (Al_2O_3). A detailed analysis of structural, optical and electrical properties of these films were studied and the modulation in the properties of thermally evaporated ZnO thin films with different third group dopants is reported.

5.3 Indium doped ZnO thin films

A. Optimization of dopant concentration

In the present investigation indium (In) doped ZnO thin films were obtained by evaporating a mixture containing pure ZnO and pure In metal powder using “W” boat. The evaporation conditions are maintained almost identical to that of undoped ZnO thin films. To study the effect of doping concentrations on ZnO thin films, films doped with 3%, 5% and 7% of In are obtained. Thickness of films in all the cases is maintained to be 200 nm. In the as deposited condition the films were found to be dark brown in color and opaque in nature. These films were annealed at 300 for 2 hours so that they turn transparent.

Films were subjected to optical transmittance study in the visible region in a wavelength range of 350 nm 850 nm. The transmittance spectra of ZnO thin films doped with 3%, 5% and 7% In is shown in the Fig 5.1. It was observed that the ZnO films doped with 3%, and 5% of In have average transmittance of up to 90% in the visible region of the electromagnetic radiation spectrum. In the case of ZnO thin film doped with 7% In the transmittance of the film decreased up to 60%. The similar observation was reported by Hafdallah *et al* (2011). This research group observed a decrease in the transmittance of the film when the dopant concentration was increased to 8%.

The conductivity of ZnO films doped with 3%, 5% and 7% of In are found to be $140 \Omega^{-1}\text{cm}^{-1}$, $580 \Omega^{-1}\text{cm}^{-1}$ and $1.683 \times 10^3 \Omega^{-1}\text{cm}^{-1}$ respectively. The I-V characteristics of ZnO thin films doped with 3%, 5% and 7% of In is shown in the Fig 5.2. Thus from electrical and optical studies of ZnO thin films doped with 3%, 5% and 7% it can be concluded that ZnO film doped with 5% has a good combination of conductivity and transmittance. Since the present work was focused to improve the conductivity of the vacuum deposited ZnO thin films retaining its transmittance, doping concentration of indium metal is limited to 5% and the film doped with 5% of indium is subjected for further characterization.

B. Structural characterization

The X-ray diffactogram of indium doped ZnO thin films did not show any peak in the θ range 20° to 80° . This confirms the amorphous nature of the film.

The scanning electron microscope (SEM) image is shown in the figure 5.3. From the SEM image it is observed that the In doped films were found to have smooth and continuous surface and there was no significant modification in the the surface topography of the film.

C. Optical characterization

The optical transmittance spectra of ZnO thin film doped with 5% of indium is compared with that of undoped ZnO thin film in the figure 5.4. As mentioned earlier ZnO thin film doped with 5% indium has average visible region transmittance of up to 90% which is almost equal to that of undoped ZnO thin film. This proves that the doping in this case did not disturb the transmittance of the film.

The optical band gap of the ZnO thin film doped with 5% metallic indium powder is compared with that of undoped ZnO thin films is shown in figure 5.5. The optical band gap of the undoped ZnO thin films is found to be 3.27 eV. It decreased to 3.2 eV on doping with 5% of metallic indium. This decrease in band gap of the film due to doping is because of the formation additional donor levels below the conduction band which will absorb photons having energy lower than the band gap value.

D. Electrical characterization

The conductivity of ZnO thin films doped with 5% of indium is found to be $580 \Omega^{-1}\text{cm}^{-1}$. The I-V characteristics of ZnO thin films doped with 5% indium compared with undoped ZnO thin film is shown in the figure 5.6. The I-V characteristics in figure shows the improvement in the conductivity of vacuum evaporated ZnO film after doping and stability in the conductivity of these films over a range of voltage from -5V to +5V.

The activation energy of 5% of indium doped ZnO thin films is measured by measuring the resistance of the film with the variation of temperature. A representative graph of variation of $\log(R)$ with the reciprocal of temperature ($1/T$) is shown in the figure 5.7. From the logarithmic resistance profile with respect to reciprocal of temperature, the thermal activation energy is calculated using the equation 5.3.1.

$$E_a = \frac{2.303 \times k_b \times (slope)}{e} \quad (5.3.1)$$

$\log(R)$ verses $1/T$, for In_2O_3 doped ZnO thin film curve shows a linear behavior in two regions. The first one from (1.7-2.1) $1/K$ and the other from (2.3-3.2) $1/K$. In these two ranges the activation energy is proportional to the slope and indium doped ZnO thin film presents a donor level with activation energy of 74 meV in the 1000($1/T$) range (2.3-3.2 [$1/K$]) and another donor level with activation energy of 375 meV in the 1000($1/T$) range (1.7-2 [$1/K$]).

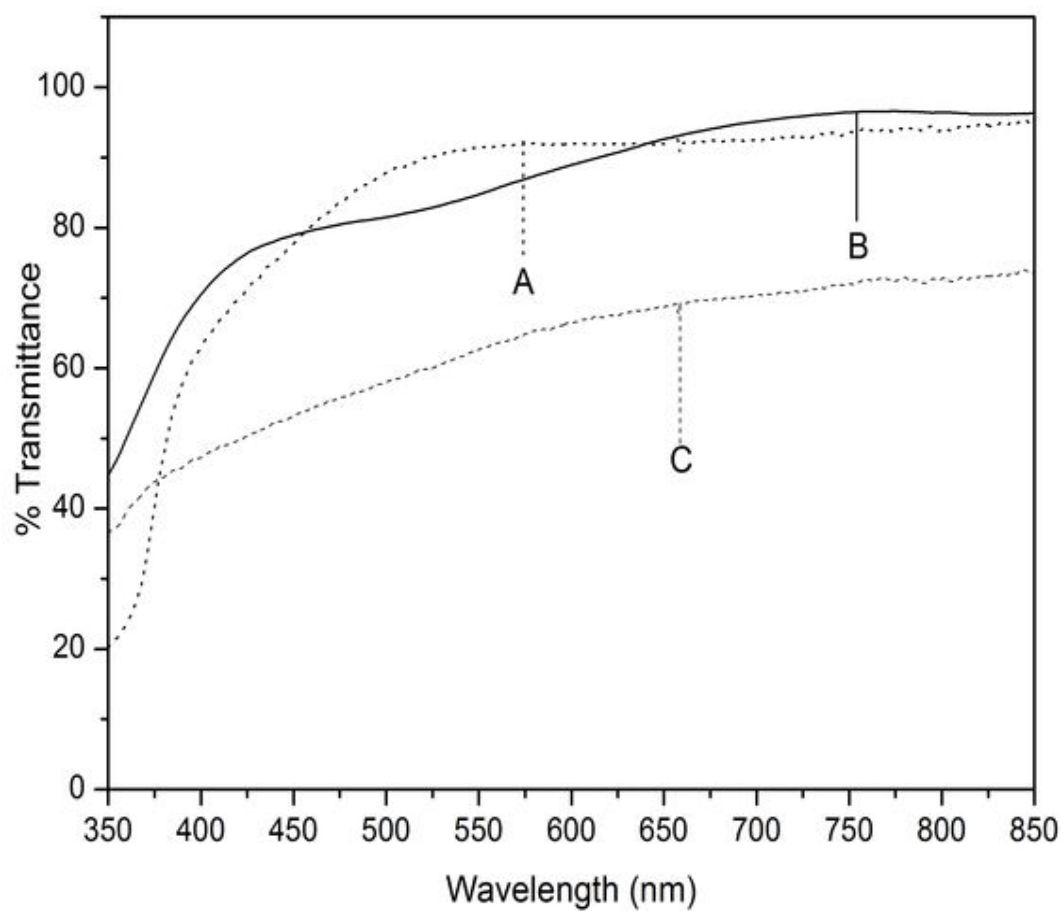


Figure 5.1: Transmittance spectra of ZnO thin films doped with (A) 3% of indium, (B) 5 % of indium and (C) 7% of indium

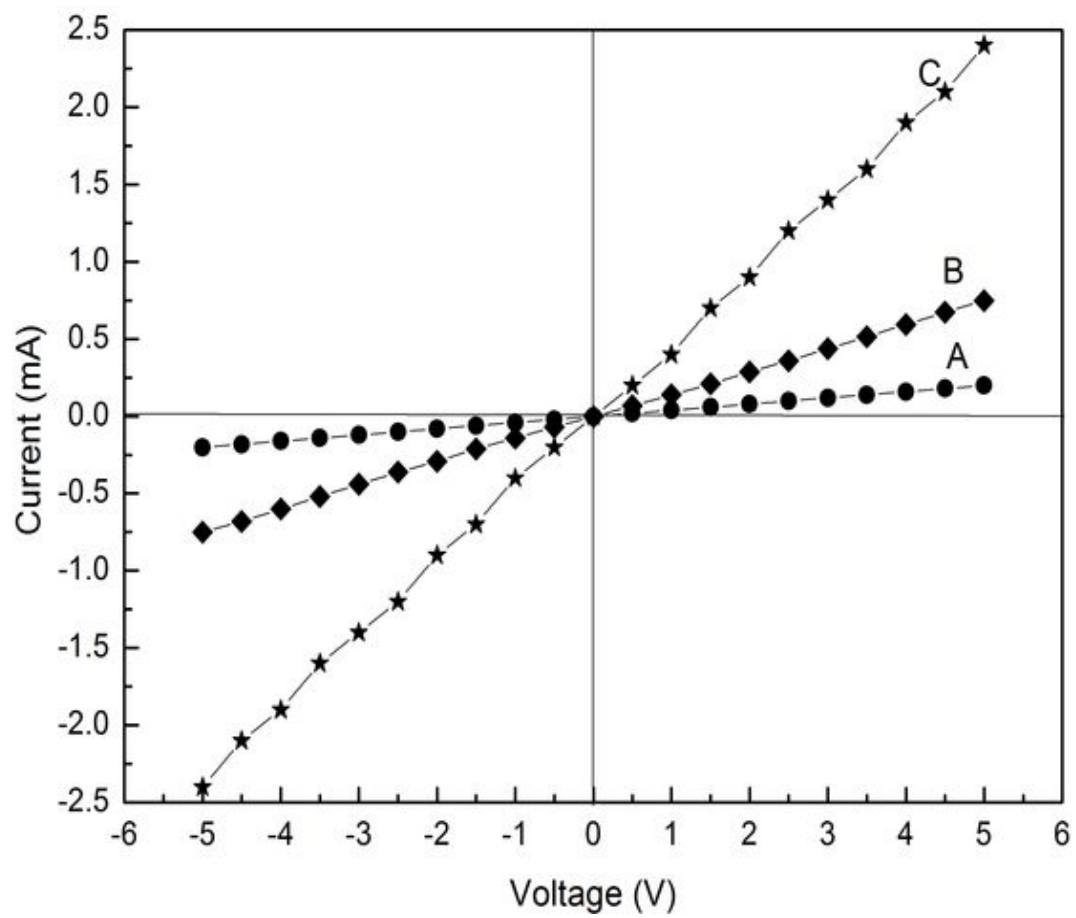


Figure 5.2: I-V characteristics of ZnO thin films doped with (A) 3% of indium, (B) 5 % of indium and (C) 7% of indium

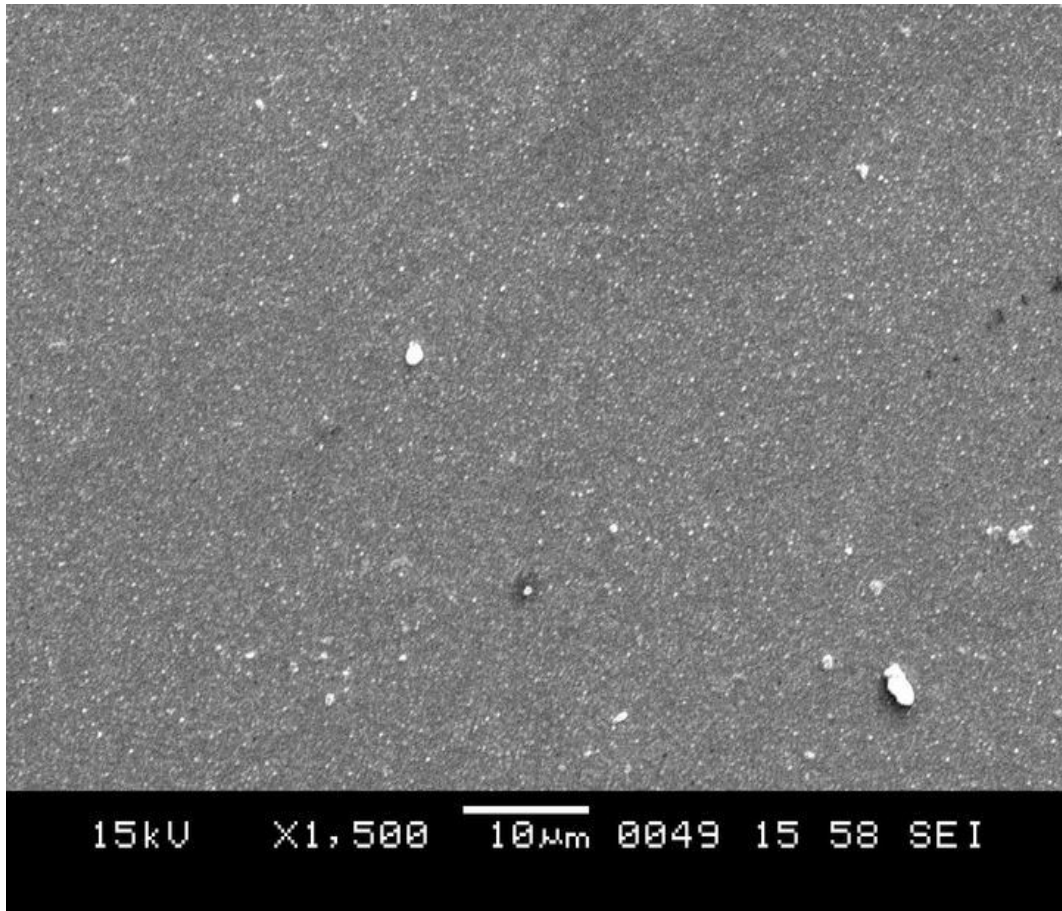


Figure 5.3: SEM image of ZnO thin film doped with 5 % of indium

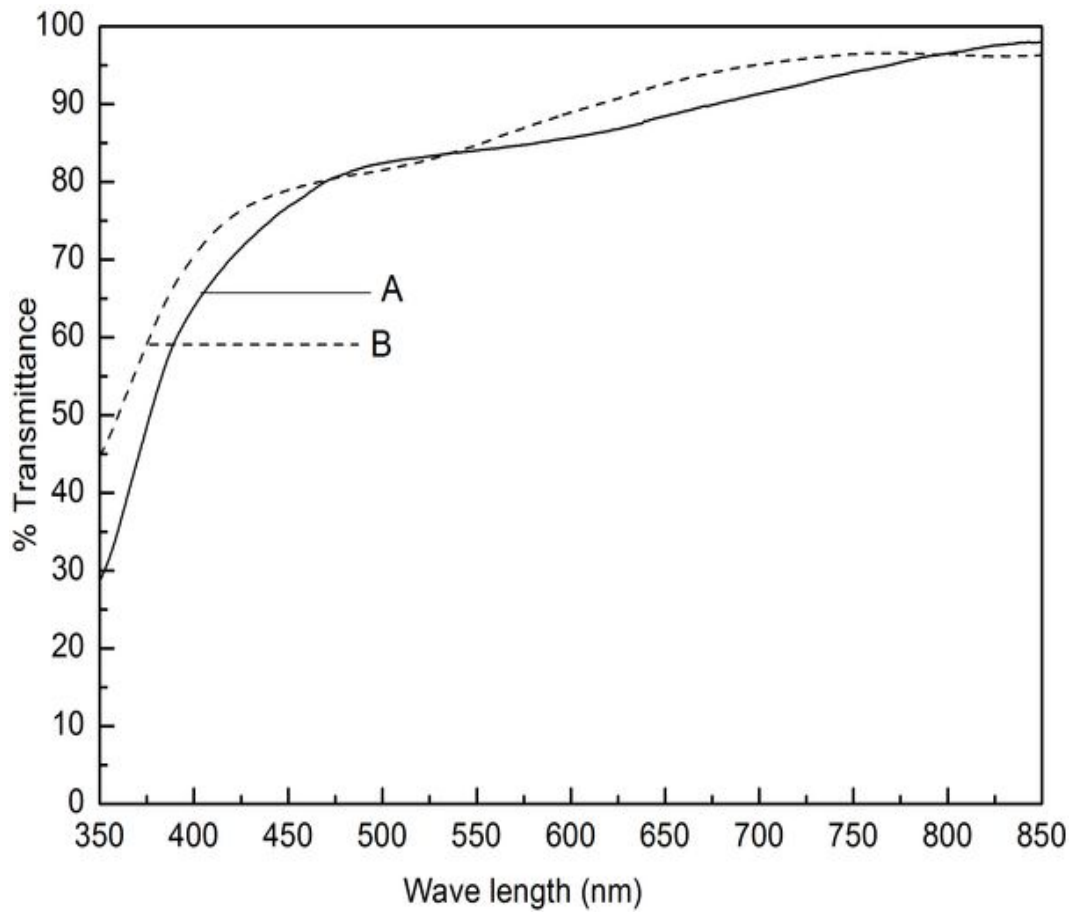


Figure 5.4: Transmittance spectra of (A)undoped and (B) 5 % of indium doped ZnO thin films

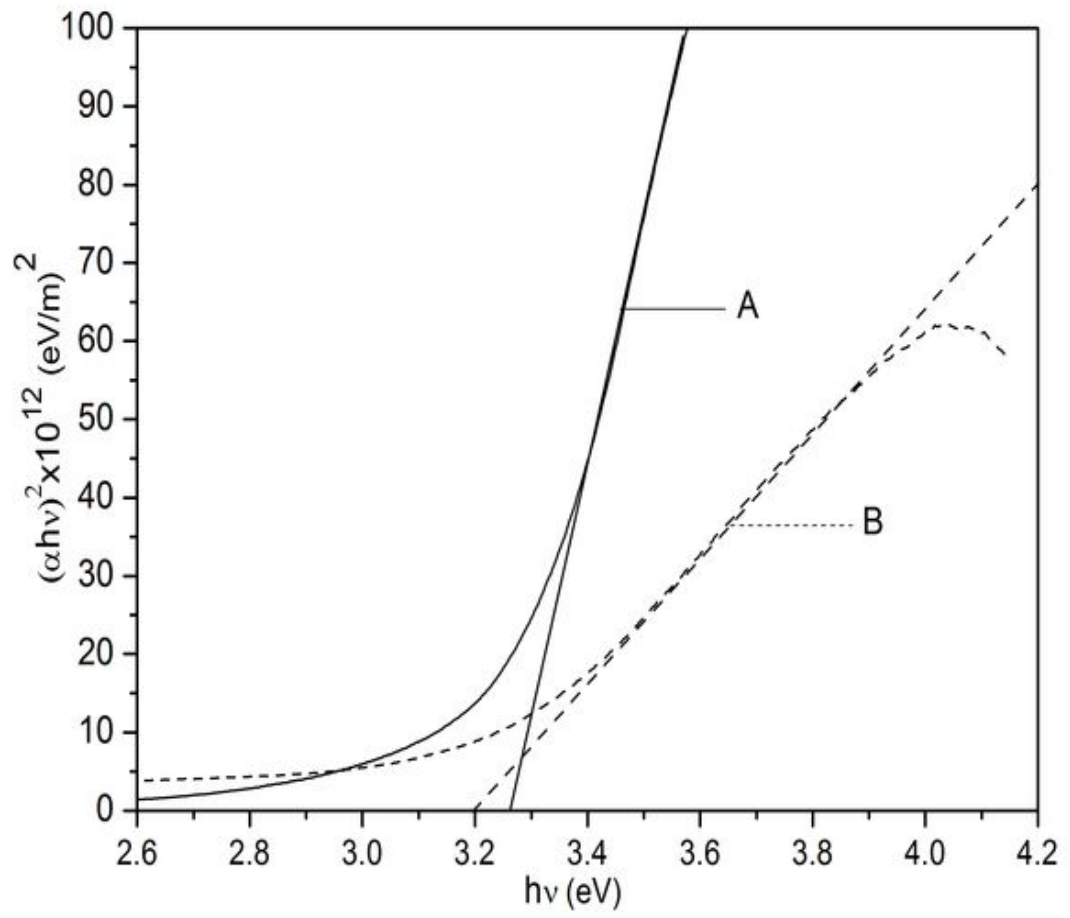


Figure 5.5: Optical band gap measurements of (A)undoped and (B) 5 % of indium doped ZnO thin films

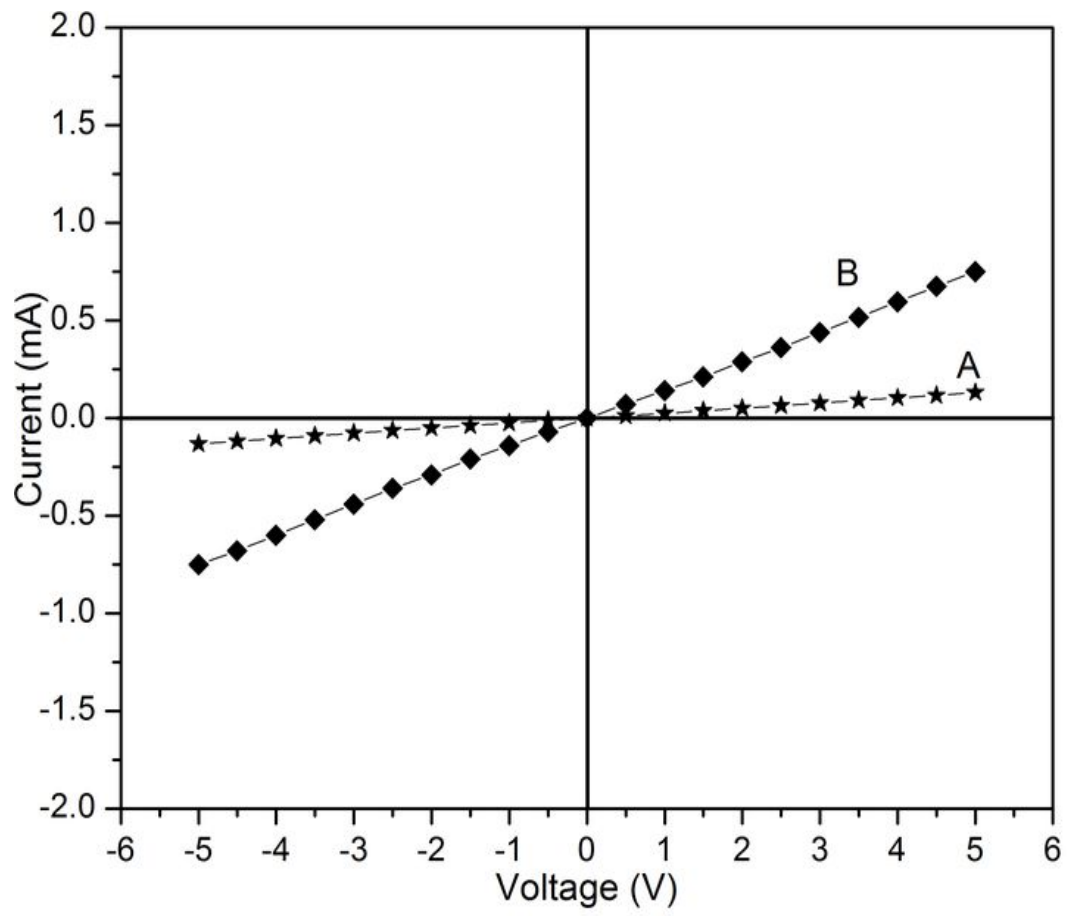


Figure 5.6: I-V Characteristics of (A)undoped and (B) 5 % of indium doped ZnO thin films

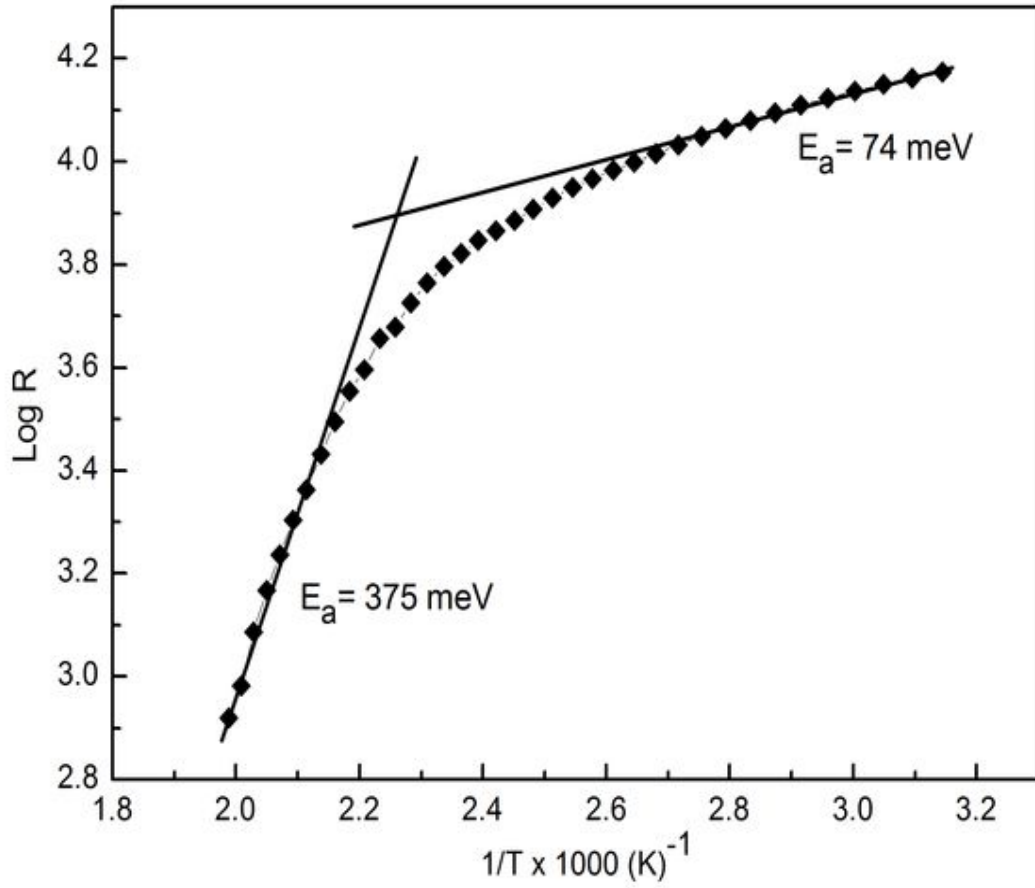


Figure 5.7: Logarithmic resistance profile of 5 % of indium doped ZnO thin film with respect to the reciprocal of temperature

5.4 Indium oxide doped ZnO thin films

In this section results of the investigations carried out on indium oxide (In_2O_3) doped ZnO thin films are presented. A mixture of 95% of ZnO powder and 5% of In_2O_3 powder is mixed and evaporated using “W” boat. The evaporation condition is maintained almost identical to that of undoped ZnO thin films and film thickness is maintained to 200 nm. Films in the as deposited condition were found to be dark brown in color in the as deposited condition. Films were annealed for two hours at 300°C so that they regain their stoichiometry and turn transparent. Transparent films were further subjected to different structural, electrical and optical characterizations.

A. Structural characterization

As in the previous cases the X- ray diffractogram of the In_2O_3 doped ZnO thin film ($\text{ZnO}:\text{In}_2\text{O}_3$) also did not show any peak in the θ range 20° to 80° . Thus the amorphous nature of the film is confirmed.

The scanning electron microscopy of $\text{ZnO}:\text{In}_2\text{O}_3$ thin film is shown in the figure 5.8. From the SEM image it can be concluded that the film has smooth and continuous surface with out significant modifications due to doping. As shown in previous cases the film was with flat surface.

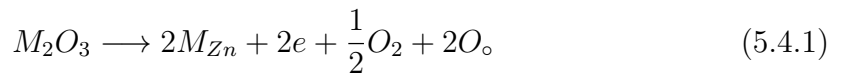
B. Optical characterization

The optical characterizations of $\text{ZnO}:\text{In}_2\text{O}_3$ thin films were carried out in the visible region of the electromagnetic radiation spectrum. The transmittance spectra of $\text{ZnO}:\text{In}_2\text{O}_3$ films compared with undoped ZnO thin film in the visible region of the electromagnetic spectrum is shown in the figure 5.10. From this figure it can be concluded that the transmittance of $\text{ZnO}:\text{In}_2\text{O}_3$ films did not disturb significantly due to doping. The transmittance of the film is found to be up to 90% which is almost same as that of undoped ZnO thin films.

The optical band gap of ZnO:In₂O₃ film compared with optical band gap of undoped ZnO thin film is shown in the figure 5.9. As it is mentioned in the previous sections, optical band gap of undoped ZnO thin films is 3.27 eV. This band gap is widened to 3.3 eV when the film is doped with 5 % of In₂O₃. This widening of optical band gap is generally attributed to the Burstein-Moss shift (Kykyneishi *et al* 2010), which results from the filling of electronic states near the bottom of the conduction band, due to the increase of carrier concentration in the ZnO film. In this process, the apparent band gap of a semiconductor is increased as the absorption edge is pushed to higher energies, because of all states close to the conduction band being populated. Tokumoto *et al* (2002) also made the same observation when ZnO thin film grown by spray pyrolysis method was doped with indium. In this case indium acetylacetonate was used as the source of dopant.

C. Electrical characterization

The I-V characteristics of undoped ZnO thin film and In₂O₃ doped ZnO thin film is shown in the figure 5.11. Graph shows the improvement in conductivity of thermally evaporated ZnO thin film due to doping and stability of current over a range of voltage from -5V to +5V. When the film is doped with 5% of In₂O₃, very good room temperature conductivity of $3.5 \times 10^3 \Omega^{-1} \text{cm}^{-1}$ is observed. This conductivity is found to be significantly high as compared to the room temperature conductivity of ZnO:In films. The high conductivity of indium oxide doped ZnO thin film can be explained by considering equation 5.4.1 (Elmer 2010).



where “M” represents III group metal. This can be indium, gallium or aluminum. According to equation 5.3.1, when In₂O₃, which is a group III oxide, is added to ZnO, it is assumed that, being a group III dopant atom, indium will occupy the zinc lattice site spending additional electrons which are not required for the bonding, to the conduction band (Elmer 2010). These additional electrons will contribute in improving the n-type conductivity of the film. Hence, the conductivity of the films doped with In₂O₃ is found to be very high as compared to that of films doped with

metallic indium.

The activation energy of ZnO:In₂O₃ film is found out by measuring the resistance of the film with the variation of temperature. The study was carried out by increasing the temperature of the film up to 300°C from room temperature. The graph, Log(R) versus 1000/T, for ZnO:In₂O₃ films is shown in figure 5.12. This curve shows a linear behavior in two regions. The first one from (1.7-2.1) 1/K and the other from (2.3-3.2) 1/K. In these two ranges the activation energy is proportional to the slope and the activation energy can be calculated using the equation 5.3.1. In the case of ZnO:In₂O₃ an activation energy of 29 meV was measured in the 1000 x (1/T) range (2.3-3.22 [1/K]) and another of 71 meV in 1000 x (1/T) range (1.7-2.1) [1/K]. Basically electron concentration in ZnO thin film increases by III group oxide doping and the trapping levels with activation energy bellow 55 meV contribute to the electrical conductivity with very low energy cost which improves the dark conductivity of the film (Gonzales *et al* 1998).

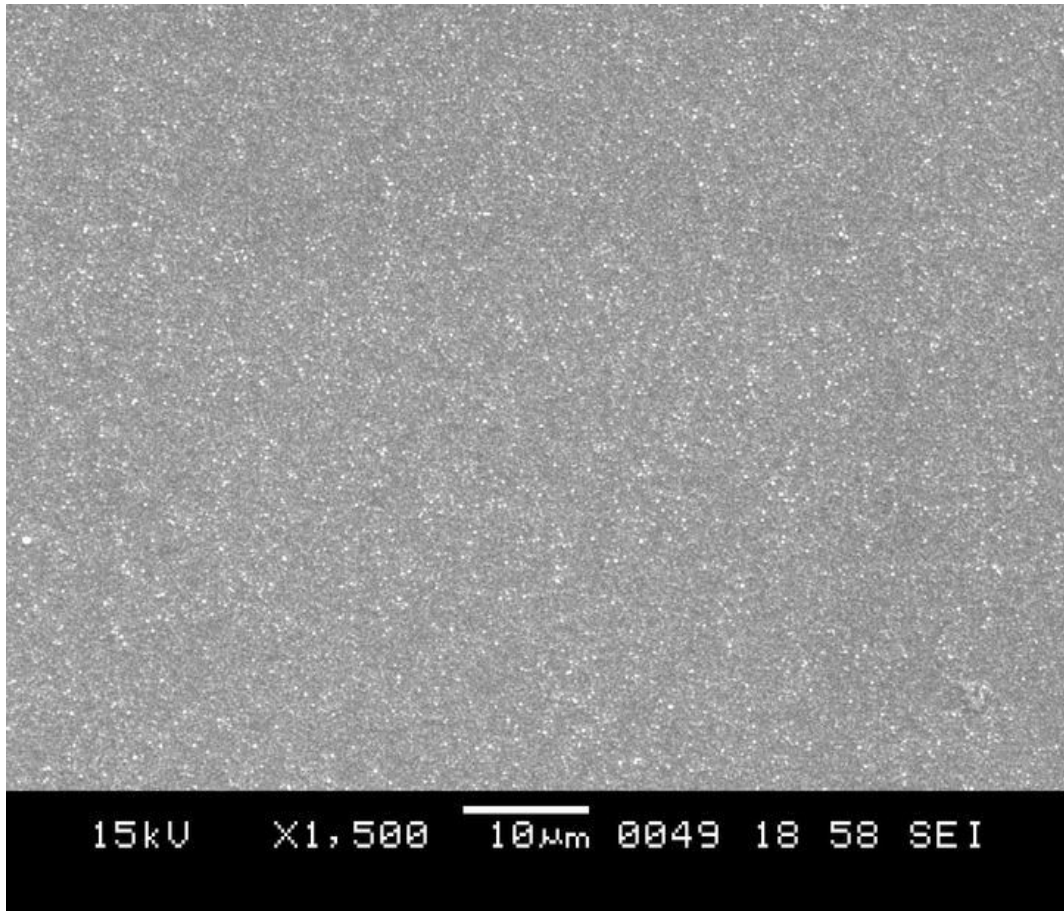


Figure 5.8: SEM image of the surface of ZnO:In₂O₃ thin film

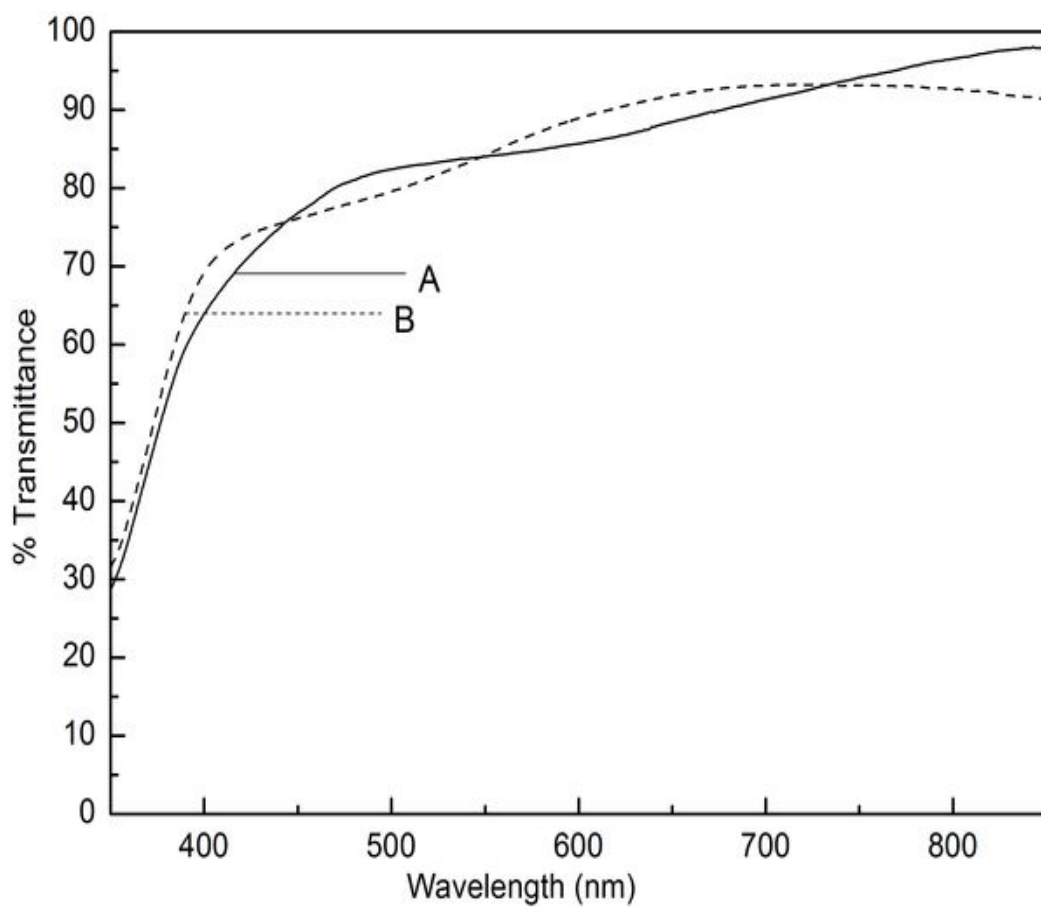


Figure 5.9: Transmittance spectra of (A) undoped and (B) ZnO:In₂O₃ thin films

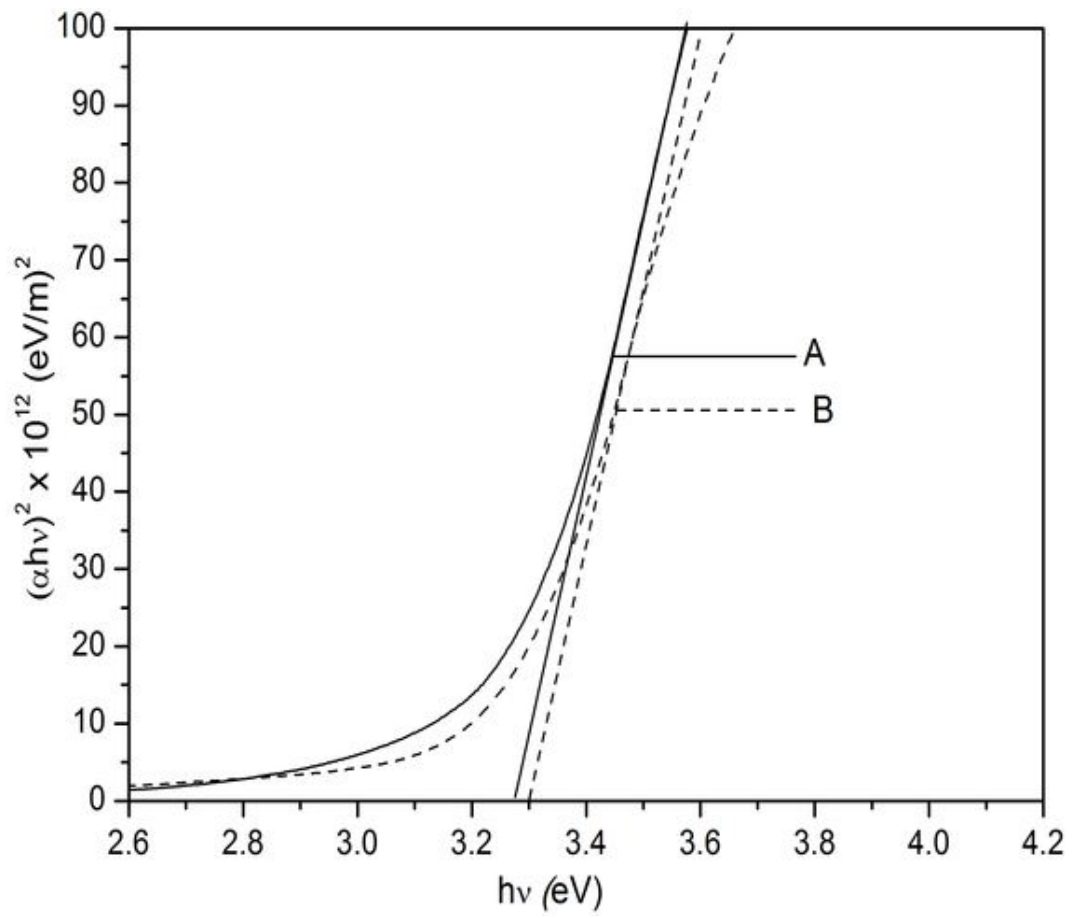


Figure 5.10: Optical band gap measurements of (A) undoped and (B) ZnO:In₂O₃ thin films

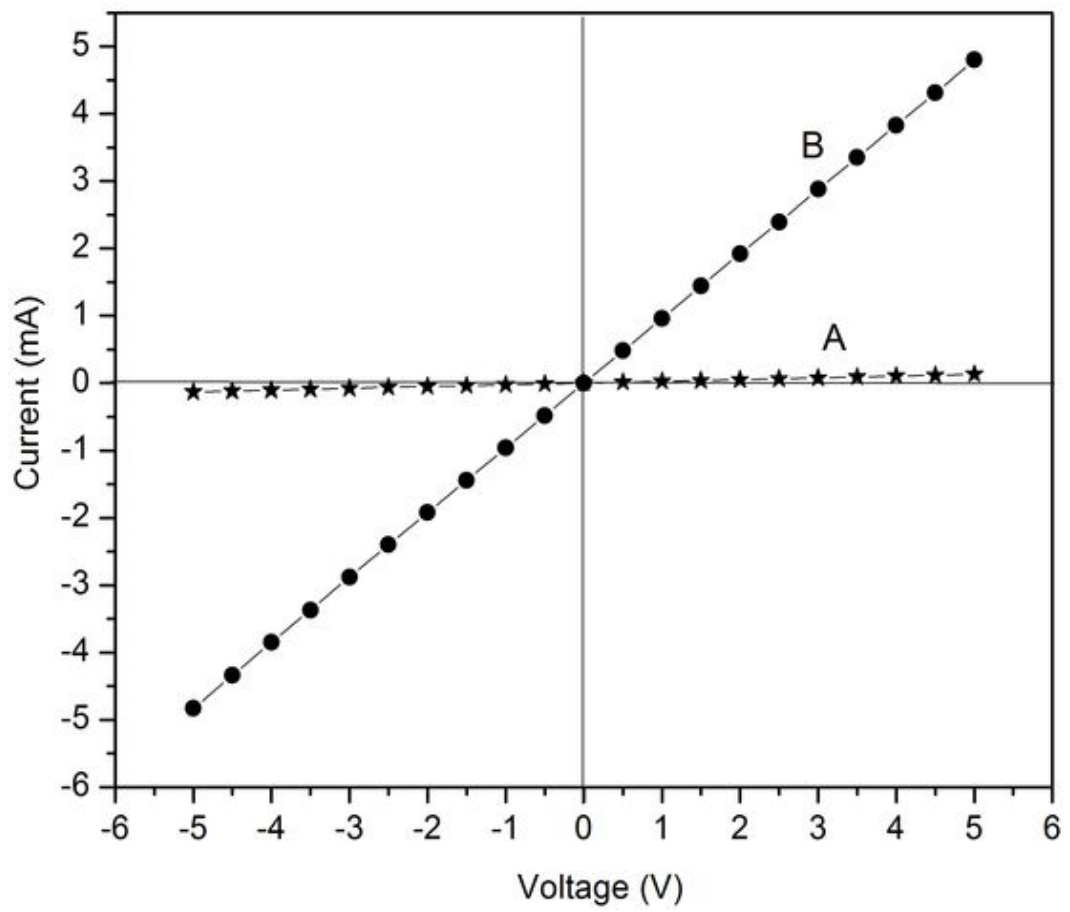


Figure 5.11: I-V characteristics of (A) undoped and (B) ZnO:In₂O₃ thin films

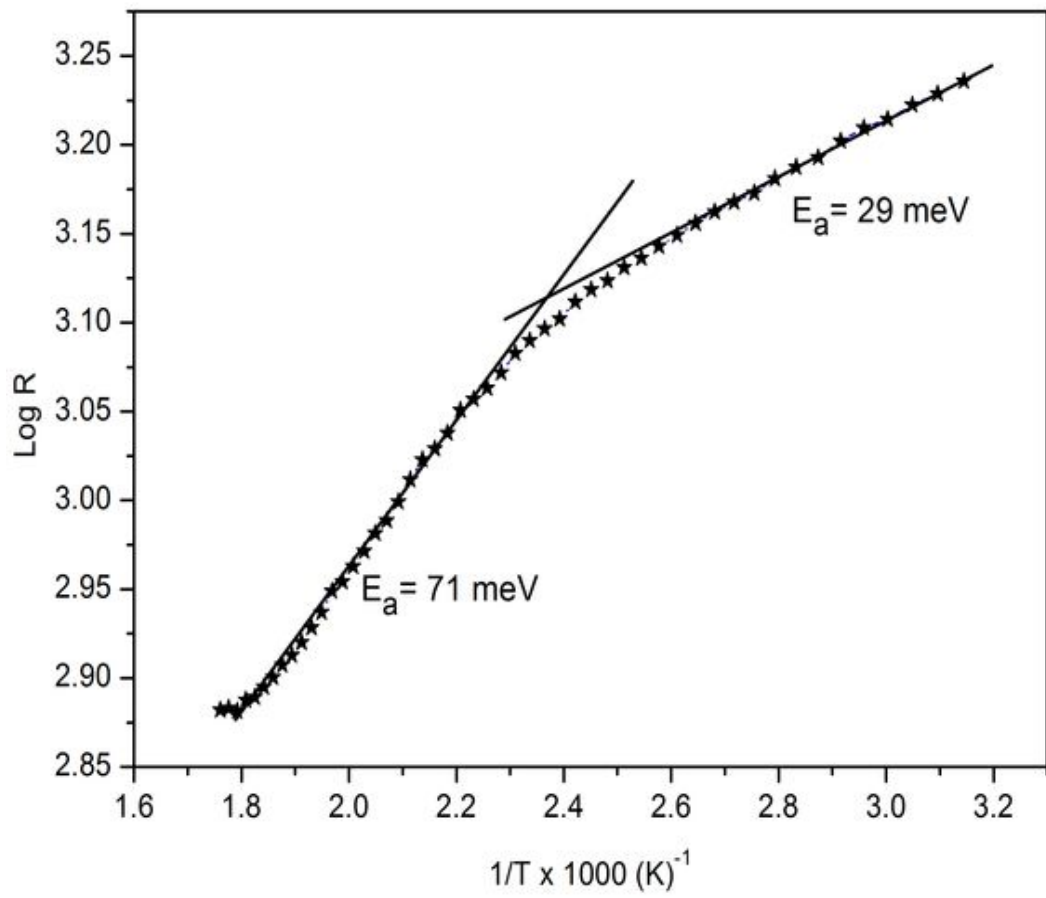


Figure 5.12: Logarithmic resistance profile of ZnO:In₂O₃ thin film with respect to the reciprocal of temperature

5.5 Gallium oxide doped ZnO thin films

In the present section of study, thermally evaporated ZnO thin film is doped with 5% of gallium oxide. The films were prepared by evaporating a mixture of 95% of zinc oxide powder and 5% of gallium oxide powder using “W” boat. The vacuum maintained during the process of evaporation is of the order of 10^{-5} mbar. The other evaporation conditions were maintained almost identical to that of undoped ZnO thin films. In this case also, thickness of the film is maintained to 200 nm. These films were dark brown in appearance in the as deposited condition and on annealing at 300°C for two hours these films turned transparent. These transparent films were subjected to different characterization as explained in the following sections.

A. Structural characterization

As it is reported in the previous sections, ZnO thin film doped with gallium oxide (ZnO:Ga₂O₃) also did not show any peak in the θ range 20° to 80°, which confirms the amorphous nature of the film. The scanning electron microscopy of ZnO:Ga₂O₃ thin film is shown in the figure 5.13. From the SEM image it can be concluded that the ZnO:Ga₂O₃ film also has smooth and continuous surface with out significant modifications due to doping. As reported in previous cases, in this case also the film had flat surface with out much disturbance in the surface topography.

B. Optical characterizations

The optical transmittance of ZnO:Ga₂O₃ thin films is measured in the visible region. The transmittance spectra of ZnO:Ga₂O₃ compared with that of undoped ZnO thin films is shown in the figure 5.14. From spectra we observe that transmittance of ZnO thin film is reduced after 600 nm on doping with Ga₂O₃. In this case average transmittance of the film is found to be only up to 85%.

The optical band gap of ZnO:Ga₂O₃ films compared with that of undoped ZnO thin films is shown in the figure 5.15. As it is reported in the previous sections, optical band gap of undoped ZnO thin films is 3.27 eV and after doping with 5% of

Ga₂O₃ the band gap of the film is reduced to 3.25 eV. This reduction in the band gap is due to the formation of additional levels below the conduction band as already mentioned in section 5.3.

C. Electrical characterizations

On doping ZnO thin film with 5% of Ga₂O₃, a great improvement in the conductivity of the film is observed. Doped films showed a room temperature conductivity of $8.7 \times 10^3 \Omega^{-1} \text{cm}^{-1}$. This considerably high improvement in electrical conductivity brought in by Ga₂O₃ doping can be explained again by considering equation 5.4.1. When group III oxides like Ga₂O₃ are added to zinc oxide, it is assumed that group III dopant atoms will built into the zinc lattice sites spending additional electrons which are not required for the bonding to the conduction band according to the equation 5.4.1. These additional electrons will contribute in improving the conductivity of the film. Thus metal oxide doped ZnO thin films show significantly high electric conductivity. The I-V characteristic of ZnO:Ga₂O₃ film is presented in figure 5.16.

To calculate the activation energy, variation in the resistance of films with the change in temperature is recorded. Study was carried out by increasing the temperature of the film up to 300°C from room temperature. In this low temperature, extrinsic conduction predominates since ZnO has a wide band gap of the order of 3.3 eV. The graph shown in figure 5.17 represents $\log(R)$ verses $1/T$ curve of ZnO:Ga₂O₃ thin films. The curve shows a linear behavior in two regions. The first one from (1.7-2.1) 1/K and the other from (2.3-3.2) 1/K. In these two ranges the activation energy is proportional to the slope and can be calculated using equation 5.2.1. ZnO:Ga₂O₃ thin film presents activation energy of 26 meV in the 1000(1/T) range (2.3-3.2 [1/K]) and another activation energy of 68 meV in the 1000(1/T) range (1.7-2 [1/K]). Thus like ZnO:In₂O₃ films, ZnO:Ga₂O₃ film is also found to have one energy level with activation energy lower than 55 meV. This will contribute to the electrical conductivity of the film with very low energy cost and thus improving the dark conductivity of the film (Gonzales *et al* 1997).

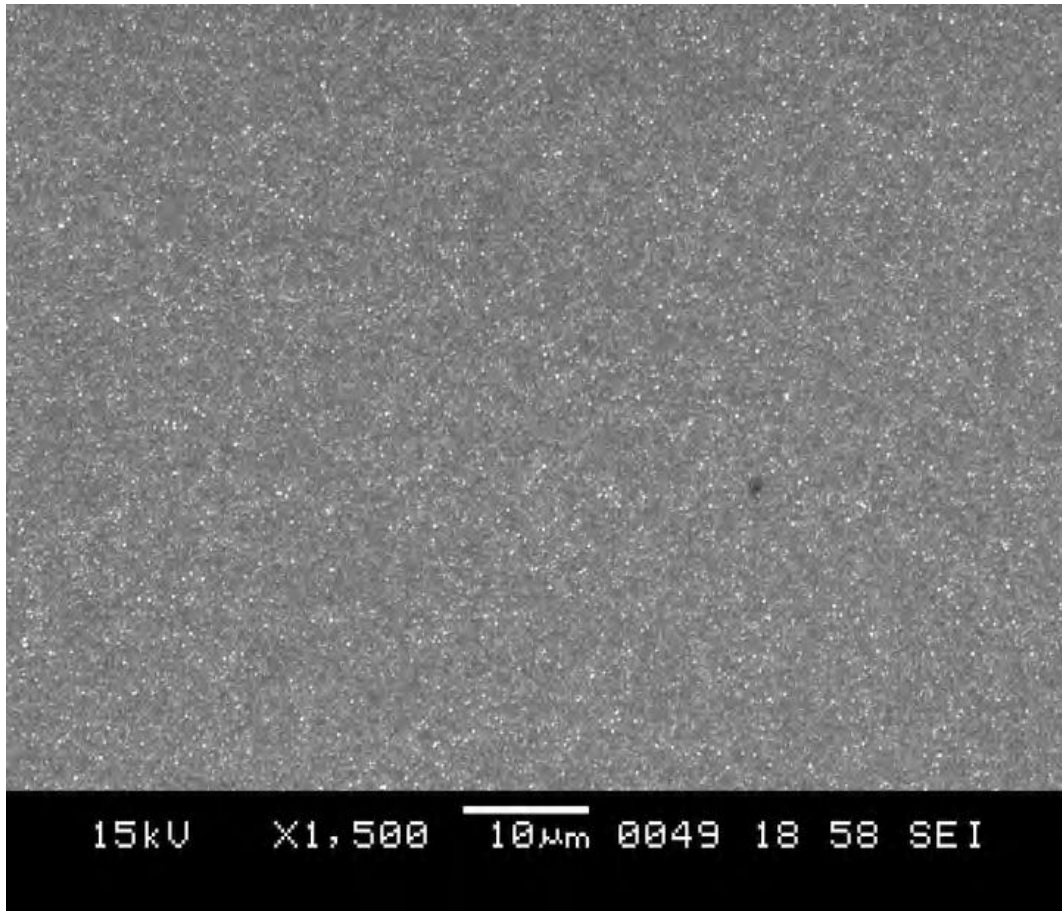


Figure 5.13: SEM image of ZnO:Ga₂O₃ thin film

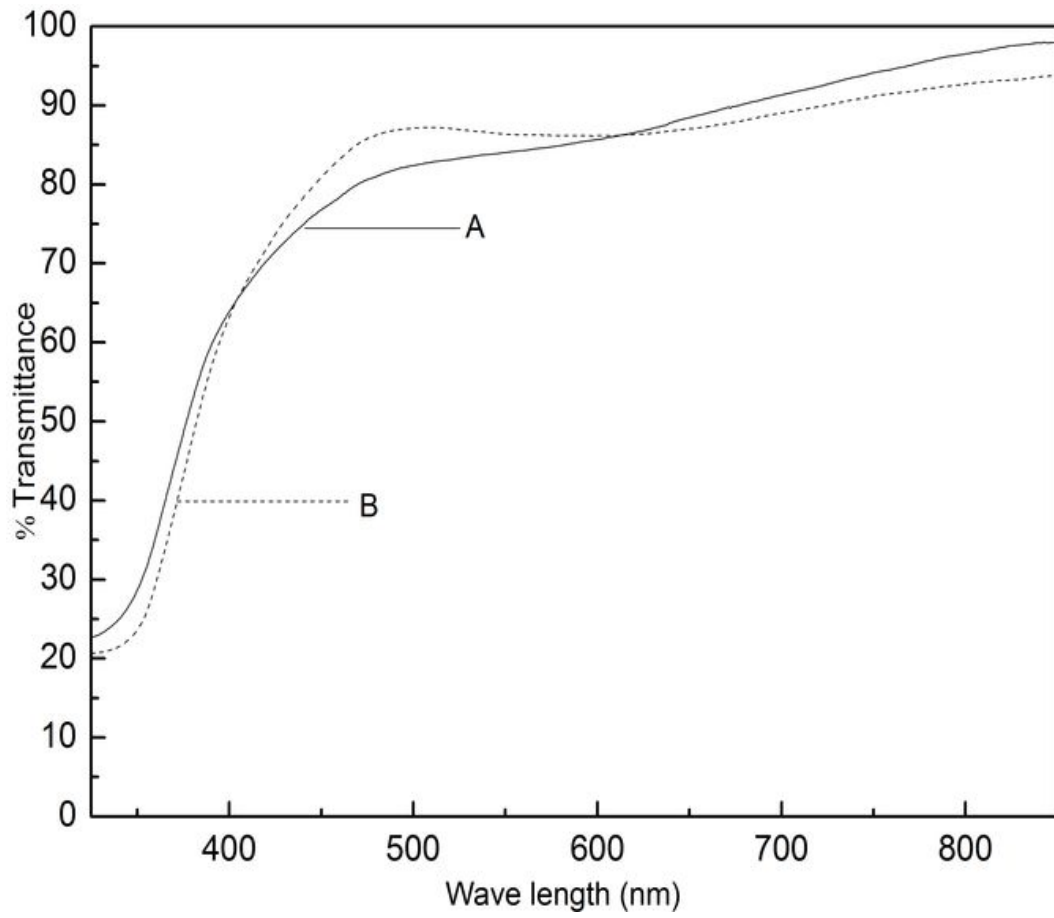


Figure 5.14: Transmittance spectra of (A) undoped and (B) ZnO:Ga₂O₃ thin films

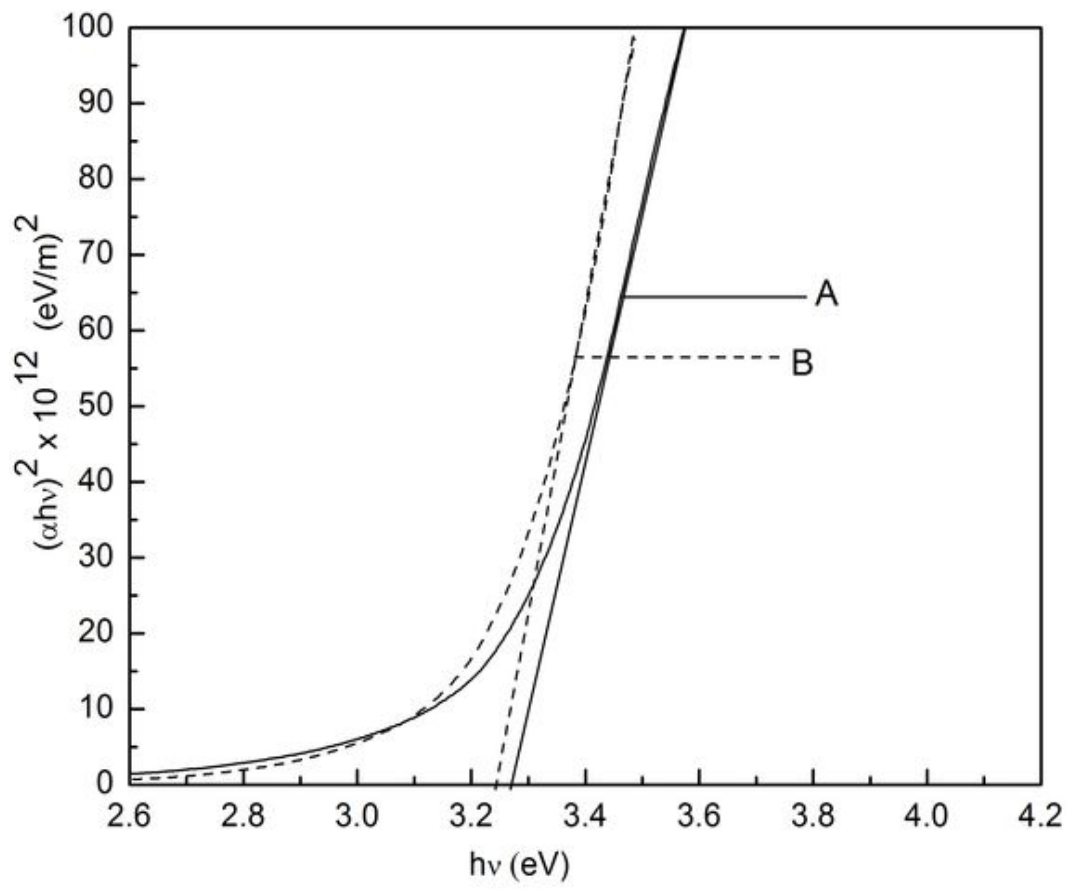


Figure 5.15: Optical band gap measurements of (A) undoped and (B) ZnO:Ga₂O₃ thin films

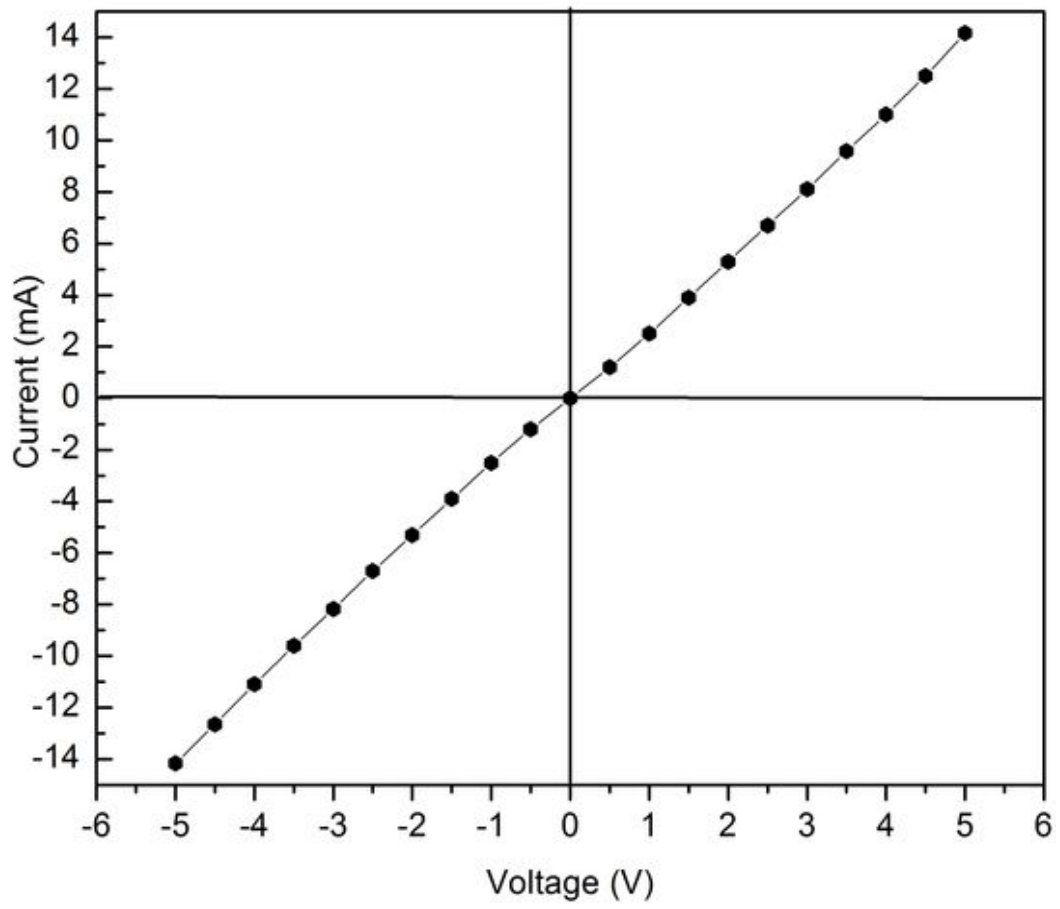


Figure 5.16: I-V characteristic ZnO:Ga₂O₃ thin film

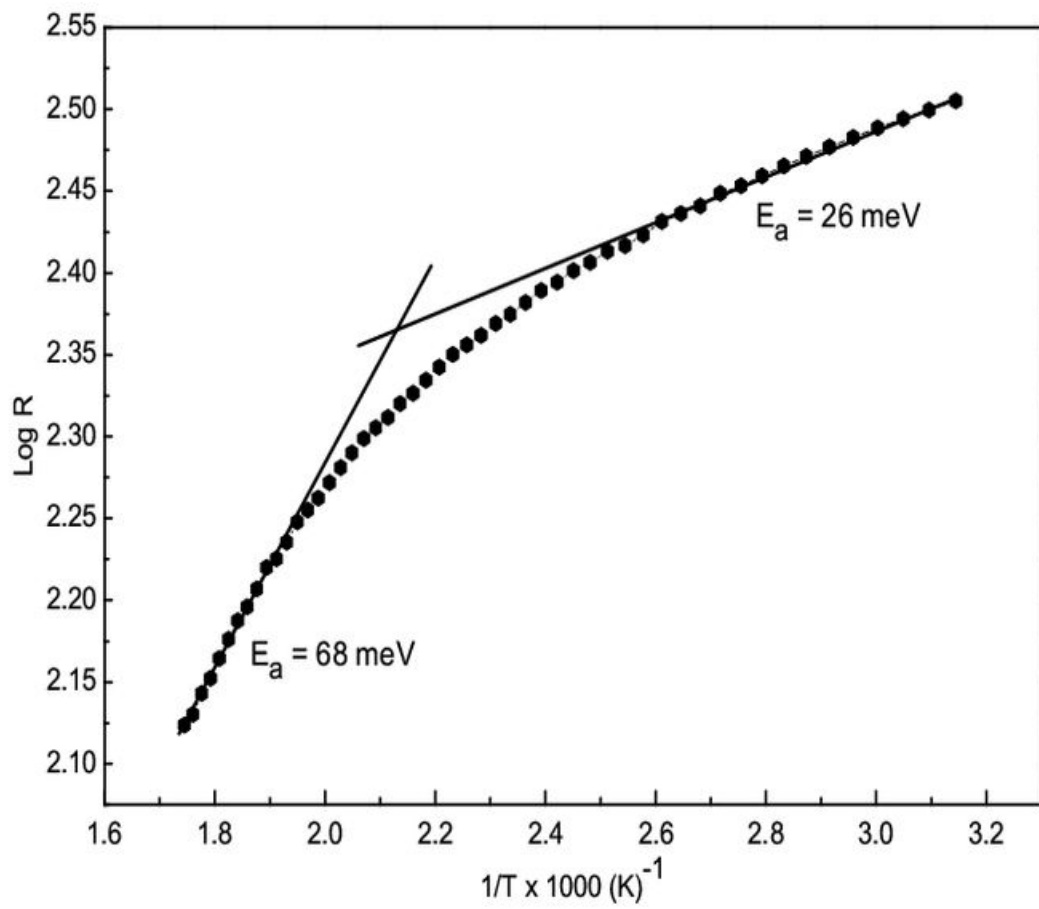


Figure 5.17: Logarithmic resistance profile of of ZnO:Ga₂O₃ thin film with respect to the reciprocal of temperature

5.6 Aluminum oxide doped ZnO thin films

The last section of this investigation concentrated on doping of thermally evaporated ZnO thin film with aluminum oxide (Al_2O_3). A mixture of 95% ZnO powder and 5% of Al_2O_3 powder is evaporated using a “W” boat. The evaporation was carried out under a vacuum of the order of 10^{-5} mbar, maintaining other evaporation conditions almost identical to that of undoped ZnO thin films. The film thickness was maintained to 200 nm. As in previous cases the aluminum oxide doped ZnO thin films ($\text{ZnO}:\text{Al}_2\text{O}_3$) appeared dark brown in color in the as deposited condition. The films turned transparent on annealing them for 2 hours at 300°C . These transparent films were further subjected to different structural, optical and electrical characterization and results of these characterization are mentioned as follows.

A. Structural characterization

ZnO thin films doped with aluminum oxide are also found to be amorphous in nature since X-ray diffractogram of these films did not show any peak in the θ range 20° to 80° ,

The scanning electron microscopy of $\text{ZnO}:\text{Ga}_2\text{O}_3$ thin film is shown in the figure 5.18. From the SEM image it can be concluded that the $\text{ZnO}:\text{Al}_2\text{O}_3$ film also has smooth, continuous and flat surface.

B. Optical characterization

The transmittance spectra of $\text{ZnO}:\text{Al}_2\text{O}_3$ film compared with that of undoped ZnO thin film is shown in the figure 5.19. Interestingly it is found that transmittance of ZnO thin film has been increased after doping them with Al_2O_3 . It is observed that the films have an excellent transmittance of up to 95% in the visible region of the electromagnetic radiation spectrum. Similar observation was reported by Alaeddin *et al* (2009) who obtained aluminum doped ZnO thin films by spray pyrolysis method using aluminum chloride as the source of dopant and Gonzalez *et al* (1998), who obtained aluminum doped ZnO thin films by sol-gel technique, using aluminum chloride

and aluminum nitrite as the source of dopants.

The plot of variation of $(\alpha h\nu)^2$ with $(h\nu)$ for ZnO:Al₂O₃ films in comparison with that of undoped ZnO thin films is shown in figure 5.20. From this graph we find that optical band gap of ZnO:Al₂O₃ thin films is 3.24 eV which is lower than the band gap of undoped ZnO thin films (3.27 eV). This may be due to the formation of donor levels below the conduction band. These donor levels will absorb the photons having energy lower than the band gap value and thus reduce band gap value.

C. Electrical characterization

On doping ZnO thin film with 5% of Al₂O₃, the conductivity of the film is found to increase up to $5 \times 10^3 \Omega^{-1} \text{cm}^{-1}$. As repeatedly mentioned in this chapter this high conductivity is due to the contribution of additional electrons which are liberated on doping third group metal oxide to ZnO, according to equation 5.4.1. In addition to the III group metal atoms which occupies zinc lattice site and act as donors, these electrons also contribute in the conductivity of the films. Thus significantly high conductivity in the film is observed. The I-V characteristic of ZnO:Al₂O₃ film is shown in the figure 5.21.

The activation energy of ZnO:Al₂O₃ films is found out by raising the temperature of the film from room temperature to 300°C and recording the variation of resistance of the film with temperature. The graph in figure 5.22 represents the logarithmic resistance profile of ZnO:Al₂O₃ film with respect to the reciprocal of temperature. The graph in the figure shows two linear regions. The first one from (1.7-2.1) 1/K and the other from (2.3-3.2) 1/K. The activation energy of the film is proportional to the slope of the linear portions of the graph and can be calculated using equation 5.3.1. ZnO:Al₂O₃ thin film shows first activation energy of 43 meV in the range [2.3-3.2(1/K)] and second activation energy of 142 meV in the range of [1.7-2(1/K)]. As in the case of ZnO:In₂O₃ and ZnO:Ga₂O₃ thin films, ZnO:Al₂O₃ thin film also has one trapping level with activation energy lower than 55 meV. This will contribute in improving the dark conductivity of the film.

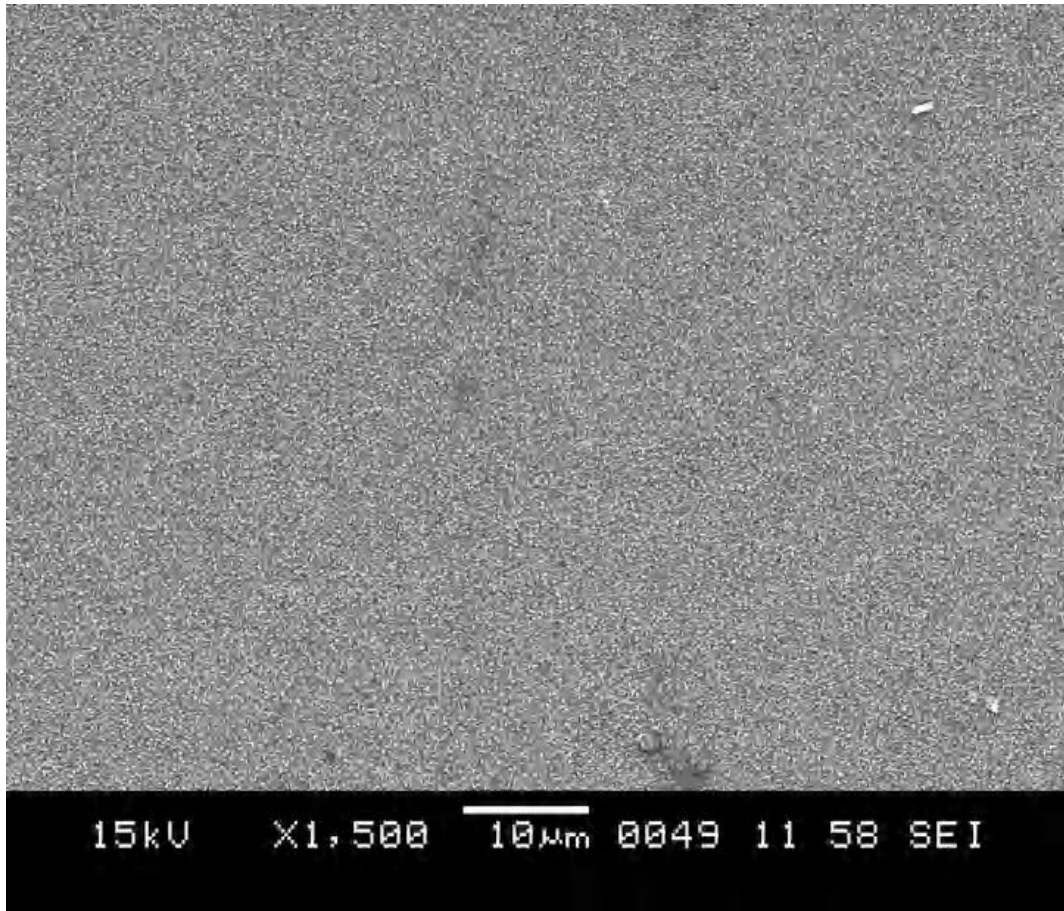


Figure 5.18: SEM image of ZnO:Al₂O₃ thin film

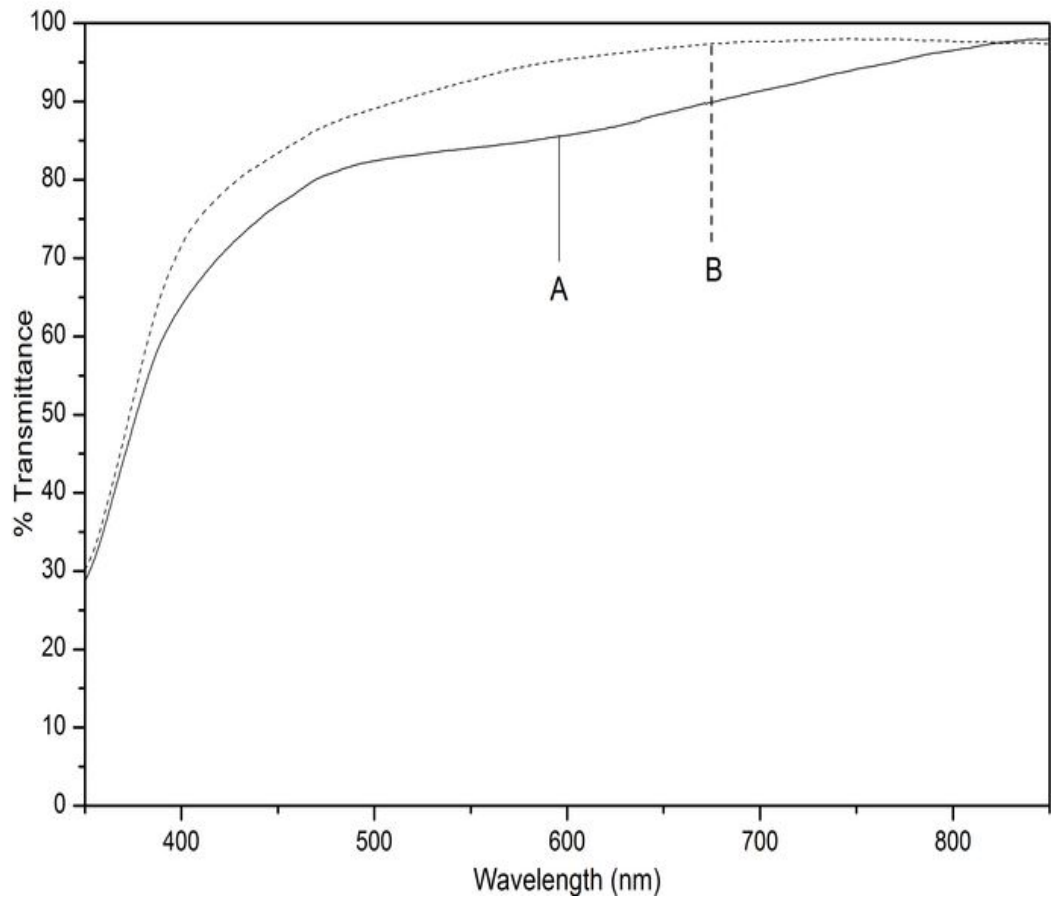


Figure 5.19: Transmittance spectra of (A) undoped and (B) ZnO:Al₂O₃ thin films

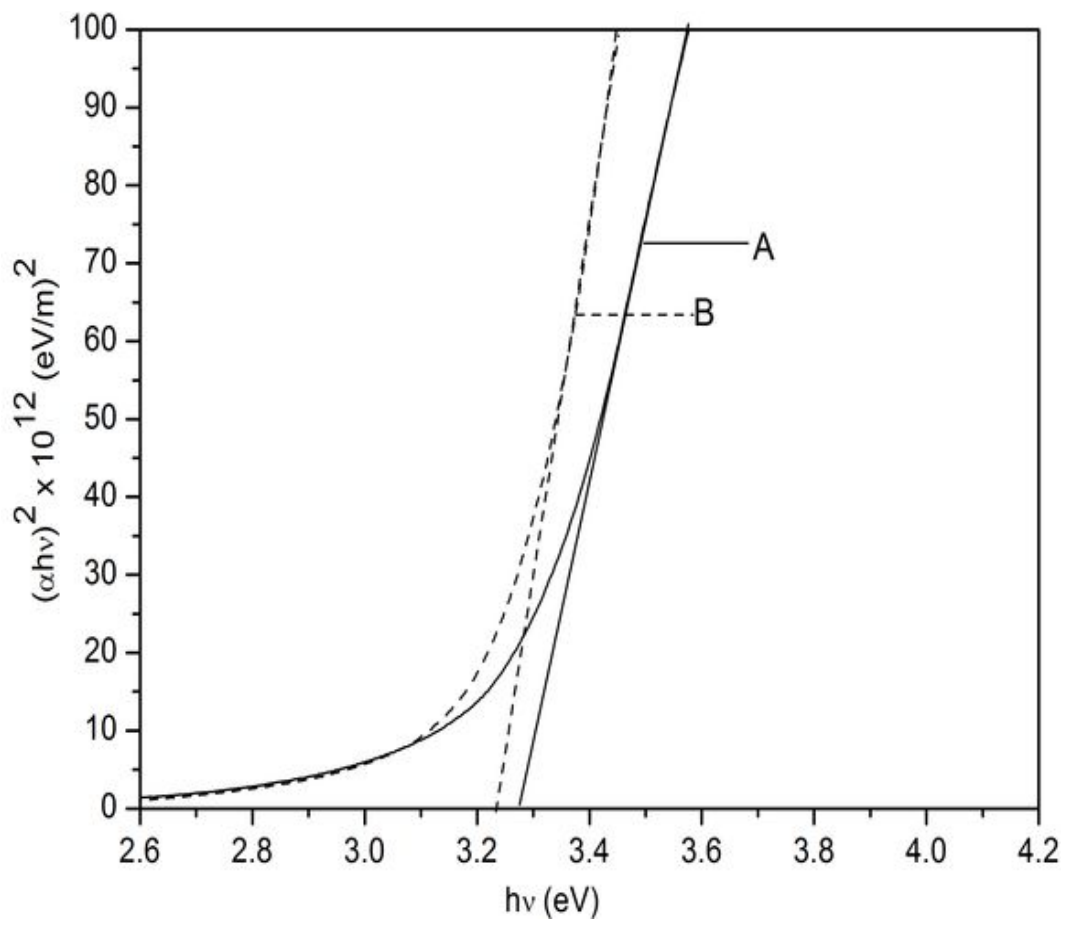


Figure 5.20: Optical band gap measurements of (A) undoped and (B) ZnO:Al₂O₃ thin films

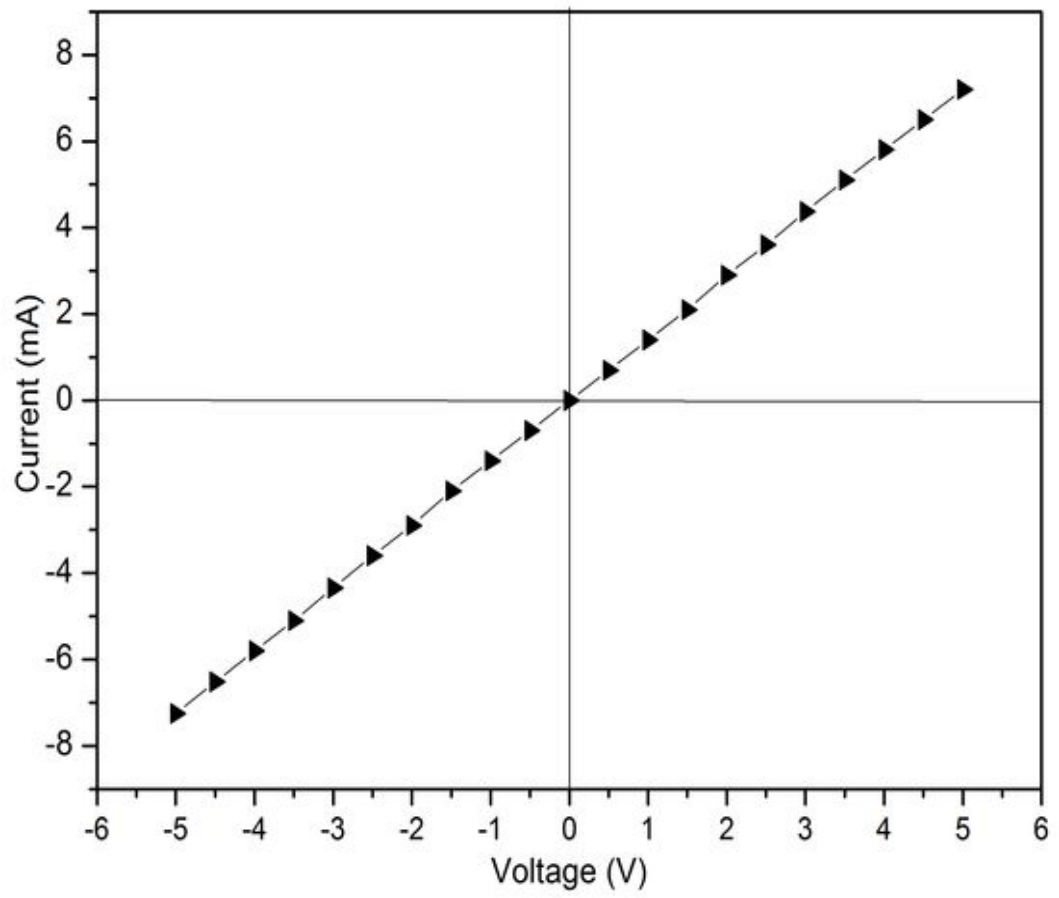


Figure 5.21: I-V characteristic ZnO:Al₂O₃ thin film

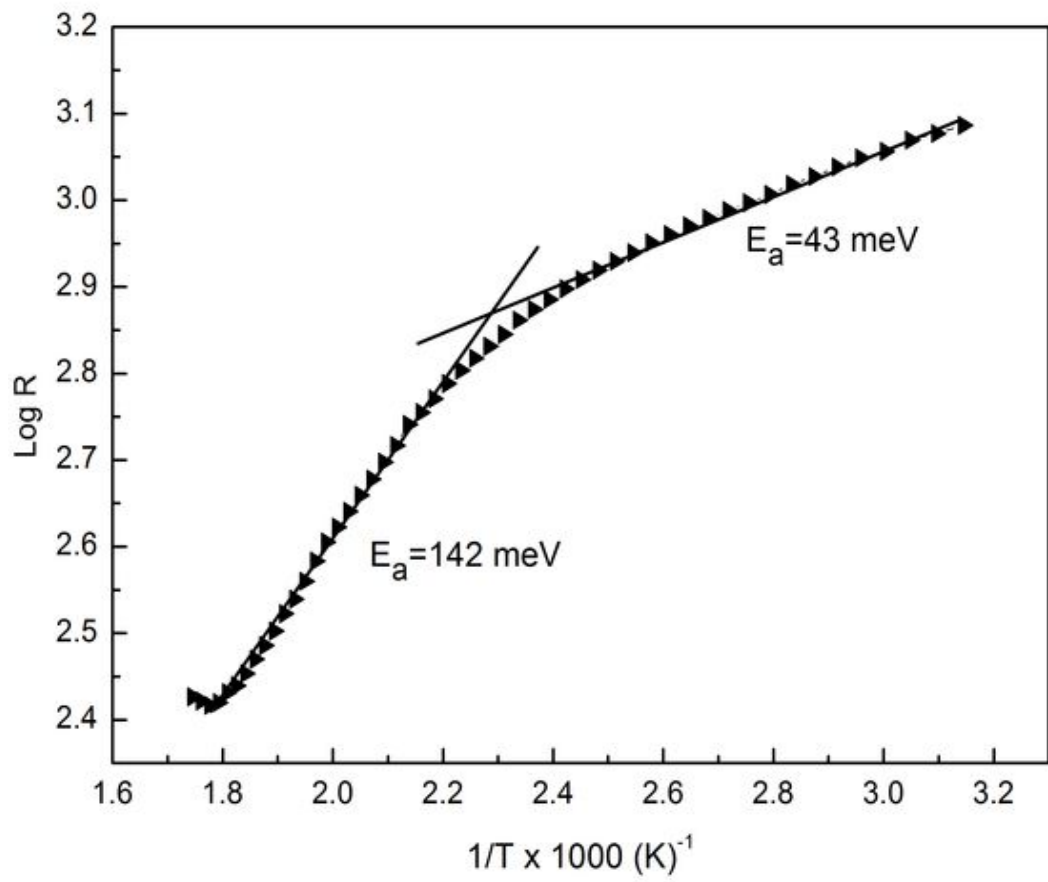


Figure 5.22: Logarithmic resistance profile of of ZnO:Al₂O₃ thin film with respect to the reciprocal of temperature

Thus, third group oxide doped ZnO thin films with a good combination of conductivity and transmittance are obtained by vacuum deposition technique. All three third group oxide doped ZnO thin films are found to be amorphous in nature with smooth and flat surface topography, which will lead to the low internal stress and are well suited for the application of flat panel displays. The absence of grain boundaries excludes the associated carrier scattering mechanism and thus higher performance of the material is expected. Activation energy measurements studies have shown that all doped films have two donor levels below the conduction band. Third group oxide doped films have one donor level with activation energy below 55 meV. This will contribute in the electrical conductivity of the film with very low energy loss.

It can be concluded that doping of vacuum evaporated ZnO thin films with n-type dopants improves its electrical properties while retaining its transmittance and among different n-type dopants aluminum oxide is the suitable dopant for ZnO thin film since it improves the room temperature conductivity with visible region transmittance of the film.

The electrical and optical properties of undoped and doped ZnO thin films studied in this work are summarized in table 5.1.

Table 5.1: Opto electronic properties of undoped and doped ZnO thin films studied in the present work.

Sample	Transmittance (%)	Conductivity ($\Omega^{-1}cm^{-1}$)	Eg (eV)	Ea for shallow donor level	Ea for deep donor level
ZnO	90	90	3.27	130 meV	261 meV
ZnO:In	90	500	3.2	74 meV	375 meV
ZnO:In ₂ O ₃	90	3.8×10^3	3.3	29 meV	71 meV
ZnO:Al ₂ O ₃	95	5×10^3	3.24	46 meV	142 meV
ZnO:Ga ₂ O ₃	85	8.7×10^3	3.25	28 meV	68 meV

Chapter 6

Summary and conclusions

6.1 Summary of the present work

ZnO thin film has gained substantial interest in the research community in past two decades. Various physical and chemical methods have been employed to obtain good quality of ZnO thin films. Irrespective of the interest in ZnO thin films and its technological importance, only few reports have been devoted to study its preparation by vacuum evaporation method. The present work concentrated on the study of structural, compositional optical and electrical properties of ZnO thin films prepared by thermal evaporation technique. Further, modulations in the properties of these films by doping with third group metal and metal oxides is studied in detail.

In this investigation ZnO thin films with thickness 500 nm were obtained by using both molybdenum (Mo) and tungsten(W) evaporation sources. The ZnO thin films obtained in both the cases were found to be dark brown in color and opaque in nature in the as deposited condition. This is due to the decomposition of ZnO powder in to zinc and atomic oxygen during the process of evaporation. These films were expected to be zinc rich in the as deposited condition based on the previously reported results. Hence film was then annealed at different temperature, so that it undergoes oxidation, regains its stoichiometry and turns transparent. Films obtained using W evaporation source gained average visible region transmittance of up to 75% after annealing at 400°C for 4 hours. Whereas, in the case of films obtained using Mo

evaporation source 70% transmittance is achieved after annealing the film at 500°C for 4 hours.

The X-ray diffractogram of ZnO thin films deposited using Mo and W evaporation sources did not show any peak in the as deposited condition as well as after annealing. This confirmed the amorphous nature of films. SEM images of the films showed the flat and smooth surface in the as deposited condition as well as after annealing in both the cases with out significant change after annealing.

The compositional analysis of the film carried out with the help of EDAX showed the incorporation of atoms of evaporation source materials in ZnO thin films in both the cases. ZnO thin film obtained using W boat contained 3% of W atoms. It is shown that after annealing the film at 400°C for 4 hours the percentage of W atoms reduced to 2.5%. In the case of ZnO thin film obtained using Mo boat, the percentage of Mo atoms in the film in the as deposited condition was found to be 18%. This was reduced to 9.71% after annealing the film at 400°C for 4 hours. The percentage of incorporated atoms of boat material in this case is further reduced to 4.16% after annealing the film at 500°C for 4 hours. This incorporation of boat materials in to the film during the process of evaporation is explained by considering the vapor pressure curve of the elements. The reduction in the percentage of Mo atoms and W atoms in the films after annealing may be due to the re-evaporation of volatile MoO and WO which might have formed during the process of deposition of the films.

Based on these results it was concluded that W is the better source for the evaporation of ZnO powder and for further investigations ZnO thin films of thickness 200 nm were obtained using W evaporation source. ZnO thin films of thickness 200 nm were dark brown in color, and opaque in nature in the as deposited condition. These films attained visible region transmittance of up to 90% after annealing them at 300°C for 2 hours. Since complete oxidation temperature and duration depends on thickness, structure and composition of films, annealing duration and temperature is reduced in this case as compared to the films of thickness 500 nm. The XPS analysis made to study the composition of the film after annealing showed that the film is

having 45.563 at% of zinc, 40.048 at% of oxygen bonded to the zinc and 14.389 at% oxygen loosely bonded to the surface of the film. This confirms the oxygen deficiency in the film.

The electrical characterization of this film made using silver contacts showed that the vacuum evaporated ZnO thin film is having a room temperature conductivity of $92 \Omega^{-1}\text{cm}^{-1}$. This conductivity is significantly high as compared to the conductivity of undoped ZnO thin films reported previously. This high conductivity of film at room temperature is attributed to the oxygen vacancies present in the the film. The hot probe study showed the n-type nature of carrier concentrations and the activation energy measurements showed that the vacuum evaporated ZnO thin film has two donor levels below the conduction band, one with activation energy of 130 meV and other with activation energy 261 meV.

In the next step these vacuum evaporated ZnO thin films were doped with third group dopants to improve the n-type conductivity of films. The objective of this research is to improve the conductivity of vacuum evaporated ZnO films, retaining transmittance of the films. Initially vacuum evaporated ZnO thin films were doped with 3%, 5% and 7% of pure indium metal and the transmittance and conductivity of these films were measured. The conductivity measurement of these films showed that the ZnO thin films doped with 3%, 5% and 7% of indium metal had conductivity of $140 \Omega^{-1}\text{cm}^{-1}$, $580 \Omega^{-1}\text{cm}^{-1}$ and $1683 \Omega^{-1}\text{cm}^{-1}$ respectively. The transmittance study of indium doped vacuum evaporated ZnO films showed that films doped with 3% and 5% of indium metal have visible region transmittance of up to 90% which is almost equal to the transmittance of undoped ZnO thin films. But in the case of 7% doped ZnO thin films the transmittance of the film decreased to 60%. Based on these studies the concentration of dopants to be added to the vacuum evaporated thin film is limited to 5% since our work was focused on improving the conductivity of the ZnO film with out disturbing its transmittance.

The optical band gap measurements of 5% doped ZnO thin film showed that the optical band gap of the films decreases to 3.2 eV, from 3.27 eV in the as deposited

condition. This decrease in the band gap is due to the formation of additional donor levels below the conduction band which will absorb photons having energy lower than the band gap value. The activation energy measurement of the film showed that 5% indium doped film is having two donor levels below the conduction band with activation energies 375 meV and 74 meV.

Further the film was doped with 5% of indium oxide to study the nature of indium as a dopant in the form of metal and metal oxide. The films of thickness 200 nm were obtained. After annealing at 300°C for 2 hours films are found to have transmittance of up to 90% which is almost equal to the transmittance of undoped film. The optical band gap of the film is found to be widened up 3.3 eV after doping. This widening of the optical band gap is due to the Burstein Moss shift effect in the film. Electrical characteristics of these films show that films are having very high room temperature conductivity of the order of $3.5 \times 10^3 \Omega^{-1} \text{ cm}^{-1}$. This significantly high conductivity in the film compared to that of indium doped film is due to the liberation additional electrons on doping with third group metal oxides. These electrons does not take part in bonding and transfered conduction band, thus contributing in improving the conductivity of film. The activation energy measurement of the film show that the film is having two donor levels below the conduction band, one with activation energy 29 meV and other with activation energy 71 meV. It has been already reported that donor levels with activation energy lower than 55 meV will contribute to conductivity of films with very low energy cost and thus support the dark conductivity of the film. The SEM analysis of these films show that films are having smooth and continuous surface. This confirms that there is no significant modification in the surface topography of films due to doping.

The film is then doped with 5% gallium oxide. A detailed study of its structural, optical and electrical properties were carried out. As in the previous cases the film was found amorphous with smooth surface. The visible region transmittance spectrum of the film showed a transmittance of up to 85%. The band gap of the film in this case is reduced to 3.25 eV. This reduction in the band gap is due to the formation of energy levels below the conduction band. The room temperature conductivity of

the film is found to be $8.7 \times 10^3 \Omega^{-1} \text{ cm}^{-1}$. In this case also the film is found to have two donor levels with activation energies 26 meV and 68 meV.

Finally the film is doped with 5% of aluminum oxide and its structural, optical and electrical properties were investigated. Similar to the other films studied in this work the film was found to be amorphous with flat and smooth surface topography. The optical studies show that the transmittance of aluminum oxide doped ZnO thin films up to 95% which was more than the transmittance of the undoped ZnO thin film and the optical band gap of the film is reduced to 3.24 eV due to doping. The room temperature conductivity of the film is found to be $5 \times 10^3 \Omega^{-1} \text{ cm}^{-1}$. Activation energy measurements of this film showed that the film is having two donor levels with activation energies 43 meV and 142 meV.

6.2 Conclusions of the present work

The conclusions drawn out of the detailed investigations carried out in the present study are listed as follows.

- Vacuum deposition technique is shown to be one of the efficient and simple methods to obtain highly conducting and transparent ZnO thin films.
- Incorporation of evaporation source atoms in to ZnO thin films, and reduction in the percentage of these incorporated atoms due to annealing is observed when ZnO thin films were obtained using both “W” and “Mo” evaporation sources.
- Through EDAX analysis it is shown that the incorporation of “W” atoms in the film is considerably less compared to the incorporation of “Mo” atoms. Hence it is concluded that “W” is better suitable source to evaporate ZnO powder compared to that of “Mo” source.
- Vacuum evaporated ZnO thin films of thickness 200 nm were found to have a combination of visible region transmittance of up to 90% and room temperature conductivity of $92 \Omega^{-1}\text{cm}^{-1}$. To the best of our knowledge this is one of the best combination of conductivity and transmittance achieved in the undoped state of ZnO thin films.
- The vacuum deposited ZnO thin film was doped with 3%, 5% and 7% of indium and only the film doped with 5% of indium is found to have good combination of conductivity of the order of $580 \Omega^{-1}\text{cm}^{-1}$ and average transmittance of up to 90% in the visible region.
- ZnO thin films doped with 5% of indium oxide are found to have an excellent improvement in the conductivity of up to $3.5 \times 10^3 \Omega^{-1}\text{cm}^{-1}$ with visible transmittance of up to 90%. This significantly high conductivity of the film compared to the conductivity obtained by doping the film with metallic indium can be attributed to the additional electrons liberated during the process of doping with third group metal oxides.

- The addition of 5% of aluminum oxide to ZnO thin film improved even the transmittance of the film with conductivity.
- Vacuum deposited ZnO thin films are found to have two donor levels below the conduction band in the undoped as well as doped condition and third group oxide doped films are found to have one donor level with activation energy below 55 meV. This will contribute in the electrical conductivity of the film with very low energy loss and thus support the dark conductivity of the film.
- In all the cases films are found to be amorphous in nature with smooth and flat surface topography, which will lead to the low internal stress and are well suited for the application of flat panel displays. The absence of grain boundaries excludes the associated carrier scattering mechanism and thus higher performance of the material is expected.
- It can be concluded that doping of vacuum evaporated ZnO thin films with n-type dopants improves its electrical properties while retaining its transmittance and among different n-type dopants aluminum oxide is the suitable dopant for ZnO thin film since it improves the room temperature conductivity with visible region transmittance of the film.
- Thus highly conducting and transparent ZnO thin films with flat and smooth surface which are well suited for the application of transparent electrodes are obtained by vacuum deposition technique.

6.3 Scope for further work

The present work mainly focused on finalizing the optimum conditions for obtaining highly conducting and transparent ZnO thin films by vacuum evaporation technique. The work also presented the results on successful n-type doping of these films. Since not much results on the investigations of vacuum evaporated ZnO thin films have been reported yet, the research groups have tremendous opportunities to study the the nature of vacuum evaporated ZnO thin films. Still there are lots of possibilities of study in the case of vacuum evaporated ZnO thin films. As a concluding remark a few of them are suggested here.

The previous works on vacuum evaporated ZnO thin films have reported the evaporation of ZnO powder using Mo or W evaporation source. Since in any of these studies an analysis of the composition of the films was not performed, none of the reports mentioned the incorporation of the atoms of boat materials in the film. The present study confirmed the incorporation of atoms of evaporation source materials in ZnO thin films deposited using both Mo as well as W evaporation sources through EDAX analysis. The study can be further continued in detail to know the effect of incorporated atoms on the structural electrical and optical properties of the films.

The present investigation achieved 200 nm thick amorphous and smooth surfaced vacuum evaporated ZnO thin films with an excellent combination of visible region transmittance of up to 90% and room temperature conductivity of $92 \Omega^{-1}\text{cm}^{-1}$. The study can be further carried out to know the stability of these properties of the films at ambient conditions and the device suitability of these undoped films.

The present work is successful in n-type doping of vacuum evaporated ZnO thin films. The research can be further concentrated on improving the combination of n-type conductivity and transmittance achieved in the present case. The vacuum evaporated films can also be doped with other elements to improve its properties other than conductivity.

Until very recently, the p-type doping ZnO thin films is one of the major problems. However after successful breakthroughs, achieved of late, this problem has been solved to a great extent. Studies of p-type doping of vacuum deposited ZnO thin films will be highly desirable in this direction. If p-type doping of vacuum evaporated ZnO thin films is achieved it will certainly boost the commercialization of ZnO based semiconductor devices.

Bibliography

- Agne, T., Guan, Z., Li, X. M., Wolf, H., Wichert, T., Natter, H. and Hempelmann, R. (2003), ‘Doping of the nanocrystalline semiconductor zinc oxide with the donor indium’, *Appl. Phys. Lett.* **83**(6), 1204–1206.
- Agura, H., Suzuki, A., Matsushita, T., Aoki, T. and Okuda, M. (2003), ‘Low resistivity transparent conducting Al-doped ZnO films prepared by pulsed laser deposition’, *Thin Solid Films* **445**(12), 263–267.
- Aida, M. S., Tomasella, E., Cellier, J., Jacquet, M., Bouhssira, N., Abed, S. and Mosbah, A. (2006), ‘Annealing and oxidation mechanism of evaporated zinc thin films from zinc oxide powder’, *Thin Solid Films* **515**(4), 1494 – 1499.
- Aksoy, S., Caglar, Y., Ilican, S. and Caglar, M. (2012), ‘Sol–gel derived Li–Mg co-doped ZnO films: Preparation and characterization via XRD, XPS, FESEM’, *J. Alloys. Compd.* **512**, 171–178.
- Alaeddine, A., Raichidi, I., Bahsoun, F., Mohanna, Y., Bazzi, O. and Hasan, F. E. H. (2003), ‘Influence of aluminum dopant on the optical and electrical properties of zinc oxide thin films prepared by spray pyrolysis technique’, *J. Appl. Sci.* **91**(8), 1588–1592.
- Aly, S. A., Sayed, N. Z. E. and Kaid, M. A. (2001), ‘Effect of annealing on the optical properties of thermally evaporated ZnO thin films’, *Vacuum* **61**(1), 1–7.
- Aoki, T., Hatanaka, Y. and Look, D. C. (2000), ‘ZnO diode fabricated by excimer-laser doping’, *Appl. Phys. Lett.* **76**(22), 3257–3258.

- Assunção, V., Fortunato, E., Marques, A., Águas, H., Ferreira, I., Costa, M. E. V. and Martins, R. (2003), 'Influence of the deposition pressure on the properties of transparent and conductive ZnO:Ga thin-film produced by r.f. sputtering at room temperature', *Thin Solid Films* **427**(1-3), 401–405.
- Ataev, B. M., Bagamadova, A. M., Djabrailov, A. M., Mamedov, V. V. and Rabadanov, R. A. (1995), 'Highly conductive and transparent Ga-doped epitaxial ZnO films on sapphire by CVD', *Thin Solid Films* **260**(1), 19–20.
- Ataev, B. M., Bagamadova, A. M., Mamedov, V. V., Omaev, A. K. and Rabadanov, M. (1999), 'Highly conductive and transparent thin ZnO films prepared in situ in a low pressure system', *J. Cryst. Growth* **198-199**(2-3), 1222–1225.
- Bachari, E. M., Baud, G., Amor, S. B. and Jacquet, M. (1999), 'Structural and optical properties of sputtered ZnO films ', *Thin Solid Films* **348**(1), 165–172.
- Bagnall, D. M., Chen, Y. F., Zhu, Z., Yao, T., Koyama, S., Shen, M. Y. and Goto, T. (1997), 'Optically pumped lasing of ZnO at room temperature', *Appl. Phys. Lett.* **70**(17), 2230–2232.
- Banerjee, A. N., Ghosh, C. K., Chattopadhyay, K. K., Minoura, H., Sarkar, A. K., Akiba, A., Kamiya, A. and Endo, T. (2006), 'Low-temperature deposition of ZnO thin films on PET and glass substrates by DC-sputtering technique ', *Thin Solid Films* **496**(1), 112–116.
- Boris, V. L., Ugolkov, V. L. and Grekov, F. F. (2004), 'Kinetics and mechanism of free-surface vaporization of zinc, cadmium and mercury oxides analyzed by the third-law method ', *Thermochim. Acta* **411**(2-3), 187–193.
- Bouhssira, N., Abed, S., Tomasella, E., Cellier, J., Mosbah, A., Aida, M. S. and Jacquet, M. (2006), 'Influence of annealing temperature on the properties of ZnO thin films deposited by thermal evaporation ', *App. Surf. Sci.* **252**(15), 5594–5597.
- Cao, H. and Zhao, Y. G. (1999), 'Random Laser Action in Semiconductor Powder', *Phys. Rev. Lett.* **82**(11), 2278–2281.

- CASA-XPS (2011), www.casaxps.com/help_manual/manual_updates/xps_spectra.pdf.
Online; accessed on 17-October-2012.
- Chakraborty, A., Mondal, T., Bera, S. K., Sen, S. K., , R. G. and Paul, G. (2008), 'Effects of aluminum and indium incorporation on the structural and optical properties of ZnO thin films synthesized by spray pyrolysis technique ', *Mater. Chem. Phys.* **112**(15), 162–166.
- Chang, J. F., Kuo, H. H., Leu, I. C. and Hon, M. H. (2002), 'The effects of thickness and operation temperature on ZnO:Al thin film CO gas sensor ', *Sens. Actuators, B* **84**(2-3), 258–264.
- Craciun, V., Elders, J., Gardeniers, J. G. E. and Boyd, I. W. (1994), 'Characteristics of high quality ZnO thin films deposited by pulsed laser deposition ', *Appl. Phys. Lett.* **65**(23), 2963–2965.
- Desnica, U. V. (1998), 'Doping limits in II-VI compounds-challenges, problems and solutions ', *Prog. Crystal growthand Charact* **366**(4), 291–357.
- Dghoughi, L., Ouachtari, F., Addou, M., Elidrissi, B., Erguig, H., Rmili, A. and Bouaoud, A. (2010), 'The effect of Al-doping on the structural, optical, electrical and cathodoluminescence properties of ZnO thin films prepared by spray pyrolysis', *Physica B* **405**(9), 2277–2282.
- Elmer, K. (2010), *Hand Book of Transparent Conducting Oxides* , 1 edn, Springer, New York, chapter :Transparent conducting zinc oxide and its derivatives, pp. 193–265.
- Florescu, D. I., Mourokh, L. G., Pollak, F. H., Look, D. C., Cantwell, G. and Li, X. (2002), 'High spatial resolution thermal conductivity of bulk ZnO (0001) ', *J. Appl. Phys.* **91**(2-3), 890–892.
- Funakubo, H., Mizutani, N., Yangetsu, M., Saiki, A. and Shinozaki, K. (1999), 'Orientation Control of ZnO Thin Film Prepared by CVD ', *J. Electron.* **4**(S1), 25–32.

- Ghoniem, N. M. (1998), 'High temperature oxidation of Tungsten and Molybdenum ', <http://www.fusion.ucla.edu/apex/meeting5/1ghoniem1198.pdf>. Online; accessed 19-July-2010.
- Golan, G., A. Axelevitch, Gorenstein, B. and Manevych, V. (2006), 'Hot-Probe method for evaluation of impurities concentration in semiconductors ', *Microelectr. J* **37**(9), 910–915.
- Gomez, H., Maldonado, A., Olvera, M. and Acosta, D. R. (2005), 'Gallium-doped ZnO thin films deposited by chemical spray ', *Sol. Energy Mater. Sol. Cells.* **87**(1-4), 107–116.
- Gong, H., Wang, Y., Yan, Z. and Yang, Y. (2002), 'The effect of deposition conditions on structure properties of radio frequency reactive sputtered polycrystalline ZnO films ', *Mater. Sci. Semicond. Process.* **515**(1), 31–34.
- Gonzales, A. E. J., Urueta, J. A. S. and Parra, R. (1998), 'Optical and electrical characteristics of aluminum doped zinc oxide thin films prepared by sol-gel method ', *J. Cryst. Growth* **192**(3-4), 430–438.
- Hafdallah, A., Yanineb, F., Aida, M. and Attaf, N. (2011), 'In doped ZnO thin films', *J. Alloys. Compd.* **509**(26), 7267–7270.
- Hichou, A. E., Addou, M., Ebothé, J. and Troyon, M. (2005), 'Influence of deposition temperature (Ts), air flow rate (f) and precursors on cathodoluminescence properties of ZnO thin films prepared by spray pyrolysis', *J. Lumin.* **113**(3-4), 183–190.
- Huang, M. H., Mao, S., Feick, H., Yan, H., Wu, Y., Kind, H., Weber, E., Russo, R. and Yang, P. (2001), 'Room-Temperature Ultraviolet Nanowire Nanolasers', *Science* **292**(5523), 1897–1899.
- Hwang, D.-K., Kim, H.-S., Lim, J.-H., Oh, J.-Y., Yang, J.-H., Seong-Ju, Park, Kim, K.-K., Look, D. C. and Park, Y. S. (2005), 'Study of the photoluminescence of phosphorus-doped p-type ZnO thin films grown by radio-frequency magnetron sputtering ', *Appl. Phys. Lett.* **86**(15).

- Janotti, A. and Vandewalle, C. G. (2009), ‘Fundamentals of zinc oxide as a semiconductor’, *Rep. Prog. Phys.* **72**(126501), 1–29.
- Kato, H., Sano, M., Miyamoto, K. and Yao, T. (2002), ‘Growth and characterization of Ga-doped ZnO layers on a-plane sapphire substrates grown by molecular beam epitaxy’, *J. Cryst. Growth* **237-239**(1), 538–543.
- Kim, K. H., Park, K. C. and Ma, D. Y. (1997), ‘Structural, electrical and optical properties of aluminum doped zinc oxide films prepared by radio frequency magnetron sputtering’, *J. Appl. Phys.* **81**(126501), 7764–7772.
- Kim, K. K., Kim, H. S., Hwang, D. K., Lim, J. H. and Park, S. J. (2003), ‘Realization of p -type ZnO thin films via phosphorus doping and thermal activation of the dopant’, *Appl. Phys. Lett.* **83**(1), 63–65.
- Kittel, C. (1996), *Introduction to Solid State Physics*, Wiley, New Jersey.
- Ko, H. J., Chen, Y. F., Hong, S. K., Wenisch, H., Yao, T. and Look, D. C. (2000), ‘Ga-doped ZnO films grown on GaN templates by plasma-assisted molecular-beam epitaxy’, *J. Appl. Phys.* **77**(23), 3761–3763.
- Kykynteshi, R. (2010), *Hand Book of Transparent Conducting Oxides*, 1 edn, Springer, New York, chapter ; Transparent conducting oxides based on tin oxides, pp. 171–192.
- Lee, J. H., Yeo, B. W. and Park, B. O. (2004), ‘Effects of the annealing treatment on electrical and optical properties of ZnO transparent conduction films by ultrasonic spraying pyrolysis’, *Thin Solid Films* **457**(23), 333–337.
- Liu, Z. F., Shan, F. K., Li, Y. X., Shin, B. C. and Yu, Y. S. (2003), ‘Epitaxial growth and properties of Ga-doped ZnO films grown by pulsed laser deposition’, *J. Cryst. Growth.* **259**(1-2), 130–136.
- Look, D. C. (2001), ‘Recent advances in ZnO materials and devices’, *Mat. Sci. Eng.B.* **80**(1-3), 383–387.
- Minami, T., Nanto, H. and Takata, S. (1984), ‘Highly Conductive and Transparent Aluminum Doped Zinc Oxide Thin Films Prepared by RF Magnetron Sputtering’, *Jpn. J. Appl. Phys. Part 2:Letters* **23**(1), L280–L282.

- Minami, T., Oda, J.-i., Nomoto, J.-i. and Miyata, T. (2010), ‘Effect of target properties on transparent conducting impurity-doped ZnO thin films deposited by DC magnetron sputtering’, *Thin Solid Films* **519**(1), 385–390.
- Minami, T., Sato, H., Nanto, H. and Takata, S. (1986), ‘Highly Conductive and Transparent Silicon Doped Zinc Oxide Thin Films Prepared by RF Magnetron Sputtering’, *Jpn. J. Appl. Phys. Part 2:Letters* **252**(9), L776–L779.
- Minami, T., Yamamoto, T. and Miyata, T. (2000), ‘Highly transparent and conductive rare earth-doped ZnO thin films prepared by magnetron sputtering’, *Thin Solid Films* **366**(1-2), 63–68.
- Minegishi, K., Koiwai, Y., Kikuchi, Y., Yano, K., Kasuga, M. and Shimizu, A. (1997), ‘Growth of p-type Zinc Oxide Films by Chemical Vapor Deposition’, *Jpn. J. Appl. Phys. Part 2:Letters* **366**(11A), L1453–L1455.
- Mishra, U. K. and Singh, J. (2008), *Semiconductor Device Physics and Design.*, Springer, Netherlands.
- Morkoc, H. and Ozgur, U. (2007), *Zinc Oxide: Fundamentals, Materials and Device technology*, 1 edn, WILEY-VCH Verlag, Weinheim, chapter 4, pp. 245–268.
- Musat, V., Teixeira, B., Fortunato, E., Monteiro, R. C. C. and Vilarinho, P. (2004), ‘Al-doped ZnO thin films by sol–gel method’, *Surf. Coat. Technol.* **180-181**(1), 659–662.
- Myong, S. Y., Baik, S. J., Lee, C. H., Cho, W. Y. and Lim, K. S. (1997), ‘Extremely Transparent and Conductive ZnO:Al Thin Films Prepared by Photo-Assisted Metalorganic Chemical Vapor Deposition (photo-MOCVD) Using AlCl₃(6H₂O) as New Doping Material’, *Jpn. J. Appl. Phys. Part 2:Letters* **366**(8B), L1078–L1081.
- Ndong, R. O., Ferblantier, G., Delannoy, F. P., Boyer, A. and Foucaran, A. (2003), ‘Electrical properties of zinc oxide sputtered thin films’, *Microelectron. J.* **34**(11), 1087–1092.

- Ntep, J.-M., Hassani, S. S., Lusson, A., Tromson-Carli, A., Ballutaud, D., Didier, G. and Triboulet, R. (1999), 'ZnO growth by chemical vapour transport', *J. Cryst. Growth.* **207**(1-2), 30–34.
- Ohshima, T., Ikegami, T., Ebihara, K., Asmussen, J. and Thareja, R. (2003), 'Synthesis of p-type ZnO thin films using co-doping techniques based on KrF excimer laser deposition', *Thin Solid Films* **435**(1-2), 49–55.
- Özgür, Ü., Alivov, Y. I., Liu, C., Teke, A., Reshchikov, M. A., Doğan, S., Avrutin, V., Cho, S.-J. and Morkoç, H. (2005), 'A comprehensive review of ZnO materials and devices ', *J. Appl. Phys.* **98**(041301), 1–103.
- Park, C. H., Zhang, S. B. and Wei, S.-H. (2002), 'Origin of p-type doping difficulty in ZnO: The impurity perspective', *Phys. Rev. B* **66**(7), 073202–073204.
- Prasada, T. R. and Santhosh, M. C. K. (2010), 'Physical properties of Ga-doped ZnO thin films by spray pyrolysis ', *J. Alloys Compd. Journal of Alloys and Compounds* **506**(23), 788–793.
- Reynolds, D., Look, D. and Jogai, B. (1996), 'Optically pumped ultraviolet lasing from ZnO', *Solid State Commun* **99**(126501), 873–875.
- Rhoderick, E. H. and Williams, R. H. (1988), *Metal-Semiconductor Contacts* , Oxford Science Publications, Oxford.
- Robert W., B., Murrey M., H. and Peter M., H. (1968), *Thin Film Technology*, Van Nostrand Rainhold Company, New York.
- Rusu, G. G., Rusu, M. and Apetroaei, N. (2007), 'On the structural changes during thermal oxidation of evaporated Zn thin films ', *Thin Solid Films* **515**(24), 8699–8704.
- Ryu, Y. R., Zhu, S., Look, D. C., Wrobel, J. M., Jeong, H. M. and White, H. W. (2000), 'Synthesis of p-type ZnO films', *J. Cryst. Growth* **216**(1-4), 330–334.
- Schroder, D. K. (2005), *Semiconductor Material and Device Xharacterization*, Wiley Inter Science, New Jersey.

- Shelke, V., Sonawane, B. K., Bhole, M. P. and Patil, D. S. (2012), 'Electrical and optical properties of transparent conducting tin doped ZnO thin films ', *J. Mater. Sci. - Mater. Electron.* **23**(23), 451–456.
- Shibata, T., Unno, K., Makino, E., Ito, Y. and Shimada, S. (2002), 'Characterization of sputtered ZnO thin film as sensor and actuator for diamond AFM probe ', *Sens. Actuators, A* **102**(1-2), 106–113.
- Shigesato, Y. (2010), *Hand Book of Transparent Conducting Oxides* , 1 edn, Springer, New York, chapter In based TCOs, pp. 161–169.
- Shree Harsha, K. S. (2006), 'Principles of Vapor Deposition of Thin Films ', <http://www.sciencedirect.com/science/book/9780080446998>. Online Book.
- Sze, S. M. (2006), *Physics of Semiconductor Devices.* , Wiley, New York.
- Takeshi Ohgaki, Kawamura, Y., Kuroda, T., Ohashi, N., Adachi, Y., Tsurumi, T., Minami, F. and Haneda, H. (2003), 'Optical Properties of Heavily Aluminum-Doped Zinc Oxide Thin Films Prepared by Molecular Beam Epitaxy ', *Key Eng. Mater.* **248**, 91–94.
- Tellier, J., Kuščer, D., Malič, B., Cilenšek, J., Škarabot, M., Kovač, J., Gonçalves, G., Mušević, I. and Kosec, M. (2010), 'Transparent, amorphous and organics-free ZnO thin films produced by chemical solution deposition at 150 C ', *Thin Solid Films* **518**(18), 5134–5139.
- Tokumoto, M., Smith, A., Santilli, C., Pulcinelli, S., Craievich, A., Elkaim, E., Traverse, A. and Briois, V. (2002), 'Structural electrical and optical properties of undoped and indium doped ZnO thin films prepared by the pyrosol process at different temperatures ', *Thin Solid Films* **416**(1-2), 284–293.
- Tolansky, S. (1950), 'Interferometric evaluation of thicknesses of thin films ', *Le Journal De Physique* **112**, 373–374.
- Tuomisto, F., Ranki, V. and Saarinen, K. (2003), 'Evidence of the Zn Vacancy Acting as the Dominant Acceptor in n-Type ZnO', *Phys. Rev. Lett.* **91**(20), 205502–205505.

- Van-de Walle, C. G. (1997), *Doping of wide band gap II- VI compounds: Theory*, Vol. 44, Academic Press, Massachusetts U. S. A.
- Van-de Walle, C. G. (2000), 'Hydrogen as a Cause of Doping in Zinc Oxide', *Phys. Rev. Lett.* **85**(5), 1012–1015.
- Wang, C., Ji, Z., Liu, K., Xiang, Y. and Ye, Z. (2003), 'p-Type ZnO thin films prepared by oxidation of Zn₃N₂ thin films deposited by DC magnetron sputtering ', *J. Cryst. Growth.* **259**(3-4), 279–281.
- Wang, R., King, L. L. H. and Sleight, A. W. (1996), 'Highly conducting transparent thin films based on zinc oxide', *J. Mater. Res.* **112**(7), 1659–1664.
- Wenas, W. W., Yamada, A., Takahashi, K., Yoshino, M. and Konagai, M. (1991), 'Electrical and optical properties of borondoped ZnO thin films for solar cells grown by metalorganic chemical vapor deposition ', *J. Appl. Phys.* **70**(11), 7119–7123.
- Xu, H. Y., Liu, Y. C., Mu, R., Shao, C. L., Lu, Y. M., Shen, D. Z. and Fan, X. W. (2005), 'F-doping effects on electrical and optical properties of ZnO nanocrystalline films', *Appl. Phys. Lett.* **86**(12), 123107–123107–3.
- Yacobi, B. G. (2004), *Semiconductor Materials - An Introduction to Basic Principles.*, Kluwer Academic Publishers, New York.
- Ye, Z. Z., Lu, J. G., Chen, H. H., Zhang, Y. Z., Wang, L., Zhao, B. H. and Huang, J. Y. (2003), 'Preparation and characteristics of p-type ZnO films by DC reactive magnetron sputtering ', *J. Cryst. Growth* **253**(1-4), 258–264.

List of Publications:

International Journal Publications

1. **Sowmya Palimar**, Kasturi V. Bangera, G. K. Shivakumar
“Study of the aluminum oxide doped zinc oxide thin films prepared by thermal evaporation technique”; **Journal of Applied Sciences**, 12,(2012),1775-1777.
2. **Sowmya Palimar**, Kasturi V. Bangera, G. K. Shivakumar
“Highly conducting and transparent Ga₂O₃ doped ZnO thin films prepared by thermal evaporation method”; **Semiconductors**, 46,(2012),1545-1548.
3. **Sowmya Palimar**, Kasturi V. Bangera, G. K. Shivakumar
“Study of the doping of thermally evaporated zinc oxide thin films” with indium and indium oxide“; **Applied Nano Science**.
Available online:<http://link.springer.com/article/10.1007/s13204-012-0161-1>
4. **Sowmya Palimar**, Kasturi V. Bangera, G. K. Shivakumar
“Influence of doping with third group oxides on the properties of zinc oxide thin films”; **Semiconductors** (To appear).

Conference Presentations

1. **Sowmya Palimar**, G. K. Shivakumar, and Kasturi V. Bangera.
Conductive and transparent undoped ZnO thin films prepared by thermal evaporation method **56th DAE Solid State Physics Symposium**; SRM University, Chennai, Dec 15-19, 2011.
Published by AIP Conference Proceedings.
Citation: <http://dx.doi.org/10.1063/1.4710154>

2. **Sowmya Palimar**, Kasturi V. Banger, and G. K. Shivakumar.
"Study of the aluminum oxide doped zinc oxide thin films prepared by thermal evaporation technique"
International Conference of Thin Films and Applications;
SASTRA University, Thanjavur, March 15-17, 2012.
One Among the top 20 papers selected for publication in Journal of Applied Science

3. **Sowmya Palimar**, Kasturi V. Banger and G. K. Shivakumar. "Study of the indium oxide doped zinc oxide thin films prepared by thermal evaporation technique"
National Conference on Condensed Matter Physics and Applications:
Manipal Institute of Technology, Manipal, Dec 27-29, 2012.
Won Best Presentation Award

Bio-Data

Sowmya Palimar
Research Scholar
Department of Physics
National Institute of Technology Karnataka
P O Srinivasanagar
Mangalore - 575 025.

Email: sowmya0124@gmail.com

Education: M. Sc., (Material science), Mangalore University, 2007.

Selected Accomplishments

1. Beneficiary of C. V. Raman Scholarship during the period 2002–2005.
2. Won Best Presentation Award in National Conference of Condensed Matter Physics and Applications – 2012